Abanoub A. Gad

Abanoubakbg@gmail.com

Ph.D. Candidate, 4th Year

Program in Molecular Medicine Cancer Biology

Department of Surgery- Marlene and Stewart Greenbaum Comprehensive Cancer Center

Education

06/2018-05/2022	*Ph.D., Molecular Medicine*
	University of Maryland, Baltimore, MD
	Advisors: Nariman Balenga, Ph.D. & John A. Olson, Jr, M.D., Ph.D.
	Degree Conferred: May 2022
08/2015-06/2017	*M.S., Pharmacology*
	Thomas Jefferson University, Philadelphia, PA
	Advisor: David Teachey, M.D.
08/2011-05/2015	*B.S., Psychology*
	University of Maryland, College Park, MD

Research Experience

06/2019-Present	*Graduate Research Assistant*
	University of Maryland, Baltimore
	Laboratories of Dr. Nariman Balenga, Ph.D and John A. Olson, Jr, M.D., Ph.D.
06/2018-09/2018	*Ph.D. Rotation Student*
	University of Maryland, Baltimore
	Laboratory of Dr. John Eley, Ph.D.
12/2018-03/2019	*Ph.D. Rotation Student*
	University of Maryland Baltimore County
	Laboratory of Dr. Aikaterini Kontrogianni-Konstantopoulos, Ph.D.
03/2019-05/2019	*Ph.D. Rotation Student*
	University of Maryland Baltimore County

	Laboratory of Dr. Gregory Szeto, Ph.D.
06/2017-05/2018	*Research Technician II*
	Dana-Farber Cancer Institute, Boston, MA
	Laboratory of Dr. Abner Louissaint, M.D., Ph.D.
06/2015-06/2017	*Research Technician I*
	Children's Hospital of Philadelphia, Philadelphia, PA
	Laboratory of Dr. David Teachey, M.D.
01/2012-06/2015	*Undergraduate Research Assistant*
	University of Maryland, College Park
	Laboratory of Dr. Patrick Kanold, Ph.D.

Publications

Gad, A.A., Azimzadeh, P. & Balenga, N. Conserved residues in the extracellular loop 2 regulate *Stachel*-mediated activation of ADGRG2. *Sci Rep* **11,** 14060 (2021). https://doi.org/10.1038/s41598-021-93577-y

Gad, A. A., & Balenga, N. (2020). The emerging role of adhesion GPCRs in cancer. *ACS pharmacology & translational science*, *3*(1), 29-42.

Loya, J. M., McCauley, K. L., Chronis-Tuscano, A., Chen, S. Z., **Gad, A. A.**, MacPherson, L., & Lejuez, C. W. (2019). An experimental paradigm examining the influence of frustration on risk-taking behavior. *Behavioral processes*, *158*, 155-162.

Proffered Communications

Gad, A. A., Balenga, N. (2021) *A Conserved Extracellular Motif Regulates Signaling and Trafficking of ADGRG2*. Poster presented at Experimental Biology 2021 Annual Meeting.

Zhao, C. **Gad, A. A**, Balenga, N., (2020) Identifying N-glycosylation Sites and Tumor-Associated Mutations on the N-terminal Fragment of ADGRG2 for in vitro Signaling Studies. Presented as part of the University of Maryland 2020 Student Research Forum.

Gad, A. A., Balenga, N. (2020) *Molecular Determinants of Signaling and Posttranslational Modifications of GPR64*. Accepted for presentation at The American Society for Pharmacology and Experimental Therapeutics annual meeting 2020. (meeting canceled due to pandemic).

Guardia, T., **Gad, A**. **A.**, & Kontrogianni-Konstantopoulos, A. (2019) Investigating Tumor Suppression Function of Obscurins in Breast Cancer, Poster session presented at

the annual Cancer Biology retreat at the University of Maryland School of Medicine, Baltimore, MD.

Professional Affiliations

American Society for Pharmacology and Experimental Therapeutics, 2019-Present

Abstract

The parathyroid glands sense serum calcium levels and release parathyroid hormone (PTH) in response to hypocalcemia. PTH acts at bone, intestine, and kidney to increase serum calcium. Primary hyperparathyroidism (PHPT) is an endocrine disorder characterized by neoplasia of one or more glands, dysregulated PTH release, and hypercalcemia. The mechanisms of dysregulated calcium-sensing in parathyroid adenomas are not well understood. The literature suggests that the expression of the calcium-sensing receptor (CaSR) is diminished in parathyroid adenomas. We have found that a subset of PHPT patients do not show a significant change in CaSR expression. Therefore, we hypothesized that other molecules that modify the action of CaSR might inhibit its ability to sense calcium properly. We identified ADGRG2, an adhesion G protein-coupled receptor (aGPCR), in a transcriptome screen of parathyroid tissue and hypothesized that it might serve as a modifier of CaSR function. A transgenic mouse with parathyroid-restricted ADGRG2 overexpression develops parathyroid neoplasia, hypercalcemia, and hyperparathyroidism. To understand crosstalk mechanisms between ADGRG2 and CaSR, we developed a double-expressing ADGRG2-CaSR stable cell line (FL-CaSR). Activation of ADGRG2 in this novel cell line completely ablated the $G\alpha_i$ and $G\alpha_q$ signaling pathways downstream of CaSR. We also developed a SNAP and CLIP tag system to ascertain changes in receptor trafficking. Live cell imaging studies showed that in cells expressing both ADGRG2 and CaSR, co-stimulation caused the receptors to remain on the cell surface and not traffic into the early endosome. Given the important role that the ADGRG2 plays in inhibiting CaSR activity we sought to identify targetable

motifs for future therapeutic development. We identified a conserved CWI motif in the second extracellular loop (ECL2) of ADGRG2. Mutations of the conserved tryptophan or isoleucine residues completely ablated ADGRG2 signaling. Kinetic signaling assays, homogenous time resolve FRET (HTRF), and whole-cell impedance assays all confirmed an ablation of ADGRG2-mediated Gαs activity. ECL2 mutations also caused rapid proteasomal degradation of the receptor. These studies confirm a role for ADGRG2 in modulating CaSR signaling and provide the foundation for future ADGRG2-targeted therapeutic development.

Characterizing the Signaling, Crosstalk, and Trafficking of Adhesion G Protein-Coupled Receptor G2 and the Calcium-Sensing Receptor in Parathyroid Adenoma Models

by

Abanoub A. Gad

Dissertation submitted to the Faculty of the Graduate School of the
University of Maryland, Baltimore in partial fulfillment
of the requirements for the degree of
Doctor of Philosophy
2022

Acknowledgments

I would like to thank my committee, especially Dr. Nariman Balenga, who equipped me with all the tools and skills to complete my research. His patience, drive, and attention to detail during my training were essential in my development as a scientist. I would also like to thank Dr. John Olson for his essential role in my successful transition to an independent researcher and completing this thesis. Dr. Olson always found time in his busy schedule as a surgeon and scientist to discuss my writing and data. More importantly, Dr. Olson is always encouraging, even when I thought none of these experiments would work. Dr. Stuart Martin and Dr. Michelle Vitolo were also vital to my training; I was unofficially adopted in their lab group during my last year. Dr. Martin and Dr. Vitolo were incredibly generous with their time and discussed my data, career goals, and writing. Finally, Dr. Joe Stains, Dr. Dudley Strickland, and Dr. Hee-Yong Kim for their constructive comments, sharing their expertise and support throughout the past years.

My labmates, Pedram, Ace, and Ashley, were also essential in assisting me with my research and training me on the various techniques used throughout this dissertation. I also would like to thank the Martin Lab, particularly Julia Ju, Makenzy Mull, and David Annis, for their patience in training me on various microscopy techniques. More importantly than the invaluable research training and assistance, the convivial environment and friendships helped me get through some of the most demanding challenges over the last four years. To all of my friends outside of the lab, especially Rafik Boulos, Marko Yacoub, Karim and Melanie Labib, Peter and Sandy Mansour, Matt

and Nada Galey, and the MadHouse team, thank you for keeping me sane and forgiving my constant social absence.

I also have to thank my family, Adel and Teriza Gad, and my sister, the newly minted Dr. Mary Gad. My family sacrificed their lives to immigrate to the United States, missing weddings, funerals, births, and many of our family's major life events so that my sister and I could have the opportunities afforded by an education in the United States. My parents' patience, sacrifice, and belief in me are what encouraged me to pursue my Ph.D. I hope that this degree makes them proud. Also, Mary, you will receive your doctorate first, but I defended before you, so let this serve as a written record, I was the first doctor in the family.

Finally, my wife, Christina Gad. I can say definitively that this dissertation would not have been complete without Christina's constant love, encouragement, and support. As a graduate student, you understand the challenges and sacrifices required to achieve your degree; your spouse, on the other hand, is an unwitting participant on this journey. There really should be an award for the spouses of Ph.D. students. If anyone reading this can give honorary spousal Ph.Ds., then Christina comes highly recommended.

Table of Contents

List of Tables

List of Figures

List of Abbreviations

7TM	7 Transmembrane Receptor
aGPCR	Adhesion G Protein-Couple Receptor
BMD	Bone Mineral Density
BSA	Bovine Serum Albumin
Ca2+	Calcium
CaRE	Calcium Response Element
CaSR	Calcium-Sensing Receptor
CCND1	Cyclin D1
CDC73	cell division cycle 73
CRC	Colorectal Cancer
CRE	cAMP Response Element
CTF	C Terminal Fragment
DAG	Diacylglycerol
DCIS	Ductal Carcinoma In-Situ
DGK	Diacylglycerol Kinase
ECD	Extracellular Domain
ECL	Extracellular Loop
ECM	Extracellular Matrices
EGFR	Epidermal Growth Factor Receptor
EM	Electron Microscopy
EMT	Epithelial to Mesenchymal Transition
ER	Endoplasmic Reticulum
FHH3	Familial Hypocalciuric Hypercalcemia 3
GAIN	GPCR Autoproteolysis-Inducing domain
GAPS	GTPase Activating Proteins
GPCR	G Protein-Coupled Receptor
GPS	GPCR Proteolytic Site

GRKS	G Protein-Coupled Receptor Kinases
HE6	Human Epididymis-Specific Protein 6
HER2	Human Epidermal Growth Factor Receptor 2
HPT-JT	Hyperparathyroidism Jaw Tumor
HTRF	Homogenous Time Resolve Förster resonance energy transfer
IHC	Immunohistochemistry
IP3	Inositol 1,4,5-Trisphosphate
IP3R	Inositol 1,4,5-Trisphosphate Receptor
LCNEC	Large Cell Neuroendocrine Lung Carcinomas
LPAR1	Lysophosphatidic Acid Receptor 1
MAPK	Mitogen-Activated Protein Kinase
MEN	Multiple Endocrine Neoplasia
NFAT	Nuclear Factor of Activated T Cells
NSCLC	Non-Small Cell Lunch Cancer
NTF	N Terminal Fragment
PDE	Phosphodiesterases
PHPT	Primary Hyperparathyroidism
PI3K	Phosphatidylinositol-3 Kinase
PIP2	phosphatidylinositol 4,5-bisphosphate
PKA	Protein Kinase A
PKC	Protein Kinase C
PLC-ß	Phospholipase C-ß
PTH	Parathyroid Hormone
PTHR	Parathyroid Hormone Receptor
qPCR	Quantitative Polymerase Chain Reaction
RANKL	Receptor Activator of Nuclear Factor Kappa B Ligand
RB	Retinoblastoma

RGS	Regulator of G Protein Signaling
SCLC	Small Cell Lung Cancer
SHPT	Secondary Hyperparathyroidism
SRE	Serum Response Element
THPT	Tertiary Hyperparathyroidism
VFT	Venus Flytrap

Chapter 1 - The Current Understanding of Parathyroid Physiology and Pathology.

Physiology

Anatomy

Parathyroid glands are four endocrine glands situated in the anterior neck, posterior to the thyroid gland (Fig. 1.1). The two superior glands arise from the fourth pharyngeal pouch, while the inferior glands are derived from the third pharyngeal pouch. Both superior and inferior glands share a common blood supply; the inferior thyroid arteries and parathyroid veins drain into the thyroid vein plexus. The nerve supply to the parathyroid gland derives from the cervical ganglia of the thyroid gland. The location and number of glands may differ across a population. Autopsies have found ectopic and supernumerary expression of parathyroid glands in approximately 13% to 16% of people[1].

Function

The primary function of the parathyroid glands is to maintain serum calcium (Ca^{2+}) homeostasis by regulating the secretion of parathyroid hormone (PTH). PTH functions at the kidney, intestine, and bone to increase serum Ca^{2+} levels (Fig. 1.1). Early studies by Talmage and Kranitz showed that resecting the parathyroid glands rapidly increases Ca^{2+} excretion in rats[2]. We now know that PTH promotes the reabsorption of Ca^{2+} at the ascending loop of Henle, the distal tubule, and the collecting tubule of kidney. PTH-mediated activation of the protein kinase A (PKA) cascade in the distal nephron

causes rapid phosphorylation of the TRPV5 channel to stimulate Ca^{2+} reabsorption[3, 4]. PTH also causes the up-regulation of 25-hydroxyvitamin D3 1-alpha-hydroxylase in the kidneys[4]. This enzyme converts 25-hydroxyvitamin D3 to its active form, 1,25-dihydroxyvitamin D, which increases calcium absorption in the intestines.

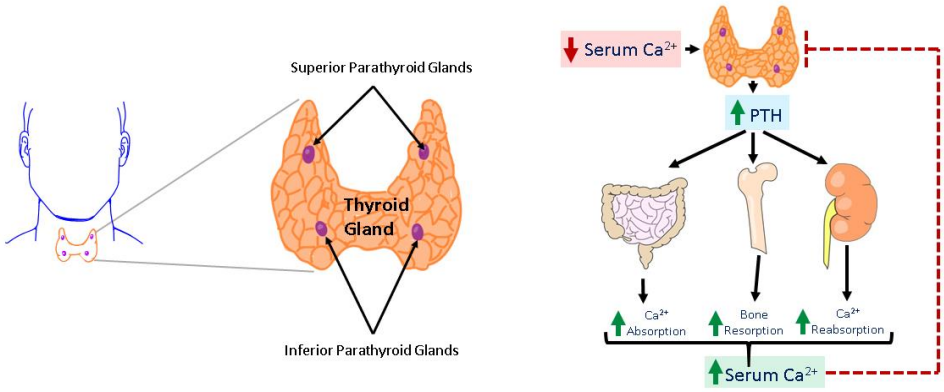

Figure 1-1 Diagram of the anatomy and function of the parathyroid glands. The four parathyroid glands are on expressed on the posterior of the thyroid gland. The chief cells of the parathyroid glands release PTH into the serum which acts at the kidneys, bone, and intestines in order to increase serum Ca^{2+} levels. The increase of serum Ca^{2+} is a negative feedback mechanism which will inhibit further PTH release.

PTH promotes release of Ca^{2+} from bone, the largest reservoir of Ca^{2+} in the human body. Bones constantly maintain a homeostatic balance between bone resorption and absorption. The resorption of bone by osteoclasts leads to the release of Ca^{2+} and phosphorous into the bloodstream. The mechanisms by which PTH causes bone resorption are indirect as osteoclast cells do not express PTH receptors. Osteoblasts, bone-forming cells, express a PTH receptor which, when stimulated, signals via the PKA to increase the expression of receptor activator of nuclear factor kappa B ligand (RANKL) and various bone-degrading proteases and cytokines[5]. RANKL mediates the differentiation of osteoclast precursors to mature osteoclasts. The PTH-mediated release of these cytokines causes prolonged activation of osteoclasts, which will, in turn, break down bone and release Ca^{2+} into the bloodstream to maintain serum Ca^{2+} levels[6]. The

parathyroid glands sense the increase in serum Ca^{2+} and inhibit further PTH release into the bloodstream, generating a negative feedback loop.

There are two distinct cell types in the parathyroid gland: chief cells and oxyphil cells. The chief cells are the primary functional cell of the parathyroid glands, responsible for PTH secretion. Chief cells contain a prominent Golgi and endoplasmic reticulum (ER) to help with the synthesis, packaging, and secretion of PTH[7]. The chief cells also express the calcium-sensing receptor (CaSR), responsible for sensing serum calcium levels (discussed in Chapter 2). Chief cells are expressed in parathyroid glands across all species, while the oxyphil cells are expressed only in humans and some animals[8].

The role of oxyphil cells in parathyroid pathobiology is not well defined. Oxyphil cells exist in small groups interspersed between chief cells and are much larger and less abundant than chief cells. Studies have found that oxyphil cells are not present in humans at birth but develop over time and increase with age[9]. The presence of CaSR on oxyphil cells is evidence that these cells are transdifferentiated from chief cells. Furthermore, oxyphil cells do not contain any secretory granules and can be defined histologically by an increased number of misshapen mitochondria[10]. While experimental evidence for the function of oxyphil cells is lacking, case reports of patients who did not respond to Ca^{2+} supplementation found that their glands consisted of 40% oxyphil cells[11]. These data suggest that oxyphil cells may play a role in resistance to calcimimetic drugs or the use of calcimimetic drugs causes a proliferation of oxyphil cells. Further research elucidating

the biology of oxyphil cells may prove critical to the treatment, diagnosis, and general understanding of parathyroid pathobiology.

Pathology

Parathyroid neoplasias range from benign hyperplasia to adenoma to rare carcinomas [12]. Parathyroid tumors generally cause hyperparathyroidism, a dysregulated increase in PTH secretion, leading to hypercalcemia. Patients afflicted with hyperparathyroidism typically describe nonspecific symptoms such as depression, lethargy, and vague aches and pains. These symptoms are likely due to the role of Ca^{2+} in synaptic transmission and neurotransmitter vesicle secretion. Patients also present with urolithiasis due to the calcium-conserving renal activity of PTH. Bone pain, decreased bone mineral density (BMD), and pathologic fractures result from PTH-mediated osteoclast activity.

Hyperparathyroidism is divided into primary, secondary, and tertiary hyperparathyroidism based upon the cause and clinical features of the disease (Table 1.1). Diseases of the parathyroid glands are defined as primary and generally present with elevated PTH and Ca^{2+} levels. Non-parathyroid mechanisms generally cause secondary and tertiary disease. The most common causes of secondary hyperparathyroidism (SHPT) are vitamin D deficiency, decreased dietary Ca^{2+} intake, or chronic renal failure[13]. Tertiary hyperparathyroidism (THPT) is the result of long-standing severe SHPT. THPT is the autonomous continuation of hyperparathyroidism after eliminating the underlying causes of SHPT. For a detailed review of SHPT and THPT, see Muppidi et al.[13] and Palumbo et al.[14], respectively.

Primary Hyperparathyroidism (PHPT)

Non-familial (Sporadic) PHPT

Primary Hyperparathyroidism (PHPT) is the most common parathyroid disorder, in the United States, with approximately 30 cases per 100,000 people[15]. PHPT is most commonly caused by sporadic adenomatosis of one parathyroid gland, although hyperplasia, multiple adenomas, and carcinomas have been observed[16, 17]. Adenomatous glands are insensitive to serum Ca^{2+} levels, which causes hypercalcemia and inappropriately high levels of PTH, given the hypercalcemic state. Practically all other hypercalcemic etiologies present with severely suppressed PTH levels. Somatic abnormalities involving the cyclin D1 (*CCND1*), retinoblastoma (*RB*), and the multiple endocrine neoplasia type 1 (*MEN1*) genes are well documented in sporadic adenomas[18]. *CCND1* was first identified in a study of parathyroid tumors and is now an established oncogene involved in numerous human cancers[18]. Approximately 40% of parathyroid adenomas have overexpression of *CCND1*, some due to a pericentromeric inversion of chromosome 11 affecting the PTH promoter and *CCND1*[19]. Whole-exome sequencing of sporadic parathyroid tumors also found inactivating mutations of *MEN1* in 30% of parathyroid tumor samples[20]. Unfortunately, *MEN1* and *CCND1* mutations are only observed in a subset of sporadic PHPT patients, making them ill-suited as therapeutic targets, suggesting other molecules may be involved in the disease pathogenesis.

Familial (Syndromic) PHPT

Five to ten percent of PHPT cases are familial, resulting from complex endocrine syndromes or hereditary germline mutations[18]. Familial PHPT is most often characterized by multiglandular disease, unlike a single-gland sporadic disease[18]. The most common PHPT-causing syndromes are MEN1, MEN2, MEN3, MEN4, and hyperparathyroidism-jaw tumor (HPT-JT). *MEN1* encodes the tumor suppressor menin, and 80% of germline *MEN1* mutations are inactivating. 95% of patients with *MEN1* mutations develop a parathyroid tumor and PHPT[21]. Mutations of the *c-ret* proto-oncogene located on chromosome 10q11.2 cause MEN2 syndromes. MEN2A and MEN2B are less common causes of PHPT, with approximately 20% of patients developing parathyroid tumors[22]. 5-10% of patients have MEN4 and present with a very similar disease as MEN1 syndrome, although these patients do not have mutations in *MEN1*[18]. The most common MEN4 mutation is a loss of function mutation in *CDNK1B,* which encodes the P27 tumor suppressor protein [23]. MEN4 is an autosomal dominant disorder and causes several different malignancies, including pituitary, parathyroid, and adrenal tumors, among others[23]. HPT-JT causes the development of several different neoplasms, including parathyroid adenomas and parathyroid, uterine, renal, and pancreatic carcinomas due to mutations in the cell division cycle 73 (*CDC73*) gene[18, 24, 25]. Interestingly, over 65% of sporadic parathyroid carcinomas express mutations in *CDC73*, which indicates these mutations give rise to an aggressive proliferative cellular phenotype in parathyroid cells[18].

Normocalcemic PHPT

Data has emerged describing patients with parathyroid adenomas and marked elevated PTH levels with no evidence of hypercalcemia[26]. To diagnose normocalcemic PHPT, all potential SHPT mechanisms must be assessed and eliminated, particularly vitamin D deficiency and low glomerular filtration rates. This iteration of PHPT was identified in a population-based analysis of over 5000 postmenopausal women[27]. This study included an 8-year follow-up where some of the patients ultimately developed hypercalcemia. Unfortunately, vitamin D levels were not collected; therefore, distinguishing between SHPT and normocalcemic PHPT cannot be done retrospectively. In subsequent observational studies, the correction of vitamin D deficiency in patients did not ameliorate the hyperparathyroid phenotypes[28]. The literature is not yet clear on the exact etiology of normocalcemia PHPT. Some researchers argue that it may be a mild or early presentation of PHPT[29], while others consider it a separate disease state[26]. Further work is needed to diagnose and explore the mutational landscape of this particular phenotype more accurately.

Diagnosis	PTH Levels	Serum Ca2+	Genetic Abnormalities	Primary Causes
Sporadic PHPT	High	Elevated	CCND1/PRAD1 MEN1 LOH	Sporadic Parathyroid adenomatosis
Familial PHPT	High	Elevated	MEN1, MEN2, MEN3 (MEN2B), MEN 4, HPT-JT	Syndromic Parathyroid adenomatosis
Normocalcemic PHPT	High	Normal	Unknown	Parathyroid adenomatosis
SHPT/THPT	High	Low	ASXL3, CIT, HGF	Vitamin D defficency Kidney Disease

Table 1-1-Various parathyroid diseases and their associated biochemical and known genetic abnormalities.

Molecular Underpinnings of PHPT

Normal serum ionized Ca^{2+} levels are between 4.4-5.2 mg/dL (1.1-1.3mM) which maintains serum PTH levels at approximately 11-51pg/mL (11-51 ng/L). The Ca^{2+} Set-

point is the level of serum Ca^{2+} needed to achieve 50% suppression of maximal PTH secretion (Fig. 1.2). Parathyroid tumor insensitivity to serum Ca^{2+} causes a shift in set point; therefore, tumors require much more serum Ca^{2+} to achieve PTH secretion inhibition, compared to a normal gland.

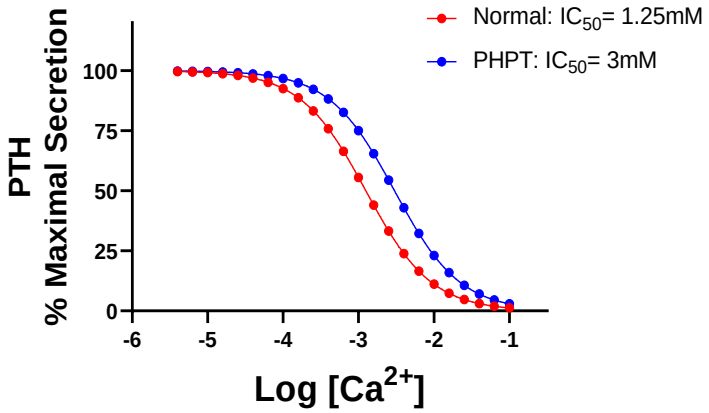

Figure 1-2 PHPT patients have an increased Ca^{2+} setpoint. The setpoint, defined as the concentration of serum Ca^{2+} required to decrease PTH secretion by 50%. PHPT patients have a much higher set point and require much more serum Ca^{2+} to inhibit PTH secretion to a physiologically acceptable level.

Genetic alterations in both familial and sporadic PHPT have helped guide the treatment of PHPT, but a fundamental question that links all forms of PHPT remains: *What is the cause of Ca^{2+} insensitivity in hyperparathyroid tumors?* The classic view postulates that parathyroid tumors have decreased CaSR expression, which causes Ca^{2+} insensitivity[30, 31]. In recent years this view has been challenged by us and several other groups who found a significant subset of PHPT patients do not show alterations in CaSR expression[32, 33]. **The fluctuations in CaSR expression among PHPT patients lead to our work's central hypothesis that the dysregulation of Ca^{2+} sensing in parathyroid tumors is not a function of CaSR expression in some patients but rather mediated by CaSR-modulating molecules.**

Current Treatments

The recommendation for all symptomatic PHPT patients is parathyroidectomy, which is curative. For patients ineligible for surgery or who refuse surgical intervention, there are medical therapies aimed at increasing CaSR sensitivity to Ca^{2+}. Unfortunately, no single agent can normalize Ca^{2+}, PTH, bone mineral density, and renal absorption of Ca^{2+}. Therefore, patients who opt out of surgery, do not meet surgical criteria due to comorbidities or have recurrent disease require consistent monitoring of serum PTH and Ca^{2+} and lifelong medical management.

The most common drug given for PHPT is Cinacalcet (Sensipar), a calcimimetic agent. Calcimimetic drugs bind allosterically to CaSR to increase the receptor's sensitivity to extracellular Ca^{2+}. In the USA, cinacalcet is approved for use in SHPT and severe PHPT patients who are not candidates for parathyroidectomy. Four randomized controlled clinical trials studied the efficacy of cinacalcet in over 700 PHPT patients, and meta-regression analysis found serum Ca^{2+} levels normalized in 90% of patients while PTH levels normalized in only 10% of cases[34]. One long-term clinical trial found that cinacalcet can achieve long-term Ca^{2+} and PTH normalization over 52-weeks[35]. Cinacalcet has been successfully utilized to correct hypercalcemia in various PHPT disease states, including sporadic, familial, intractable, and carcinomas but it has shown no effect on bone symptoms[36-39]. Due to the ubiquitous expression of CaSR across different tissue types, several side effects are associated with cinacalcet treatment. Patients primarily report gastrointestinal events, such as nausea, vomiting, and loss of appetite. Patients on cinacalcet must be monitored closely for symptoms of hypocalcemia, and over suppression of PTH may lead to adynamic bone disease.

Unfortunately, cinacalcet shows no effect on BMD; therefore, combination therapy with bisphosphonates is necessary.

Bisphosphonates decrease bone resorption to prevent BMD loss by inhibiting the activity of osteoclasts. A randomized controlled trial concluded that daily treatment with a bisphosphonate (alendronate) showed a modest increase in BMD at the spine and hip[40]. Bisphosphonates alone have little to no effect on serum Ca^{2+} or PTH levels, but studies looking at combination therapy of cinacalcet and bisphosphonates have shown significant improvements in both biochemical abnormalities and BMD[41].

Concluding Remarks

The landscape of PHPT diagnosis and treatment is continually changing with advances in cell biology, imaging modalities, genomics, and medical treatments. The accumulation of evidence thus far has successfully stratified PHPT into several different subtypes, which is essential for understanding disease pathogenesis and progression. Several studies have identified sporadic mutations in many genes among a subset of PHPT patients, most commonly the rearrangement of *PRAD1*(*CCND1*) and *PTH.* Others have described heritable syndromes which cause parathyroid adenomatosis. Although parathyroidectomy is curative, and several medical treatments have shown efficacy, they ultimately seek to correct a symptom rather than the underlying cause. The classical theory of parathyroid adenoma pathogenesis suggests a decrease in CaSR expression leads to Ca^{2+} insensitivity. Several groups have found contradictory evidence to this theory, citing several patients with PHPT that do not show any difference in CaSR

expression. The central hypothesis of this thesis is that CaSR dysfunction, in some patients, is a result of modulatory molecules rather than direct changes in CaSR. We have previously shown that RGS5 can recapitulate PHPT phenotypes in transgenic mice, which express normal CaSR. Herein we explore the function, trafficking, signaling, and crosstalk of ADGRG2 and CaSR to identify novel mechanisms of CaSR dysregulation.

Chapter 2 G-Protein Coupled Receptors: Structure, Function, and Roles in Neoplastic Diseases.

What are G Protein-Coupled Receptors (GPCRs)?

The Discovery of GPCRs: A Succinct History

Prior to the 1970s, cell surface receptors had yet to be experimentally observed and were a controversial theory in the literature. Claude Bernard conducted the earliest experiments that hinted at the existence of receptors in 1844[42]. Bernard observed that a curare-laced arrow caused complete paralysis in a rabbit, but there was no evidence that the wound could induce such a response upon autopsy. After a series of experiments on the curare poison, he concluded that the poison is acting on an 'intermediate zone' between muscles and nerves. Bernard and his student, Kuhne, would use the histological approaches of their day to try and uncover where exactly the poison was exerting its function. Bernard never successfully identified the intermediate zone, but his work laid the foundation for discovering cell receptors decades later.

In 1901, at Cambridge University, John N. Langley and his student Thomas Elliot hypothesized that cells must have a 'receptive substance.' In 1905 Langley wrote,

"*Thus there is evidence that the majority of substances which are ordinarily supposed to act upon nerve-endings act upon the receptive substances of the cells…So we may suppose that in all cells two constituents at least are to be distinguished. The chief substance which is concerned with the chief function of the cell as contraction and secretion and receptive substances which are acted upon by chemical bodies and in certain cases by nervous*

stimuli. The receptive substance affects or is capable of affecting the metabolism of the chief substance"[43]

By 1914 Langley and Ehrlich had coined the term receptor and laid the groundwork for identifying membrane receptors over 50 years later.

By the 1960s, cell receptors were an accepted theory of classical pharmacology, although none had been cloned or purified. Scientists such as Feldberg, Ahlquist, Dale, and Sakmann studied adrenaline and the acetylcholine receptors and hypothesized that distinct versions coined α and ß receptors must exist. It was not until the 1960s at Duke University that Robert Lefkowitz and Brian Kobilka purified the first receptors.

Lefkowitz developed a radioligand binding technique with Rusty Williams and Marc Caron to study the ß-adrenergic receptors. Their early experiments concluded that competition curves for the ß-adrenergic receptors were monophasic for antagonists and biphasic for agonists, a high affinity and low-affinity state[44]. Furthermore, they discovered that the addition of guanyl nucleotides mediated the transition from high affinity to low-affinity states[44]. Over the next decade, using their lab's ligand-binding experience, they developed chromatography purification techniques which allowed them to purify four distinct adrenergic receptors: α_1,α_2, $ß_1$, and $ß_2$[45]. The final hurdle was proving the functionality of the purified receptors. Rick Cerione, a post-doctoral fellow at the Lefkowitz lab, expressed the purified $ß_2$ receptor in cells from the African clawed toad, which did not contain any ß-adrenergic receptors and therefore did not respond to adrenergic agonists. By exogenously expressing the ß-adrenergic receptor, a guanine nucleotide regulator protein (G_s), and the catalytic subunit of adenylyl cyclase in African

clawed toad cells, they were able to reconstitute catecholamine signaling[46]. These experiments were the first to clone a GPCR and delineate the molecules required for signaling.

The amino-acid sequence analysis of the newly verified receptor showed a 7-transmembrane (7TM) spanning domain and homology with a light-sensing molecule, rhodopsin[47]. By 1987, Lefkowitz cloned several receptors and validated the 7TM G protein-coupled receptors (GPCRs) superfamily of functionally distinct receptors. Identifying these receptors and their functions led to innumerable discoveries, including hundreds of GPCR-targeting therapeutics. In recognition of their work on GPCRs Robert Lefkowitz and Brian Kobilka were awarded the 2012 Nobel Prize in Chemistry.

Structure and Classification

GPCRs are cell surface receptors defined by a conserved 7TM domain, alternating intracellular and extracellular loop regions, and their ability to signal through cognate G proteins (Fig. 2.1). Over 800s genes make up the GPCR superfamily, making it the largest family of genes in the human genome. There have been several attempts to classify GPCRs over the years. Herein we describe the GRAFS classification system, which divides the vertebrate GPCRs into five distinct families: Glutamate, Rhodopsin, Adhesion, Frizzled, and Secretin. The GRAF system was described in 2005 by Schiöth and Fredriksson, based on large-scale phylogenic analyses of human GPCRs[48].

The glutamate receptor family of receptors is vital for neuronal function and development. The Calcium-Sensing Receptor (CaSR) is a member of the glutamate family and is discussed in further detail below. The rhodopsin family of GPCRs is the largest, consisting of over 600 members, divided into 13 subfamilies. Rhodopsin receptors are characterized structurally by very small N termini relative to other GPCR families. Unlike the traditional A-F system of GPCR classification, the GRAFS classification differentiates between the secretin and adhesion families. Adhesion GPCRs (aGPCRs) are discussed in greater detail below. Frizzled receptors play an essential role in cell fate, developmental polarity, and proliferation. The N-termini of frizzled receptors contains over 200 amino acids with many cysteines which participate in Wnt signaling. The secretin and adhesion families contain large N-terminal fragments, but further analysis found that these two groups evolved separately and have significant differences in their N-termini. The secretin family binds large peptide ligands and most often functions in paracrine signaling.

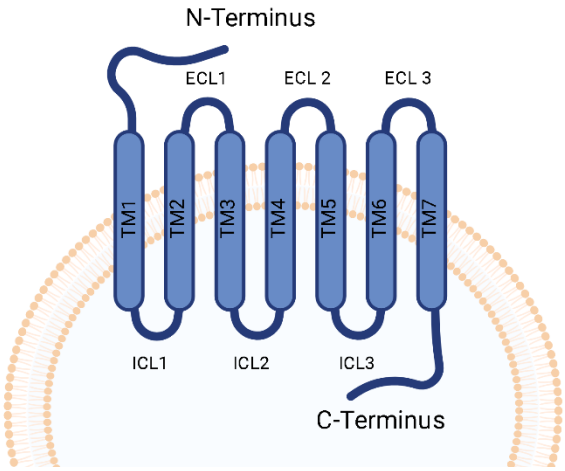

Figure 2-1 The general structure of a GPCR. GPCRs are defined by 7 conserved transmembrane regions (TM), three extracellular and intracellular loops. The N-terminus of GPCRs changes in size and peptide makeup depending on receptor classification.

Classical Signaling- The Heterotrimeric G Proteins

Heterotrimeric G proteins are the primary transducers of GPCR signaling. G proteins function as molecular switches which activate in response to ligand-induced conformational changes in GPCRs. G proteins are composed of three subunits α, ß, and γ. Unlike the diversity seen in the receptors, G proteins are a relatively small family of proteins, with 12 α, 6 ß, and 12 γ subunits[49]. Heterotrimers are divided into 4 classes based on sequence homology of the α subunit; these are $G_{s,}$ $G_{q,}$ $G_{i,}$ $G_{12/13.}$ Crystal structures of these proteins reveal a conserved GTPase domain that hydrolyzes GTP to GDP and three loops known as switches I, II, and III. All Gα subunits are post-translationally modified via palmitoylation or myristylation to allow proper trafficking and localization to the cell membranes[49]. The ß and γ subunits are a single functional unit and cannot be naturally dissociated. The ßγ subunits are bound to the hydrophobic pocket on the α subunit only when attached to a GDP and dissociate upon GTP binding. While the ßγ subunits are responsible for various downstream functions, they are not discussed in detail herein, for a comprehensive review of ßγ structure, function and signaling see Khan et al. 2013[50].

The exact coupling mechanisms of G proteins to GPCRs are not well defined. There are two opposing models of coupling; the first is the collision coupling model, which postulates interaction occurs due to lateral diffusion within the plasma membrane, allowing G proteins to interact with only activated receptors. The pre-coupling model hypothesizes that G proteins interact with receptors before agonist binding. There is data supporting and refuting both models, and it is not yet clear by which mechanism GPCRs and G proteins couple[51, 52].

The binding of a ligand to the extracellular regions of a receptor initiates downstream signaling by causing a conformational change in the intracellular domains. The change in receptor conformation leads to the exchange of GDP to GTP on the α subunit by guanine-nucleotide exchange factors (GEFs), which catalyze the exchange reaction[53]. The α subunit dissociates from the heterotrimeric complex and interacts with various effectors to cause downstream signaling followed by various signal termination mechanisms (Fig. 2.2).

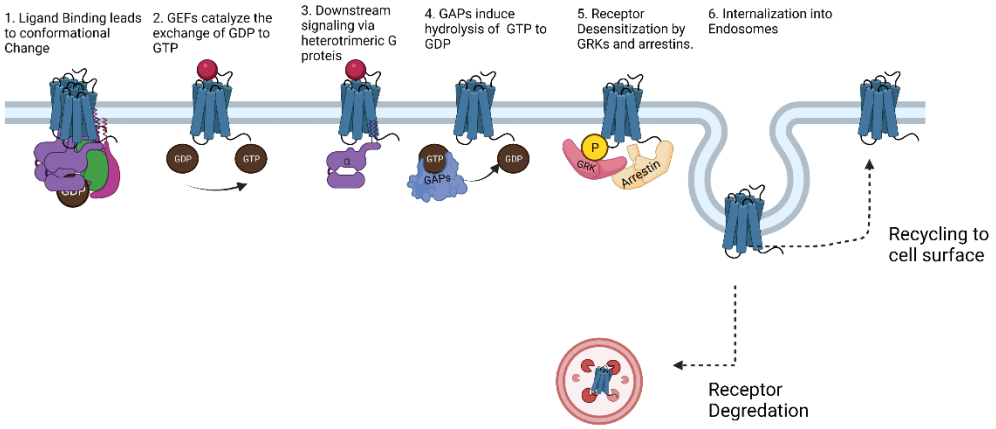

Figure 2-2 Schematic of Classical GPCR Signaling. The binding of a ligand causes a conformational change in the intracellular regions of a GPCR. GEFs will exchange a GDP for a GTP on the α subunit of the cognate G protein. The α subunit will dissociate and interact with various effectors to activate downstream signaling based on the G protein family. The GAPs will catalyze the GTPase activity of the α subunit to hydrolyze GTP back to GDP. Finally, GRKs will phosphorylate the C terminus of the activated receptor and arrestins will initiate endocytosis of the receptor.

The signaling pathways of the G protein families are well defined in the literature (Fig. 2.3). $G\alpha_q$ activates phospholipase-C ß (PLC-ß), which cleaves membrane-bound phosphatidylinositol 4,5-bisphosphate (PIP2) into diacylglycerol (DAG) and inositol 1,4,5-trisphosphate (IP3)[54]. DAG remains bound to the inner leaflet of the membrane and is an important lipid second messenger that mediates various signaling pathways, including protein kinase C (PKC). IP3 diffuses

into the cytosol and can interact with IP3 receptors (IP3R) to cause Ca^{2+} mobilization from the endoplasmic reticulum (ER).

The $G\alpha_s$ and $G\alpha_i$ signaling pathways are contrary to one another. Whereas $G\alpha_s$ activates adenylyl cyclase to increase cAMP production, $G\alpha_i$ directly inhibits adenylyl cyclase. cAMP binds the regulatory subunit of PKA, causing the release of the catalytic subunit and allowing PKA to phosphorylate downstream targets[54]. PKA phosphorylates phosphodiesterases (PDEs) to hydrolyze cAMP to 5' AMP. This negative feedback mechanism tightly regulates PKA signaling temporally and spatially.

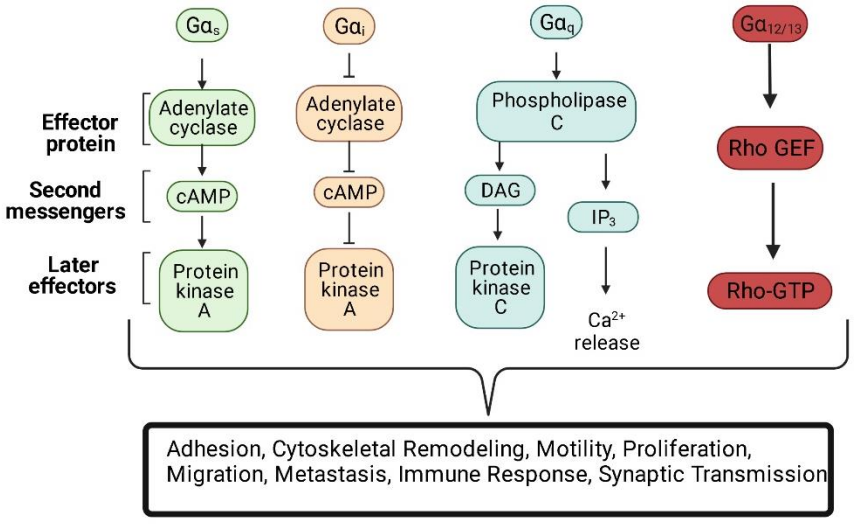

Figure 2-3 Diagram of the G protein families downstream signaling pathways.

$G_{12/13}$ is the smallest family of G proteins consisting of only G_{12} and G_{13}. These proteins were first cloned in 1991 and are challenging to study due to a series of complex overlaps between other G protein effector proteins and various other signaling networks[55-59]. Studies have found that most GPCRs that couple to G_{12} can also couple to G_{13} and vice versa, with few exceptions noted in the literature[60]. Unlike other G proteins, the effector molecules of the $G\alpha_{12/13}$ are Rho-GEFs that stimulate the exchange of GDP

for GTP on RhoA[56]. RhoA are small GTPases that regulate cellular functions, including cell adhesion, motility, and cytoskeletal rearrangements[61]. After GDP to GTP exchange on RhoA, the RhoGEFs stimulate the GTPase activity of $G\alpha_{13}$ to terminate signaling[60]. The Rho-GEFs are unique in that they function both as an effector molecule and signal terminator.

Although G proteins are GTPases and can hydrolyze GTP back to GDP, this reaction is extremely slow. The GTPase activating proteins (GAPs) (also known as GTPase accelerating proteins) accelerate the hydrolysis reaction by several orders of magnitude. GAPs show selectivity and specificity for their target G proteins, although the literature sites two opposing theories of regulation. Some studies have shown that GAPs are targeted for activation by associated G proteins, thus creating a negative feedback loop. The photoreceptor GAP, regulator of G protein signaling 9 (RGS9), is a prime example of this mechanism. RGS9 binds to cGMP PDEs, an effector in the phototransduction pathway, to enhance its activity and terminate signaling[62]. Other groups have described an inhibitory mechanism of G protein activity on its specific GAP. For example, RGS4 is a GAP with specificity to members of the G_q family of G proteins[63]. PIP3, downstream of $G\alpha_q$, binds RGS4 and inhibits its activity. Competitive binding of Ca^{2+} and calmodulin lifts the inhibition to allow GAP activation[64]. This study indicates that the inhibition of GAPs is an effect of $G\alpha_q$ early effector molecules, and the late effectors remove the inhibition to terminate signaling.

GPCR receptor kinases (GRKs) initiate the final steps of the GPCR signaling cascade by phosphorylating the C-terminus of the active receptor. While most kinases recognize their targets based on a conserved sequence, the GRKs uniquely phosphorylate

receptors based on their activation state. Studies of photoreceptors found that GRKs in the vicinity of an active receptor could phosphorylate anything accessible, including exogenous peptides[65]. These data indicate that the receptor's activation causes the activation of the proximal GRK allowing it to phosphorylate C-terminal serine/threonine residues on the active receptor[65-67]. Experiments aiming to purify GRK from protein lysates found a 40kDa protein prominently present in all extracts of phosphorylated GPCRs; this protein was later identified as ß-arrestin[68].

Four proteins make up the arrestin family, two specific to the visual system (arrestin1 and arrestin4) and two ubiquitously expressed members (ß-arrestin1 and ß-arrestin2). ß-arrestins bind to the phosphorylated form of their cognate receptors and prevent the coupling of GPCRs with their G proteins to desensitize the receptor[69]. ß-arrestins also engage clathrin to activate receptor endocytosis, which will either dephosphorylate the receptor and recycle it back to the cell surface or target the receptor for lysosomal degradation[70].

Emergent Concepts: Biased Agonism, ß-Arrestin, Intracellular Signaling, & G protein-independent functions

Over the past decade, there has been much progress in understanding GPCR dynamics, activation, and regulation, which has illuminated new concepts in GPCR pharmacology and uncovered several questions left to be answered. While the previous sections described a linear model of agonist efficacy (one ligand binds to one receptor leading to activity through a single transducer), the following section discusses the multidimensionality of GPCR-transducer complexes (i.e., receptor-G protein, receptor-ß-arrestin, transducer-independent) (Fig. 2.4).

The functionality of ß-arrestins was long-thought to be constrained to receptor desensitization by uncoupling G proteins and active GPCRs. However, new data shows ß-arrestins do not just physically obstruct the coupling of G proteins to their cognate receptors but function as membrane scaffolding proteins to inhibit the second messengers of various G protein signaling pathways. Specifically, ß-arrestins recruit PDEs and diacylglycerol kinases (DGKs) to the cell membrane to degrade cAMP (second messenger of $G\alpha_s$) and DAG (second messenger of $G\alpha_q$), respectively[71, 72]. Data also support roles for ß-arrestins in sustained G protein signaling from the endocytic pathway and G protein independent signaling[73].

After GRK-mediated phosphorylation of GPCRs, ß-arrestins interact with AP2, an adaptor protein that associates with clathrin and mediates the internalization of receptors[74]. Receptor internalization was thought to lead to signal termination followed by receptor degradation or recycling back to the cell surface. More recent data have shown sustained signaling within the early endosome prior to receptor degradation or recycling[73, 75-77]. Support for the role of the endosomes in sustained signaling came from a study of PTH-related peptide receptors (PTHR)[76]. PTHR-expressing HEK293 cells were stimulated with a PTH polypeptide, and sustained internalization corresponded with cAMP production[76]. Furthermore, immunofluorescence data showed that the PTHR, PTH peptide, and $G\alpha_s$ protein remained in a ternary complex within the endosome for the duration of the cAMP production[76]. We have uncovered a similar mechanism for ADGRG2, an adhesion GPCR, that plays an essential role in parathyroid pathology[78]. When inhibiting the endocytic pathway, we found that the total surface expression of ADGRG2 increased, but upon stimulation, the total amount of cAMP decreased. These

data indicate that a portion of the ADGRG2-mediated cAMP production is dependent on endocytic signaling[78]. Sustaining signal in the endosome has broad implications for the field, including our understanding of GPCRs and receptor biology as a whole.

ß-arrestins also scaffold proteins within the endosome to mediate G protein-independent signaling[73]. ß-arrestins trigger mitogen-activated protein kinase (MAPK/ERK) by recruiting Src family tyrosine kinases[79]. The G protein-dependent activation of ERK is transient, localized within nuclei, to promote gene transcription, whereas the ß-arrestin-dependent activation is sustained, localized within clathrin-coated structures (CCSs), and stabilized in endosomes[71, 72]. ß-arrestins can also scaffold the JNK cascade proteins, which regulate growth arrest and apoptosis. Finally, ß-arrestins exhibit receptor-dependent interactions with the phosphatidylinositol-3 kinase (PI3K) pathway. The protease-activated receptor 2 (PAR2) causes ß-arrestins-mediated inhibition of PI3K while the chemokine receptor (CCR5) actives PI3K via ß-arrestin scaffolding of various kinases[80, 81]. The interplay of ß-arrestins with GPCRs and other effector molecules is complex and still being uncovered in the literature. Several groups have identified the importance of ß-arrestins in the physiological functions of GPCRs, apart from their roles in signal termination and receptor degradation.

An essential advancement in the field has been the concept of biased agonism, which describes the ability of a single ligand to cause different signaling patterns from the same GPCR. Although structural evidence of biased agonism is lacking, the accepted hypothesis postulates that a ligand can stabilize different receptor conformations, which will, in turn, cause the formation of different receptor-transducer complexes[82, 83]. Recently, two critical studies obtained high-resolution structures of GPCRs complexed

with two different transducers but the same agonist ligand. Structures of the formoterol-bound ß$_1$-adrenergic receptor complexed with a Gα_i protein and ß-arrestin1 were resolved using cryo-electron microscopy (Cryo-EM)[84]. The iperoxo-bound M_2 muscarinic receptor structure was resolved in complex with ß-arrestin1 and Gα_i using cryo-EM[85]. These newly resolved structures show an evident change in the extracellular ligand-binding pocket based on the bound intracellular transducer.

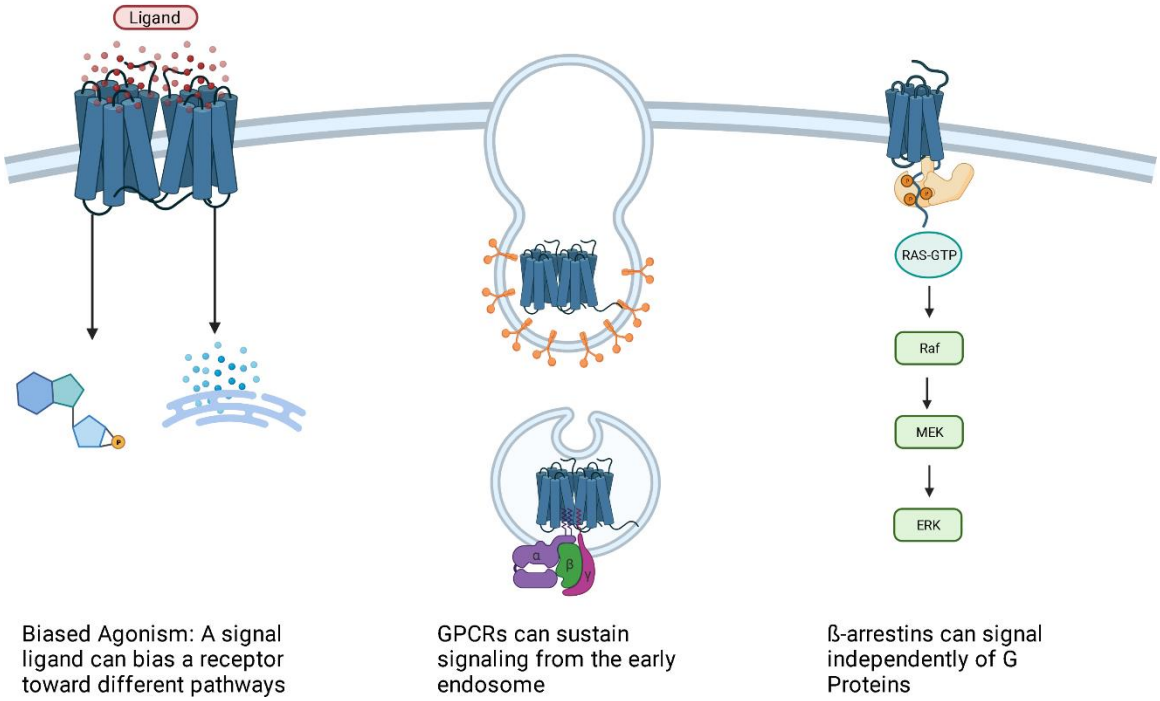

Figure 2-4 Emergent Concepts in the field of GPCRs. The discovery of biased agonism and the various role of ß-arrestins in GPCR function has altered the classical (linear) views of one ligand-one receptor-one outcome.

The exact mechanisms for how these ligands can selectively change the receptor-transducer complex are unknown, but identifying this phenomenon has important implications for future therapeutic development. Namely, the development of 'biased ligands' to selectively activate a particular signaling pathway. Further work is needed to uncover more detailed mechanisms of biased agonism, particularly the question of which

ligands produce specific responses and which responses are mediated by the various G-proteins versus arrestins.

The field of GPCR biology is rapidly expanding as technologies and techniques are developed to uncover their complex signaling networks and structures. These emerging topics in the field are slowly uncovering novel mechanisms and therapeutic targets that may lead to deeper understandings of physiology and the development of novel therapeutics.

GPCR Control of Parathyroid Function: The Calcium-Sensing Receptor.

As mentioned previously, the parathyroid glands are the primary calcium-sensing organs of the body and function to maintain serum calcium homeostasis. The calcium-sensing receptor (CaSR) is a dimeric GPCR expressed on the surface of chief cells. The CaSR expresses a large extracellular domain (ECD) which contains a venus flytrap (VFT) domain, to facilitate ligand-receptor interactions. X-ray crystallography results showed that the ECD of CaSR is heavily glycosylated and has three distinct Ca^{2+} binding sites within the VFT domain (Fig. 2.5)[86, 87]. Ligand binding causes a conformation change in the VFT, leading to downstream signaling through various cognate heterotrimeric G proteins. The intracellular and transmembrane domains of CaSR are very similar to the classic GPCR structure discussed above.

In classic stimulus-regulated secretory systems, activation leads to an increase in hormone release. The CaSR-PTH secretory pathway is unique in that the activity of CaSR causes the decrease of PTH secretion. The CaSR can couple to $G\alpha_q$, $G\alpha_i$, and $G\alpha_{12/13}$ G-proteins to initiate downstream signaling[88]. $G\alpha_q$ activates PKC, which plays a

crucial role in the proper secretion of PTH in hypocalcemic states. PKC inhibits PTH release from bovine parathyroid cells in states of hypocalcemia[89]. Furthermore, stimulating PKC using phorbol esters led to the stabilization of PTH mRNA, suggesting that PKC is essential for the synthesis and secretion of PTH[90].

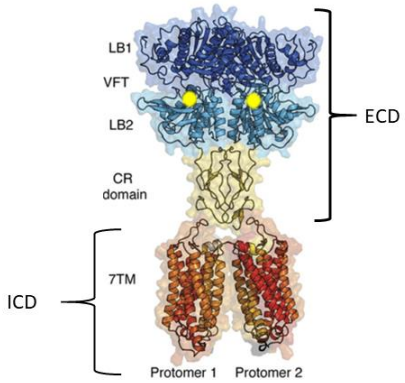

Figure 2-5- Structural representation of the CaSR homodimer.Yellow circles represent Ca^{2+} ions. The VFT Domain is made up of lobe 1 (LB1) and lobe 2 (LB2). The VFT is connected to the transmembrane region via a cysteine-rich (CR) domain. Adapted from Geng et. Al, 2016.

$G\alpha_q$ also increases intracellular Ca^{2+} via IP_3 activity on the endoplasmic reticulum (ER), which causes the release of stored intracellular Ca^{2+} and opening membrane-bound voltage insensitive Ca^{2+} channels. The increase of intracellular Ca^{2+} catalyzes the activity of PKC to decrease PTH secretion[91]. Cytosolic Ca^{2+} also plays a role in PTH transcription via a Ca^{2+} response element (CaRE), 3.6kb upstream of the *PTH* gene[92]. Finally, CaSR signaling through G_i pathways causes a decrease in cAMP, a second messenger necessary for proper PTH vesicle release.

While the exact molecular mechanisms of CaSR-mediated PTH secretion are unknown, several studies have confirmed a variety of roles for CaSR in parathyroid pathobiology. Researchers have found that slight increases in serum Ca^{2+} cause a drastic decrease in PTH release, but it is unclear whether this effect is mediated by other CaSR agonists such as polyvalent cations and various l-amino acids[93]. Patients undergoing total

parenteral nutrition (TPN) infusions containing l-amino acids have shown abnormal parathyroid activity, demonstrating that non-extracellular Ca^{2+} agonists may regulate CaSR[92]. The dimerization state of CaSR may also play a crucial role in parathyroid disease. The CaSR homodimer is the primary form of the receptor, but there is compelling evidence that CaSR also forms heterodimers with other GPCRs, although the significance of these dimers is not yet understood[93]. These studies suggest a heterogeneous function of CaSR in parathyroid cells which may explain the variability in hyperparathyroidism patients to intravenous infusion of Ca^{2+} or calcimimetic drugs[93].

IHC analysis of PHPT and other hyperplastic parathyroid tissues show a decrease in CaSR expression ranging from 30-70%, while a subset of patients show no change in CaSR expression[94, 95]. In patients with varying levels of CaSR expression, the use of a calcimimetic agent, such as cinacalcet, causes a similar decrease in PTH secretion[96]. These data suggest that CaSR expression levels alone are not responsible for dysregulated PTH levels in hyperparathyroidism patients; otherwise, the pharmacological effect of calcimimetics would vary based on CaSR levels.

There is mounting evidence supporting G-protein-independent mechanisms of CaSR activity. Activation of CaSR with increased extracellular Ca^{2+} causes the assembly of actin stress fibers and changes in cell morphology[97]. Inhibition of $G\alpha_i$ and $G\alpha_q$ in HEK-CaSR models showed no effect on CaSR's ability to alter actin polymerization and cell morphology[97]. Treatment with Rho-kinase inhibitors did attenuate the CaSR-induced actin assembly and morphological changes. These studies are of import due to the role of F-actin in the secretion of PTH from parathyroid chief cells. When treated with F-actin severing compounds, such as cytochalasin, PTH secretion increased significantly while

the stabilizing agent, jasplakinolide, decreased PTH secretion[96]. These data point to the role of CaSR-mediated actin remodeling in the inhibition of PTH-secretion.

Introduction to Adhesion G-Protein Coupled Receptors (aGPCRs).

aGPCRS are the second largest family of GPCRs consisting of 33 members with various expression patterns and functions. All aGPCRs maintain the seven-transmembrane structure common to all GPCRs and are differentiated by a large N-terminal fragment (NTF). In some aGPCRs, the NTF contains several domains, including EGF-like, cadherin, pentraxin, and leucine-rich repeats, which enable cells to interact with adhesion molecules (e.g., ADGRE5 with integrins[98]) or extracellular matrices (ECM) (e.g., ADGRG1 with collagen III[99]; ADGRG6 with collagen IV[100]). aGPCRs, except ADGRA1, contain a GPCR Autoproteolysis-Inducing domain (GAIN), which is located N-terminally to the first transmembrane domain[101]. Within the GAIN domain is a highly conserved GPCR proteolytic site (GPS) and a stretch of residues that connects GPS to the first transmembrane domain[102]. Proteolytic cleavage at the GPS during protein translation divides aGPCRs into NTF and C-terminal fragments (CTF), which remain associated via noncovalent interactions (Fig. 2.6).

Several modes of activation of aGPCRs have been proposed, some of which are unique to specific aGPCRs and cellular contexts (reviewed in detail in [103, 104]). Dissociation of NTF from CTF by an extracellular molecular partner unmasks a 15-25 amino acid tethered agonist, known as the *Stachel* peptide, that remains extracellularly on the N-terminus of CTF. Several studies have reported that NTF-truncated mutants of ADGRB2 [105], ADGRG1 [106], ADGRG2 [94, 107, 108], ADGRF1 [109], and ADGRE5 [110] show constitutive activation of downstream signaling pathways. Further studies proved that this activity is

due to the interaction of the tethered agonist with the cognate receptors. For instance, the deletion of tethered agonists in NTF-truncated ADGRD1 [111], ADGRG2 [107], and ADGRG6 [111] abolished specific signaling pathways and exogenous addition of synthetic peptides, which are identical to tethered agonists, stimulated receptor signaling [107-109, 112]. Alternative mechanisms of activation of aGPCRs exist. Unlike the receptors mentioned above, the interaction of NTF and CTF is required for proper signaling and function of ADGRC2 in the brain [113]. Moreover, circulating NTF of several aGPCRs have been reported [105, 114, 115], and the secreted NTF of ADGRB1 (Vasculostatin, a.k.a. Vstat120) showed antiangiogenic and antitumorigenic functions in glioma xenograft models [116], pointing to CTF-independent roles that NTF may play in distant or neighboring cells. To add to the complexity of aGPCR activation and signaling, recent studies have shown that while NTF and tethered agonist are required for certain signaling pathways of ADGRG1 [117], ADGRB1 [117], and ADGRG2 [107], they can be dispensable for interaction of these receptors with ß-arrestins. Together, these studies suggest that GPS, NTF, CTF, tethered agonist, and other domains of aGPCRs play various functional roles.

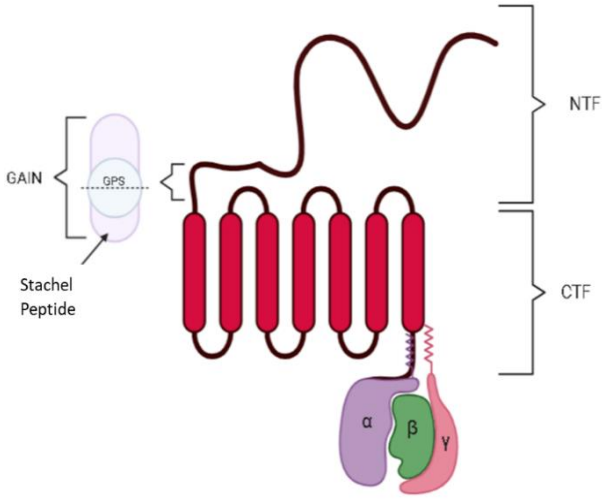

Figure 2-6 The general structure of an aGPCR. All aGPCRs, except ADGRA1, contain a GPCR Autoproteolysis-Inducing domain (GAIN) 23 that includes the GPCR proteolysis site (GPS) and a tethered agonist sequence 31. The cleavage at GPS results in a two-subunit molecule, including an N-terminal fragment (NTF) and a C-terminal fragment (CTF) that remain associated via noncovalent interactions. In some aGPCRs, NTF includes additional domains such as EGF-like, cadherin, pentraxin, and leucine-rich repeats. These domains interact with other cell adhesion molecules and extracellular matrices, by which they orchestrate the intracellular signaling.

The Emerging Role of aGPCRs in Cancer.

Multidomain NTF of aGPCRs enables cell-cell communication and cell-extracellular matrix interaction, processes that are dysregulated in cancer. Current evidence suggests that some aGPCRs regulate the cell cycle, proliferation, survival, and dissemination of cancer cells (Table 2.1). For example, knockdown of ADGRL4 reduced the proliferation of glioblastoma cells *in vitro*[118, 119]. ADGRG1 is upregulated in colorectal cancer tissues and cell lines and promotes tumor growth and metastasis via induction of epithelial to mesenchymal transition (EMT)[120]. However, in melanoma cell lines, ADGRG1 suppressed the production of vascular endothelial growth factor, a known stimulator of tumor angiogenesis, and inversely correlated with melanoma progression in mouse tissues and human melanoma xenografts [121]. Anti-growth [122] and pro-metastasis [123] roles have also been reported for ADGRG1 in melanoma studies. ADGRB1 functions as

an inhibitor of angiogenesis in pulmonary adenocarcinoma [124], glioblastoma [125], colorectal cancer [126], and astrocytoma [127]. Carcinoma-associated mutations in ADGRL1 revealed altered surface expression and exaggerated basal activity of the receptor [128]. In the era of -omics, there is now evidence of aberrant expression and mutational profile of aGPCRs in different malignancies that warrant future translational studies. Here, we review the current body of knowledge regarding the expression and function of aGPCRs in the five most common types of cancer[129].

Lung Cancer

Lung cancer is the leading cause of death and the most common cancer globally, totaling approximately 12% of new cancer cases in 2018 [130]. ADGRB3 was shown to be one of the most significantly mutated genes in 13% of lung squamous and 5% of lung adenocarcinoma tumors [131]. These mutations span the NTF, 7TM, and C-terminus of ADGRB3, and authors suggested that this protein might act as a putative tumor suppressor. This is in line with the reported anti-angiogenic and anti-neurogenic activity of other members of this subfamily, ADGRB1 and ADGRB2 [132, 133]. Currently, small cell lung cancer (SCLC) and large cell neuroendocrine lung carcinomas (LCNEC) are differentiated based on morphological analysis, which tends to be a poor determinant of the cancer subtype. Immunohistochemical (IHC) analysis of human lung tumors showed that ADGRB3 is expressed in the nucleus of a majority of SCLC samples but is either absent or expressed at low levels in the cytoplasm of LCNEC tissues [134]. The ability to use ADGRB3 staining to differentiate between SCLC and LCNEC could be of significant clinical importance. Nuclear localization and signaling of some GPCRs [135, 136] and ß-arrestins [137, 138] have been reported in HEK293 cells and tumor cells. Interestingly, the

NTF-truncated ADGRB3 was shown to interact with ß-arrestin2 [139]. Whether the nuclear ADGRB3 in SCLC cells is the activated form of the receptor that is transported to the nucleus by ß-arrestin2 requires further studies.

MicroRNAs (miRNAs) are a family of non-coding small RNAs that regulate gene expression, are dysregulated in various cancers, and are either tumor suppressors or oncogenes [140]. Down-regulation of miR-138-5p increased the expression of ADGRA2 in non-small-cell lung carcinoma (NSCLC) cell lines and patient-derived cells [141]. NSCLC patients who are treated with gefitinib, a common tyrosine kinase inhibitor, often become resistant to this drug [142]—interestingly, introducing miR-138-5p to resistant NSCLC cells down-regulated ADGRA2 and resensitized cells to gefitinib [141]. Although the endogenous ligand of ADGRA2 is unknown, this receptor has been implicated in tumor angiogenesis, a known mechanism of gefitinib resistance in lung cancer patients [141-144]. Whether inhibition of ADGRA2 by a small molecule or biologic can resensitize patients to gefitinib is yet to be explored.

Expression profiling revealed that 97 miRNAs were differentially expressed in NSCLC patients' lungs compared with normal lung tissues, of which miR-099a was one of the most downregulated miRNAs in NSCLC tissues. Expression of miR-099a in NCI-H1650, NCI-H1975, and NCI-H1299 lung adenocarcinoma cell lines reduced expression of ADGRE2 and increased cell cycle arrest and apoptosis [145]. Rescue experiments suggested that ADGRE2, a target of miR-099a, mediates NSCLC cell migration and its knockdown increases adhesion and decreases proliferation. ADGRE2 expression also correlated with ß-catenin expression [145], a known marker for EMT and metastasis in lung adenocarcinoma [146]. IHC analysis of 119 lung cancer patient biopsies revealed that

ADGRE2 is upregulated in approximately 12% of cases [145]. ADGRE2 binds to chondroitin sulfate [147], a proteoglycan that is involved in lung growth [148] and is present at elevated levels in lung tumors [149]. This evidence, combined with the fact that ADGRE2 couples to Gα15 [150], a promiscuous Gα protein that activates phospholipase Cß, provide strong grounds for the screening of small molecules that interfere with ADGRE2-mediated signaling and migration of NSCLC cells.

Insertional mutagenesis experiments, either by retroviruses or lentiviruses, have been exploited as a tool to identify genes that potentially regulate cell growth and culminate in tumorigenesis [151]. Genomic localization of proviral sequences after a retroviral screen in mice suggested that ADGRF1 is a proto-oncogene in mouse leukemia [152], which was corroborated by additional reported insertions sites [153, 154]. Lum et al. followed this proto-oncogenic indication by mRNA and protein expression analysis and found that whereas ADGRF1 expression was low in lung cancer cell lines, lung adenocarcinoma tumor samples showed upregulated ADGRF1 compared to either normal lug, squamous or small lung tumor samples [152].

Breast Cancer

Breast cancer was the second most commonly diagnosed cancer in 2018 with over 2,000,000 newly diagnosed cases [130]. Several aGPCRs show altered expression or mutation in breast malignancies[155-158]. ADGRC2 was initially shown to be down-regulated in human epidermal growth factor receptor 2 (HER2)-positive breast carcinomas [159]. Further immunohistochemical studies by the same group did not identify a significant correlation between ADGRC2 expression and either HER2 or estrogen receptor (ER) status of lung tumor tissues or cell lines [156]. However, they identified a

small group of cell lines and tumors that show striking downregulation of ADGRC2, pointing to a potential impact of this receptor in a subset of breast cancers. ADGRC2 is a member of the non-classical cadherin family of proteins due to the presence of several cadherin domains in its NTF. Interestingly, cadherins are involved in cell-cell communication and cell adhesion and E-cadherin promotes metastasis in diverse models of invasive ductal carcinomas [160-162]. Therefore, it would be interesting to know whether the deletion of cadherin domains in ADGRC2 changes the metastatic potential of breast cancer cells.

Similar to ADGRC2, localization, and expression of ADGRE2 are also correlated with breast cancer patient prognosis [163]. While ADGRE2 is not expressed in normal breast epithelial cells, invasive breast carcinomas and ductal carcinoma in situ (DCIS) showed upregulation of ADGRE2 [163]. Nuclear expression of ADGRE2 was correlated with lower tumor grades and a longer disease-free survival [163]. Since active GPCRs do not reside in the nucleus, it is possible that ADGRE2 is either activated on the cell surface and endocytosed to the nucleus or it is not shuttled to the plasma membrane after translation. Further research is necessary to define the mechanism by which ADRGE2 regulates breast cancer cell function and to confirm nuclear localization as a prognostic biomarker.

Data from the Cancer Genome Atlas (TCGA) show that 52% of patients with invasive ductal carcinoma have reduced levels of ADGRB1, which correlates inversely with patient survival [164]. This is consistent with the down-regulation of ADGRB1 in several other tumors including glioblastoma [125], colorectal [126], and lung cancer [124]. The secreted N-terminal fragment of ADGRB1 (Vasculostatin, a.k.a. Vstat120) was shown to

suppress growth in xenograft models of glial tumors [116]. Vstat120 contains an arginine-glycine-aspartate domain and five thrombospondin type-1 repeats, motifs that are known modulators of angiogenesis [165, 166]. Overexpression and consequent secretion of Vstat120 reduced the viability of various subtypes of breast cancer cell lines [164]. Injection of Vstat120-expressing virus into the brain of breast cancer-derived brain metastases (BCBM) mouse models significantly decreased the tumor size and disease burden and increased survival [164]. This experiment is of significant clinical importance because BCBM is a feature of treatment-resistant HER2-positive and triple-negative breast cancer, for which the standard of care is systemic chemotherapy and radiation with poor prognosis and low survival rates [167]. Given the antiangiogenic effects of Vstat120 and its motifs, it would be important to investigate their stability and bioavailability in mouse models of cancer. Also, the therapeutic efficacy of these molecules in combination with other current therapies warrants future research.

ADGRE5 is upregulated in MDA-MB231, MDA-468, MCF-7, and T47D breast cancer cell lines and its knockdown decreased cell growth, proliferation, and migration [158]. However, the mechanisms by which ADGRE5 regulates these cellular functions in breast cancer cell lines are mainly unknown. Independent studies have provided contradictory results whether the expression of the endogenous ligand of ADGRE5, CD55, correlates with breast cancer prognosis positively or negatively [168, 169]. This might be due to the different methods used by authors to define “high and low expression”. It is noteworthy that ADGRE5 [158] and CD55 [169] are co-expressed on the surface of MCF-7 cells. Further studies may reveal whether these receptor-ligand pairs are co-localized in breast tumor tissues as well and if deletion of either or both proteins alters the *in vivo*

manifestation of breast tumor. As elaborated in more detail later in this minireview, the expression of ADGRE5 in various epithelial carcinomas correlates with the stage and progression of the tumor.

As great strides are made in cancer treatments, there are still many patients who develop resistance to targeted therapies. Bhat et al. recently showed that several aGPCRs are expressed in cancer stem cells and anti-HER2 therapy-resistant cells. Using Aldefluor, a non-immunological fluorescent marker for stemness, Baht et al. found that ADGRB3, ADGRE2, ADGRA2, ADGRF5, and ADGRF1 are all overexpressed in cancer stem cells [155]. The only aGPCR found to be expressed in both cancer stem cells and anti-HER2 therapy-resistant cell lines was ADGRF1 [155]. Knockdown of ADGRF1 in BT747 cells decreased anchorage-independent growth, a common feature of metastatic cell lines, and reduced the mammosphere formation, suggesting a role for ADGRF1 in cancer stemness [155]. These data warrant further investigation into the downstream effects and potential targeting of ADGRF5 in HER2+ breast cancer.

Knockdown of ADGRF5 in highly metastatic breast cancer cell line, MDA-MB-231 reduced the cell migration *in vitro* and metastasis in mammary tumor mouse models *in vivo* [170]. The potential role of ADGRF5 in cell invasion was further confirmed by the ectopic expression of the receptor in less-metastatic breast cancer lines (MCF-7 and Hs578T) [170]. Activation of a well-known cytoskeletal remodeling signaling cascade, Gαq, p63RhoGEF, and small GTPases, RhoA and Rac1 was confirmed as the potential mechanism of cell motility by ADGRF5 in breast cancer cells [170]. The increased expression of ADGRF5 in human breast cancer tissues correlated with cancer metastasis

and poor prognosis [170], further suggesting this receptor as a potential candidate for breast cancer therapy.

The expression of ADGRG2 in breast cancer cell lines has been debated. Richter et al. showed low to no expression of ADGRG2 transcripts in MDA-MB-231 and Hs578T breast cancer cell lines [171]. We have also not been able to show the expression of ADGRG2 in MDA-MB231 cells at either mRNA or protein level (data not shown). However, Peeters et al. revealed the effect of ADGRG2 knockdown on migration and adhesion of these cell lines, presumably via its effect on RelB, a member of the NF-κB family [172]. Surprisingly, Peeters et al. did not provide expression data for ADGRG2 at either mRNA or protein level in either cell line. An impedance-based assay (xCELLigence) showed that ADGRG2 knockdown delays breast cancer cell adhesion but does not modulate cell proliferation [172]. Constitutive activation of the serum response element (SRE) transcription factor was dependent on the autoproteolysis of ADGRG2 at its GPS site when the receptor was overexpressed in HEK293 cells [172]. Unlike reports on the inhibitory function of NTF in ADGRG2 signaling [94, 107, 108], Peeters et al. showed that NTF plays a crucial role in the activation of both NF-κB and SRE pathways by ADGRG2 [172]. Further studies to profile the expression and localization of ADGRG2 in breast cancer cell lines and patient breast tumor-derived cells are necessary to provide a thorough understanding of its function in this disease.

Colorectal Cancer

The current standard of care for colorectal cancer (CRC), the third most commonly diagnosed cancer [129], is surgical resection, radiotherapy, and chemotherapy [173]. In recent years targeted therapies such as inhibitors of angiogenesis, immune

checkpoint, and epidermal growth factor receptor (EGFR) have turned CRC into a highly treatable disease. However, resistance due to tumor mutation and recurrence following surgery warrants further studies [174].

The expression of several aGPCRs is changed in CRC. While ADGRB1 is down-regulated in the colon mucosa of CRC patients [175], ADGRB2 is upregulated in advanced CRC [175], and ADGRE3 is upregulated in CRC biopsies of relapsed patients compared with patients who are disease-free [176-178]. In addition, expression of ADGRE1 is decreased in colon tissue biopsies of mouse models of colorectal carcinoma compared with control mice [176]. Unfortunately, these aGPCRs have no prognostic indications and no further work has been done to elucidate their mechanistic roles in CRC.

Other aGPCRs have shown more promise in laboratory and clinical settings. Analysis of three Gene Expression Omnibus (GEO) datasets and one dataset from TCGA (151 cases of CRC) revealed that ADGRA3 is down-regulated in 78% of CRC specimens and its elevated expression in 22% of the samples is associated with prolonged recurrence-free survival [179]. CRC patients with upregulated ADGRA3 showed reduced KRAS mutation, smaller tumors, and less metastasis [179]. Interestingly, gain-of-function mutations in KRAS contribute to the transition from adenoma to CRC [180] and are good predictors of resistance to EGFR therapy [174]. Overexpression of ADGRA3 in a CRC cell line (HCT116) suppressed the Wnt/ß-catenin signaling pathway, a known driver of CRC [179, 181] and down-regulated c-Myc and cyclin-D1. There is compelling evidence that KRAS mutations can cause aberrant Wnt/ß-catenin signaling, which will cause an oncogenic transformation in intestinal epithelial cells [182]. Yet, it is unclear whether there is a crosstalk between ADGRA3 and KRAS at the levels of Wnt/ß-catenin signaling.

High ADGRE5-expressing CRC cells show greater localization of ß-catenin in the nucleus, indicating activation of the Wnt/ß-catenin signaling pathway [183, 184]. Wobus et al. found that CRC cells with increased expression of ADGRE5 showed an elevated invasion and a poor clinical outcome [183-185]. Given that ADGRE5 has an observable effect on tumor cell invasion, migration, and secondary metastasis in various cancers [110, 186-188], its interactions with junctional proteins were studied. Proximity ligation and co-immunoprecipitation assays in various human CRC cell lines showed a strong interaction among ADGRE5, ß-catenin, and E-cadherin when compared to normal tissues and cell lines [189]. Malignant samples had reduced membrane-bound and increased cytoplasmic ADGRE5 [189]. These results suggest that ADGRE5 plays an important role in the regulation of cell junctions in normal colon tissue. Whether the cytoplasmic ADGRE5 is an indication of its prior activation and endocytosis in CRC cells awaits further investigation. IHC staining of various rectal adenocarcinoma tissue samples showed a strong co-expression of ADGRE5 and CD55 in the invasive front of the tumor [190]. However, cells in the center of the tumor showed little to no expression of either ADGRE5 or CD55. Patients with high ADGRE5 expression showed a less favorable prognosis, more metastatic burden, and a higher rate of clinical recurrence [190]. These data indicate that ADGRE5 and its ligand, CD55, may have a prognostic role as a biomarker in CRC.

Protein and mRNA analysis of 48 colorectal carcinoma cases showed a significant increase in ADGRF5 levels when compared with normal tissues [191]. These results were confirmed in three microarrays from the Oncomine database and IHC staining of over 90 CRC samples [191]. Patients expressing high levels of ADGRF5 showed an increase in

distant metastasis and histological differentiation [191]. Univariate analysis of these results, along with several other in-silico studies, show that high levels of ADGRF5 could act as an unfavorable prognostic indicator in CRC patients. miR-511-5p is known to be down-regulated in a variety of CRC cell lines and patients who expressed elevated levels of miR-511-5p show higher survival rates [192]. *In vitro* overexpression of miR-511-5p mimetics in CRC cells reduced proliferation and colony formation and increased cell apoptosis [192]. Interestingly, miR-511-5p binds the 3'UTR of the *ADGRF5* gene to repress its transcription, and overexpression of ADGRF5 reverses the anti-tumor features of miR-511-5p [192]. Together, these data support tumorigenic roles for ADGRF5.

mRNA, IHC, and in-situ hybridization analyses showed that ADGRG1 is highly expressed in CRC specimens [193] and colonic crypt cells [193] compared with normal gastrointestinal tissues and cells. This overexpression is intensified in mice that express progastrin, a peptide that is upregulated in CRC and other cancer cell lines [194, 195]. Jin et al. found that ADGRG1 directly interacts with progastrin to increase the proliferation rate of colonic cells and the genomic deletion of ADGRG1 increases apoptosis in the colonic mucosa and decreases proliferation in mice [194]. The increased expression of ADGRG1 predicted a worse prognosis for patients suffering from CRC [120] and knockdown of ADGRG1 down-regulated mesenchymal markers, N-cadherin, and vimentin via the PI3K/AKT pathway [120]. The current screening method for CRC is an optical colonoscopy that does not detect the early stages of cancer development. It remains to be investigated whether ADGRG1 can potentially be a less invasive diagnostic biomarker for CRC.

Prostate Cancer

There were 1,276,106 newly diagnosed cases of prostate cancer in 2018, globally. Due to the indolent nature and slow progression of prostate cancer many cases go undiagnosed until later stages of the disease. Examination of prostate cancer screenings such as prostate-specific antigen and digital rectal exam lack internal validity and have shown inconsistent results and false positives [196].

Histological analysis of a prostate tissue array derived from 36 adenocarcinoma cases revealed that ADGRE5 is upregulated in these tumors compared with normal adjacent tissues [110]. This was corroborated by the high expression of ADGRE5 in some prostate cancer cell lines (PC3 and DU145) and low expression in non-transformed prostate cells. The depletion of ADGRE5 in DU145 cells reduced the serum-induced activation of RhoA small GTPase *in vitro* and cell migration and invasion in Matrigel [110]. The described mechanism of ADGRE5-mediated migration of prostate cells is consistent with a previous study, where ADGRE5 regulated the migration of neural progenitor cells through Gα12/13 G proteins and RhoA small GTPase [197]. Mice injected with ADGRE5-depleted PC3 cells showed a significant reduction in bone metastasis but no change in tumor growth when compared with mice that were injected with parental PC3 cells [110]. In addition to ADGRE5, the increased expression of lysophosphatidic acid receptor 1 (LPAR1) has been reported in prostate cancer cells [198]. Interestingly, the ectopic co-expression of ADGRE5 and LPAR1 in LNCaP cells (an androgen-sensitive prostate adenocarcinoma) revealed that these GPCRs heteromerize and ADGRE5 potentiates the LPA-induced RhoA activation [110]. Heteromerization and crosstalk of various GPCRs and the consequent regulation of tumorigenesis and metastasis of prostate [199, 200], breast [199, 200], and glioblastoma [201] cells have been previously reported. Histological examination

indicated an association between the expression of LPAR1 and ADGRE5 in prostate cancer biopsies [110]. Together, these data suggest crosstalk between LPAR1 and ADGRE5 in prostate tumor cells. Considering that LPAR1 antagonists have not yet been approved to mitigate tumor burdens and metastasis, it would be interesting to examine whether inhibition of ADGRE5 by small molecules or specific antibodies suppresses the LPAR1-mediated metastasis.

Prostate biopsies from old subjects, which are prone to benign hyperplasia or have undiagnosed cancer, showed higher expression of ADGRF1 [152]. There is a spectrum of ADGRF1 expression among main prostate cancer cell lines; high in PC3, low in LNCaP, and negative in DU145. Histological analysis with antibodies raised against two distinct peptides from the NTF of ADGRF1 showed differential staining in prostate adenocarcinoma tissues, suggesting potential expression of different splice variants [152]. Such differential staining precluded a comparative analysis of ADGRF1 expression between benign prostate hyperplasia and prostate adenocarcinomas and emphasized the importance of relative quantification of splice variants of aGPCRs in tumors.

Gastric Cancer

Gastric cancers are the 5th most commonly diagnosed cancer in the world [130]. Aust et al. found that ADGRE5 was expressed in 44 of 50 gastric cancer biopsies [202]. Alternative splicing generates 3 isoforms of ADGRE5 that contain three, four, or five repeats of EGF domains on their NTF. Overexpression of the smaller isoform, ADGRE5/EGF1,2,5 in BGC-823 stomach adenocarcinoma cells increased their invasive behavior *in vitro* [203]. In line with these findings, orthotopic mouse models of gastric carcinoma that lacked the ADGRE5/EGF1,2,5 showed reduced metastatic spread and

tumor volume [188]. However, the full-length isoform, ADGRE5/EGF1,2,3,4,5 suppressed the invasion and increased proliferation. These studies indicate that the characteristics of gastric tumor cells may be regulated by the balance of ADGRE5 splice variants [203].

Recently, Chao et al. found that the exosomes isolated from the stomach adenocarcinoma cell lines that express wild-type ADGRE5 stimulated migration of other cells in a transwell assay [204]. This was accompanied by phosphorylation of the major signaling molecules of the MAPK pathway. Consistent with these findings, exosomes released from ADGRE5-expressing tumors increased metastasis of gastric adenocarcinomas [205]. In a footpad mouse model of aggressive gastric adenocarcinoma, Liu et al. found that tumors lacking ADGRE5 show a diminished metastasis and metastatic niche formation [205]. Exosomes isolated from SGC-L, an SGC-7901 cell-derived highly metastatic gastric cancer cell line expressing ADGRE5, were also able to increase the metastatic phenotype of tumor cells [205]. Taken together, these studies suggest that ADGRE5 increases cell proliferation and metastasis in gastric cancer via vesicle-mediated tumor cell communication and activation of the MAPK pathway.

A recent study showed that ADGRF1 mRNA and protein are significantly upregulated in tumor biopsies compared with paired adjacent normal tissues resected from 117 gastric cancer patients [206]. Patients with high ADGRF1 protein levels had shorter survival and increased recurrence after surgery compared with gastric cancer patients with low ADGRF1 expression. These data suggest that ADGRF1 may be a candidate biomarker for diagnostic purposes in gastric cancer patients. N-docosahexaenoylethanolamine (synaptamide, *a.k.a.* DHEA), a stimulant of neurite growth, was recently shown to induce cyclic AMP production via ADGRF1 [207]. It would

be interesting to know (a) whether the level of synaptamide, an endogenous metabolite ligand of ADGRF1, is altered in the gastric tumor microenvironment, (b) what the pathologic impact of synaptamide-ADGRF1 interaction is, and (c) what molecular mechanism(s) are used by ADGRF1 in gastric cancer cells.

Potential Therapeutic Approaches

Although the field of aGPCR research has seen constant growth in terms of engaged signaling pathways in the past decade, the physiological functions of these receptors are yet to be explored further. In particular, their role in all aspects of cancer, from tumor initiation to metastasis, is incompletely understood. aGPCRs are implicated in diverse diseases from diabetes to various neoplasms. However, there are currently no approved drugs targeting any aGPCRs.

The difficulty in obtaining structural information from aGPCRs has hampered the process of developing small molecules or biologics to target them. On the other hand, the large NTF and its multiple domains provide potential sites to target therapeutically. The recent discovery of an ADGRG1 antagonist [208] gives hope for the development of future small molecules with proper pharmacology to regulate the function of these understudied receptors in cancer. In addition to small molecules, antibodies against domains of the NTF can be potentially interesting modulators. Salzman et al. showed that monobodies designed for certain domains on the NTF of ADGRG1 could act as activators or inhibitors of G protein signaling [209]. It remains to be explored whether antibodies against either tethered agonist or its binding site(s) will act as antagonists.

Another theoretical approach that may modulate aGPCR function is the design of cell-permeable inhibitors of autoproteolysis, as this cleavage is required for activation of certain signaling pathways by ADGRG2 and ADGRG1 [172, 210].

aGPCRs interact strongly with ß-arrestins, particularly in the absence of NTF [107, 117]. The signaling bias of classical GPCRs towards either G protein or ß-arrestin pathways and their physiological effects have challenged the drug development [211-213]. This phenomenon should be considered in the development of aGPCR modulators too.

Fibrosis in the tumor microenvironment, a side effect of protease actions and metastasis, alters the composition of ECM dramatically [214]. Given the ECM-binding domains on the NTF of some aGPCRs, it would be interesting to examine whether these changes modulate aGPCR activity and thereby proliferation and migration of tumor cells. Also, targeting the large ECM ligands of aGPCRs to interfere with the protein-protein interaction can be a potential approach to regulate aGPCR functions in cancer.

On average, aGPCRs have 19 transcript variants with tissue-dependent expression patterns, leading to functional differences [215]. As mentioned above for ADGRF1 in prostate cancer and ADGRE5 in gastric tumors, splice variants of aGPCRs show a differential impact on tumorigenesis. Therefore, it is crucial to use the genomics/bioinformatics tools such as RNA-Seq to quantify various transcripts of aGPCRs of interest in tumor specimens at the first stages of cancer studies.

The body of evidence provided here points to fundamental roles that aGPCRs may play in the promotion or prevention of cancer and we hope this would trigger future translational studies to explore their potential as therapeutic targets.

Table 2-1 A comprehensive list of aGPCRs, their endogenous ligands, signaling pathways, altered expression, and mutation in various types of cancer.

A-Various malignant cell lines show expression of the latrophilin subfamily and its receptor FLRT3, including the brain, colorectal, kidney, blood/mast cell, liver, breast, prostate, lung, and skin tumors but the study indicated has only been done in breast cancer cell lines.

B- There is contradictory evidence regarding the expression of ADGRG2 in breast cancer. Some experiments have shown very little expression[171] while others claim a functional outcome due to ADGRG2 knockdown [172].

Subfamily	Receptor	Ligand	NTF domains	Signaling Pathways	Cancer	Expression	Disease Significance
I	ADGRL1 (LPHN1)	α-latrotoxin [216], Teneurin-2 (Lasso) [217, 218], FLRT1, 2, 3 [218, 219], Neurexin-1α, -1ß, -2ß, -3ß[220]	GAIN, LDL, OML, STR, HBD [221]	$G\alpha_q$, $G\alpha_o$ [222]	AML [223]	Decreased [223]	Overexpression of ABCB1 drug transporter [223]
	ADGRL2 (LPHN2)	FLRT3 [219]		-	Breast [A, 224], Squamous Cell Lung Carcinoma [225]	Increased [224,225]	Escape immune surveillance by activating the Tim-3-Galectin-9 pathway [224]
	ADGRL3 (LPHN3)	FLRT1, 2, 3 [219, 226], Teneurin-3 [219]		-	Breast [227]	Increased [227]	Correlated with axillary lymph node metastasis [227]
	ADGRL4 (ELTD1)	-	EGF [228], EGF-Ca [101]	-	Renal [228], Colorectal [228], HNSCC [228], Ovarian [228]	Increased [228]	Correlated with a positive prognosis in various cancers by regulating angiogenesis and vessel maturation [228]
II	ADGRE1 (EMR1)	-	EGF [229], EGF-Ca [101], GAIN [101]	-	CRC [176], AML[230]	Increased [176, 230]	Azoxymethane mouse models of CRC show increased expression of ADGRE1 [176]

Table 2.1 continued

	ADGRE2 (EMR2)	Chondroitin Sulfate B [147]		$G\alpha_{16}$ [231]	Lung [145,146] AML [230], Glioblastoma[232], Breast [163]	Increased [145, 163, 230], Localization [20]	Decreases adhesion and increases proliferation in lung cancer [145] Correlated with EMT markers [146] Associated with a more invasive phenotype [163, 232] Cytoplasmic expression correlated with worse prognosis [163]
	ADGRE3 (EMR3)	-		-	Relapsed CRC [177, 178], HCC [233], Glioblastoma[234]	Increased [177, 178, 233, 234]	Hypomethylated at CpG islands [233] Increase in invasive phenotype [234]
	ADGRE4 (EMR4)	-		-	-	-	
	ADGRE5 (CD97)	CD55 [235], α5β1 integrin [98], Chondroitin Sulfate B [147], CD90 [236]	EGF [229], EGF-Ca [101], GAIN [101], RGD [237]	$G\alpha_{12/13}$ [110]	CRC [183, 184, 189, 238], Adenocarcinoma [190], Pancreatic [239], IHC [240], Gastric [204], Breast [158], HCC [186], Esophageal [241], Glioblastoma[241], Ovarian [242], Gallbladder [243], AML [244, 245], OSCC [246], Thyroid [247]	Increased [158, 183, 186, 190, 239, 240, 242-248], Localization [189]	Poor clinical outcome and increased invasion [158, 184, 190, 238, 239, 242-249] Cytoplasmic ADGRE5 correlates with more malignant phenotype [189] Expressed only on the invasive front of rectal tumor cells [190] Biliary soluble ADGRE5 is a negative prognostic biomarker in IHC [240] Exosome-mediated

Table 2.1 continued

							proliferation [240] Correlated with tumor metastasis [186] Hypomethylated promoter [241]
III	ADGRA1 (GPR123)	-	-	-	-	-	-
	ADGRA2 (GPR124)	Glycosaminoglycans [250], WNT7 [251]	GAIN [101], HBD [101], LRR [101]	β-catenin [251]	Glioblastoma[252], Osteosarcoma [253], Urothelial Carcinoma [254]	Increased and decreased [252], Increased [254]	Alteration in ADGRA2 expression leads to altered microtubule dynamics during mitosis leading to chromosomal instability [252] Contributes to tumor angiogenesis [253] and is highly expressed in tumor vasculature [255]
	ADGRA3 (GPR125)	-	-	-	CRC [179]	Increased [179]	Correlates with increased metastasis and worse prognosis [179]
IV	ADGRC1 (CELSR1)	-	GAIN [101], Cadherin [101], EGF-Ca [101] HBD [103], Laminin/EGF [101]	Rho Kinase [256]	-	-	
	ADGRC2 (CELSR2)	-		Ca^{2+} [257]	Breast [157]	Localization [157]	Cytoplasmic localization is a negative prognostic marker in HER2+ breast carcinoma [157]
	ADGRC3 (CELSR3)	-		Ca^{2+} [257]	OSCC [258], AML [230], HCC [259], HNSCC [260]	Decreased [230, 258], Increased [259, 260]	Highly methylated in oral carcinomas [258] Increased expression

Table 2.1 continued

							correlated with poor prognosis in HCC [259] Decreased expression is correlated with better survival in HNSCC [260]
V	ADGRD1 (GPR133)	-	GAIN [101], Laminin /PTX[101]	$G\alpha_s$ [261]	Glioblastoma [262], AML [263], Gastric [264]	Increased [262, 263,] Decreased [264]	Protumorigenic role in hypoxic glioblastoma tumors [262] Associated with poor clinical outcome [263] Downregulated by lncRNA and miRNAs in gastric cancer [264]
	ADGRD2 (GPR144)	-		-	Lung [265], HNSCC [260]	Increased [260]	Frequently mutated due to benzo(a)pyrene exposure [265] Increased expression is correlated with better survival in HNSCC[260]
VI	ADGRF1 (GPR110)	Synaptamide [207]	GAIN [101], SEA [101]	$G\alpha_s$ [207], $G\alpha_q$ [109]	Lung [152, 266, 267], Prostate [152], Breast [155], ALL [268], Osteosarcoma[269], HCC [270], Thyroid [271]	Increased [152, 155, 267-269]	Various polymorphisms associated with NSCLC susceptibility [266] Knockdown decreased anchorage-independent growth in BT747 breast cancer cells [155] Prostate cancer lines express splice-

Table 2.1 continued

							variants of ADGRF1 [152] Knockdown decreased proliferation and its expression served as a prognostic marker for osteosarcoma [269] Deficiency of ADGRF1 caused a decrease in hepatocellular carcinogenesis [270] The expression can be used to distinguish papillary thyroid cancer from other thyroid malignancies [271]
	ADGRF2 (GPR111)	-	GAIN [101]	-	-	-	-
	ADGRF3 (GPR113)	-	GAIN [101], HBD [101]	-	SBNET [272, 273]	Increased [272, 273]	Increased expression in the primary SBNET and secondary lesions [272, 273]
	ADGRF4 (GPR115)	-	GAIN [101]	$G\alpha_{15}$ [150]	Lung [274]	Increased [274]	Associated with TRIMP58 methylation in lung squamous cell carcinoma, may be a prognostic marker [274]
	ADGRF5 (GPR116)	Surfactant Protein D [275]	GAIN [101], IG2 [101], SEA [101], I-SET [101]	$G\alpha_{q}$ [170]	CRC [191], Breast [170], Gastric [276]	Increased [170, 191]	Patients with high levels of ADGRF5 showed distant metastasis

Table 2.1 continued

							and poor tumor differentiation [191] Expression promotes migration, invasion, and metastasis [170]
VII	ADGRB1 (BAI1)	Phosphatidylserine [277], Matrix metalloprotease 14 [278]	HBD [101], TSP [101]	$G\alpha_{12/13}$ [117], β-Arrestin [117]	Lung [124], Glioblastoma [125], CRC [126, 175], Astrocytoma [127], Breast [164]	Decreased [88,164]	Functions as an inhibitor of angiogenesis [124-127] Decrease in expression correlates with a favorable prognosis [164] Ectopic expression of NTF decreased metastasis to the brain [164]
	ADGRB2 (BAI2)	Glutaminase Interacting Protein (GIP) [279], Furin[105]		$G\alpha_{16}$ [105]	CRC [280]	Increased [280]	Correlates with tumorigenesis and tumor growth [280]
	ADGRB3 (BAI3)	C1q-like proteins [281]	HBD [101], TSP [101], CUB [101]	-	Lung [134], Glioma [282]	Increased [134], Decreased [282]	Expression is increased in SCLC and can be used to differentiate from LCNEC [134]
VIII	ADGRG1 (GPR56)	Collagen III [100], Transglutaminase II [99, 283]	GAIN [101]	$G\alpha_{q/11}$ [284], $G\alpha_{12/13}$ [197], β-Arrestin[117]	CRC [120], Melanoma [121, 123], Prostate [285], AML [286]	Increased [120] [121] [285, 286]	Promotes metastasis by inducing EMT [120] [123] [285] Suppresses the expression of VEGF [121] The increased expression can be used to differentiate

Table 2.1 continued

							leukemic stem cells [286]
	ADGRG2 (GPR64)	-		$G\alpha_q$ [78, 287], $G\alpha_s$ [94], $G\alpha_{13}$ [107], β-Arrestin [78, 287]	Breast [B] [171, 172], ES [171], Parathyroid [94], Endometrial [288]	Increased [94, 172] Decreased [288]	Knockdown of ADGRG2 decreased cell migration [172] Promotes invasiveness and metastasis [171] Regulates PTH release by parathyroid adenoma [94] Functions as a tumor suppressor in endometrial cancer [288]
	ADGRG3 (GPR97)	Beclomethasone Dipropionate [150]		$G\alpha_o$ [150]	-	-	-
	ADGRG4 (GPR112)	-			NEC [289]	Increased [289]	A novel marker for NEC cells [289]
	ADGRG5 (GPR114)	-		$G\alpha_s$ [150]	AML [230]	Increased [230]	Consistently upregulated in AML [230]
	ADGRG6 (GPR126)	Collagen IV [100], Laminin-211 [290]	GAIN [101], CUB [101], Laminin /PTX [101]	$G\alpha_s$ [111]	Bladder [291]	Intronic Mutations [291]	The mutational burden can be a prognostic marker in bladder cancer [291]
	ADGRG7 (GPR128)	-	GAIN [101]	-	Lymphoma [292]	Gene Fusion [292]	ADGRG7 fused with TRK fused gene (TFG) in lymphoma tumors [292]

Table 2.1 continued

IX	ADGRV1 (GPR98)	-	GAIN [101], EPTP [101], Laminin /PTX [101], CALX-ß [101]	$G\alpha_i$ [293], $G\alpha_s$ [294], $G\alpha_q$ [294]	CRC [295]	Increased [295]	Inhibition by miR-145 sensitizes cells to Oxaliplatin [295]

Discussion

The field of aGPCRs and our understanding of their functions in cancer biology is rapidly growing. To date, some of the most robust evidence for aGPCRs in neoplastic conditions include the role of ADGRE5 in paclitaxel resistance and its role as a prognostic biomarker for various tumors[242]. *In-vitro* results show that ADGRE5 is downregulated by administering troglitazone in human thyroid cell lines, which indicates clinical trials studying ADGRE5 as a therapeutic target may be necessary[296].

Due to their membrane localization and diversity of function, GPCRs are good pharmacologic targets, but as of 2019, only ~15% of known GPCRs are approved therapeutic targets[297]. More than 30% of non-olfactory GPCRs are orphans, meaning their endogenous ligands are unknown, and that is the primary reason for the under-representation of these receptors are drug targets. Approximately 35% of all FDA-approved drugs target GPCRs, but there are currently no approved drugs for aGPCRs, although they have long been recognized as suitable therapeutic targets. Some significant challenges facing aGPCR therapeutics are the lack of data regarding endogenous ligands, downstream signaling, cellular localization, tissue expression, and structure. With the advent of several new techniques to dissect the various aspects of aGPCRs much progress has been made to uncover the varied roles of these receptors in disease. Several studies

described above show promising results for studying and targeting aGPCRs in various cancer modalities.

The following experiments investigate ADGRG2 and aim to study its role in parathyroid neoplasms using transgenic mice and novel cell lines.

Chapter 3 – Evidence of CaSR-Modulating Molecules Recapitulating PHPT Phenotypes in Transgenic Mice

Introduction- RGS5

Using a transcriptomic approach our lab sought to identify modifiers of CaSR function. We identified the regulator of G protein Signaling 5 (RGS5) as differentially expressed in the parathyroid glands. RGS5 is a GTPase activating protein, which has previously been shown to terminate $G\alpha_q$ signaling[298]. CaSR signals via $G\alpha_{q,}$ therefore we hypothesized that the overexpression of RGS5 may play an essential role in modulating CaSR sensitivity to extracellular Ca^{2+} levels.

Our experiments found that RGS5 is selectively upregulated in parathyroid tumors where it inhibits CaSR function[33]. RGS5-null mice displayed decreased levels of PTH, which was indicative of CaSR activation[299]. To further test the ability of RGS5 to modulate the activity of CaSR, we generated a transgenic mouse that overexpressed RGS5 selectively in the parathyroid glands. This transgenic mouse model recapitulated both biochemical and bone PHPT phenotypes. Both male and female transgenic mice showed elevated PTH levels at 6 and 12 months, but only the male mice showed a significant increase in serum Ca^{2+} levels after 12 months (Fig. 3.1 A-D)[33]. We analyzed the levels of CaSR expression and parathyroid size via immunohistochemistry and found that the size of the parathyroid glands increased in the transgenic mice while there were no changes in total CaSR expression between control and transgenic mice (Fig. 3.1 E-F)[33]. The recapitulation of PHPT phenotypes in transgenic RGS5-overexpressing mice supports our hypothesis that PHPT phenotypes may be caused by modifiers of CaSR signaling rather than decreased CaSR expression.

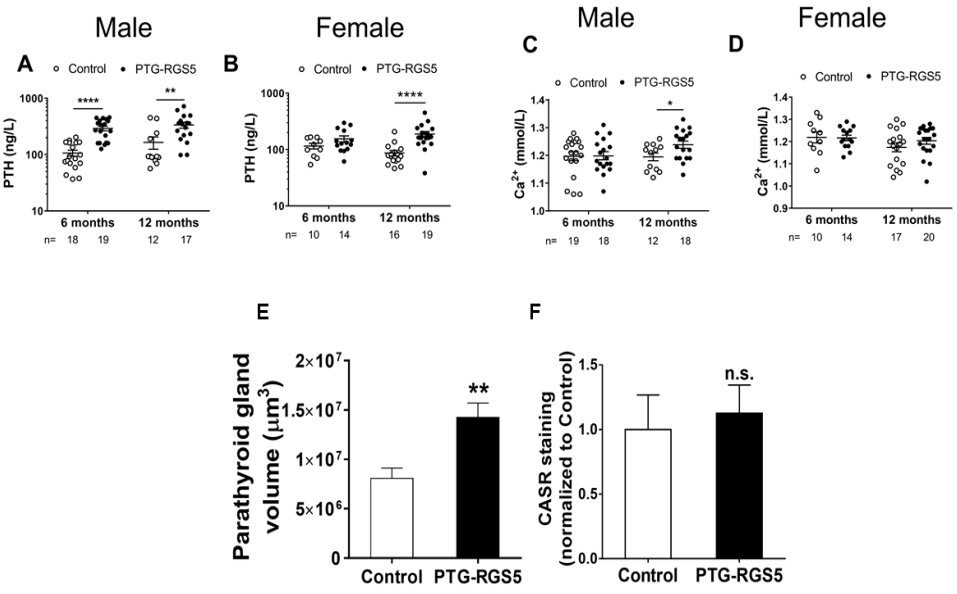

Figure 3-1- Parathyroid overexpression of RGS5 in a transgenic mouse model recapitulates PHPT phenotypes. A-B) PTH levels are increased in RGS5 overexpressing mice at 6 and twelve months. **C-D)** Serum Ca^{2+} levels are significantly increased in male mice after 12 months, but no difference is seen in female mice. Data are mean ± SEM. A nonparametric Mann-Whitney t-test was used for the analysis of A-D. *P < 0.05, **P < 0·01, ****P < 0.0001. **E)** Overexpression of RGS5 causes increased parathyroid gland volume. **D)** IHC quantification of CaSR expression shows no difference in CaSR expression in RGS5 transgenic mice.

ADGRG2

In 2015 our lab identified ADGRG2 in an RNA transcriptome screen which showed a ten-fold enrichment of ADGRG2 expression in parathyroid glands compared with a normal reference (Fig. 3.2)[94]. Furthermore, all the other genes in the RNA transcriptome screen were well characterized in various aspects of parathyroid development and function, which led us to hypothesize a significant role of ADGRG2 in parathyroid glands. To determine whether ADGRG2 played a role in parathyroid neoplasia, we conducted quantitative polymerase chain reactions (qPCR) and immunohistochemistry staining (IHC) to measure ADGRG2 expression in parathyroid tumors and normal glands (Fig. 3.2B and 3.3A). We found that ADGRG2 is significantly upregulated in parathyroid

adenomas compared to normal parathyroid glands. Due to its membrane localization, parathyroid enrichment, and lack of known function, we concluded that ADGRG2 may play an essential role in the biology of parathyroid adenomas and may serve as a potential therapeutic target.

ADGRG2 was first identified in a screening of human epididymal cDNA library in 1997 and was initially named human epididymis-specific protein (HE6)[300]. Initial studies

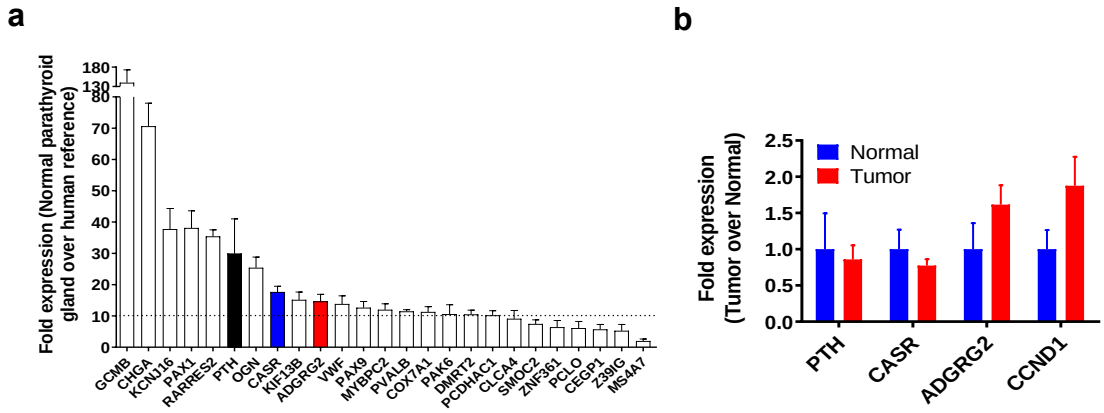

Figure 3-2 Transcriptome screening identified ADGRG2 as highly enriched in parathyroid tissue.**A)** We performed an RNA transcriptome screen to identify molecules that may modulate CaSR function in parathyroid cells. We compared RNA transcripts derived from normal parathyroid tissues to a human reference and found ADGRG2 differentially enriched 10-fold in the parathyroid glands. **B)** We also compared the expression of ADGRG2 transcripts in normal parathyroid glands and parathyroid tumor cells and found a 2-fold increase of ADGRG2 in tumors.

concluded that the expression of HE6 was restricted to the efferent ductules and the initial segment of the epididymis. Further studies found the HE6 transcript encoded a GPCR, and the HUGO Gene Nomenclature Committee then renamed this receptor GPR64. In 2015 the International Union of Basic and Clinical Pharmacology (IUPHAR) created a uniform nomenclature for all 33 members of the aGPCR subfamily[101]. Currently, this receptor is known as ADGRG2. Seven years after the initial discovery, the first hypothesized function of this protein was advanced by Davies et al. (2004)[301]. They found that targeted deletion of murine HE6 resulted in male infertility via dysregulation of fluid reabsorption within the epididymal ducts[301]. Unfortunately, due to the

technological limitations of the time, not much else was discovered about this receptor until the 2010s.

Based on sequence homology, researchers identified ADGRG2 as a GPCR that maintained the classic 7TM structure and a large NTF, common to all members of the aGPCR subfamily. Furthermore, this receptor's activation mechanism is via the autoproteolytic cleavage of the NTF and interactions of the *Stachel* peptide described above.

ADGRG2, like most aGPCRs, is an orphan receptor meaning its endogenous ligand is unknown. The lack of ligands was a significant hurdle to studying this family of GPCRs as there was no way to activate this receptor exogenously. Demberg et al., in 2015, synthesized the 15-amino acid *Stachel* peptide of ADGRG2 and used it to stimulate ADGRG2 signaling[108]. Activation using the synthetic *Stachel* lead to downstream $G\alpha_s$ signaling and cAMP accumulation. This seminal work allowed researchers to exogenously manipulate this receptor for the first time, overcoming one of the most significant challenges to understanding its biology.

To study the activity of ADGRG2 in parathyroid biology, our lab synthesized the *Stachel* peptide of ADGRG2, called P15. Using primary human parathyroid tissue, we dissociated cells and incubated with various doses of P15 and found that ADGRG2 activation in human adenoma cells leads to an increase in PTH release from these cells seeded in low and normocalcemic conditions but not hypercalcemic conditions (Fig.3.3B)[94]. These data provided compelling evidence that ADGRG2 is involved in PHPT disease and may serve as a mechanism for increased PTH secretion in these tumors.

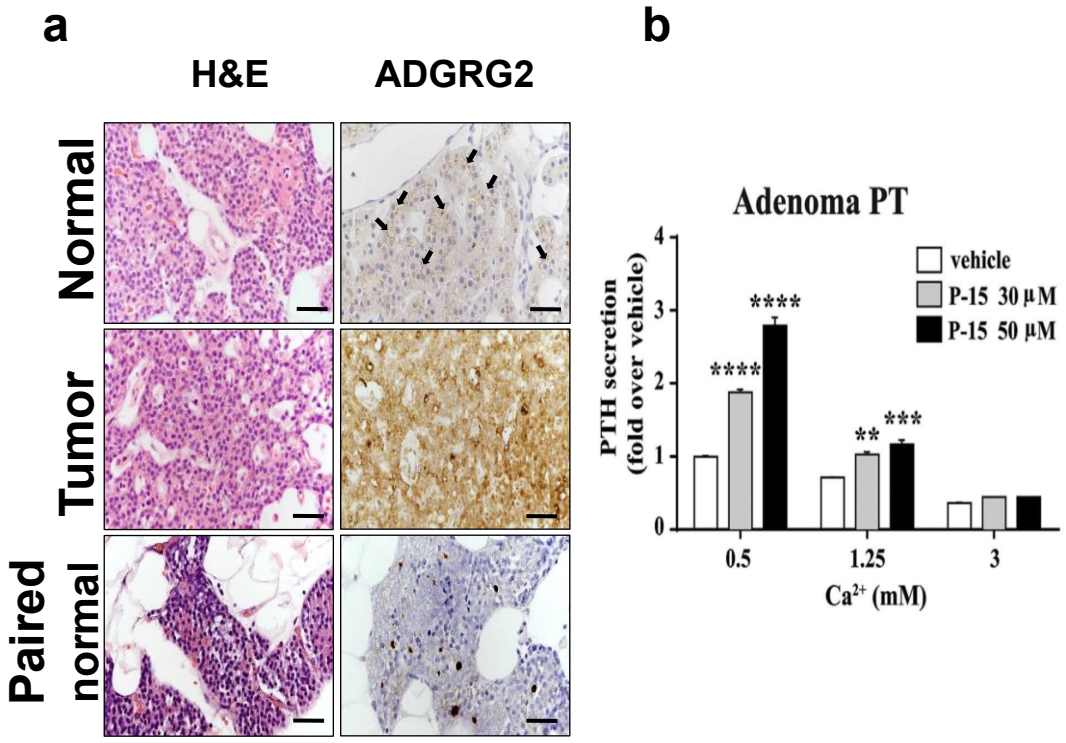

Figure 3-3 Activation of ADGRG2 in human parathyroid cells causes an increase in PTH release. A) ICH and H&E staining of normal parathyroid glands show low total ADGRG2 expression. Tumor cells show diffuse overexpression of ADGRG2 and a normal gland from the same patient show very little ADGRG2 staining indicating that overexpression is restricted to tumor cells. **B)** Primary parathyroid tumor cells were dispersed and seeded in 3 Ca^{2+} conditions followed by stimulation with P15. PTH secretion was measured using ELISA. Activation of ADGGR2 caused a significant dose-dependent increase in PTH secretion in the .5mM and 1.25mM Ca^{2+} conditions. The 3mMM Ca^{2+} overcame the Ca^{2+} insensitivity, as expected in PHPT patients.

ADGRG2 overexpressing transgenic mice develop PHPT phenotypes

We have developed a transgenic mouse strain with a parathyroid-restricted expression *of adgrg2* (Fig. 3.4a). Successful integration of the targeting construct into the murine H11 locus was confirmed by PCR to demonstrate the presence of the transgene. The *adgrg2* transgene and cloning junctions were sequenced in their entirety in genomic DNA from transgenic founder animals. Amplification with the $adgrg2^{l/fl}$ primer pair produces a 623 bp amplicon (Fig. 3.4b). This result confirms that *adgrg2* is inserted into this conditional model for parathyroid tissue-specific expression following crossbreeding

to *PTH-Cre* mice. To demonstrate Cre-dependent excision of the *STOP* sequence and expression of ADGRG2, we transduced lung fibroblasts derived from *adgrg2*$^{fl/fl}$ and WT littermates with a CRE-expressing lentiviral construct. We detected ADGRG2 protein in *adgrg2*$^{fl/fl}$ lung fibroblasts transduced with Cre, but not lung fibroblasts derived from WT or PTH-Cre mice (Fig. 3.4c).

We then aged transgenic *adgrg2*-overexpressing mice for seven months and tested their serum Ca^{2+} and PTH levels. Mice with parathyroid targeted overexpression of ADGRG2 were compared to *adgrg2*$^{fl/fl}$ mice that were not crossed with PTH-CRE. ADGRG2 overexpression caused a significant increase in serum Ca^{2+} levels compared to *adgrg2*$^{fl/fl}$ mice (Fig. 3.4d) (P-value= .0265, N=10). The slight elevation in serum Ca^{2+} caused a significant increase in PTH-release (Fig. 3.4e) (P-value= .0382, N=11). The drastic change in PTH resulting from slight changes in serum Ca^{2+} is common to parathyroid physiology and accurately recapitulates PHPT. Bone µ-CT analysis showed no significant bone phenotypes at 7 months (Supplemental Fig 3.1).

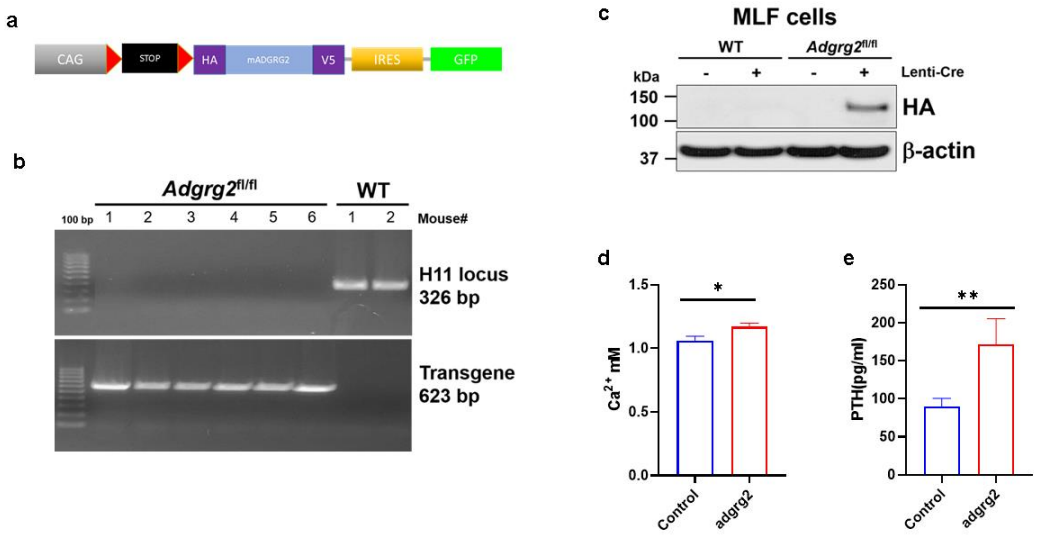

Figure 3-4 Parathyroid targeted overexpression of ADGRG2 recapitulates biochemical phenotypes of PHPT in a transgenic mouse model. A) To overexpress *adgrg2* in a transgenic mouse we employed a cre-lox system. *adgrg2* was cloned downstream of a floxed STOP codon and tagged with HA on the N-terminus and V5 on the C terminus. **B)** PCR confirmation showed the insertion of the transgene within the H11 locus. **C)** MLF cells collected from *adgrg2*$^{fl/fl}$ mice were collected and transduced with a lentivirus expressing cre recombinase. The cre recombinase successfully cleaved the STOP codon in the *adgrg2*$^{fl/fl}$ mouse which caused the expression of ADGRG2. **D)** Serum Ca^{2+} and **E)** PTH were significantly elevated in heterozygote adgrg2 overexpressing mice.

Discussion

Data generated using a transgenic mouse that overexpresses ADGRG2 in the parathyroid glands showed a recapitulation of PHPT phenotypes. After seven months, transgenic mice developed parathyroid gland neoplasia and marked hypercalcemia and hyperparathyroidism. These data implicate ADGRG2 as a modifier of the CaSR function. Analysis of bone phenotypes using µ-CT yielded no significant results (Supplemental Fig. 3.1). Based on our previous studies of RGS5 overexpressing mice, we believe that the lack of bone phenotypes is due to the mice's age. We have previously observed the onset of bone phenotypes after one year of aging. In future studies, we will age the ADGRG2-overexpressing mice for at least one year to determine if changes in bone morphology occur at the latter stages of PHPT development. Furthermore, homozygous expression of *adgrg2* was embryonically lethal. Therefore, we conducted these

experiments using heterozygote *adgrg*$^{fl/+}$ mice. This variable may have also contributed to the lack of bone-phenotype in *adgrg2* mice compared to the homozygous *RGS5* mice.

We have successfully recapitulated PHPT phenotypes in two transgenic mouse strains by overexpressing ADGRG2 or RGS5. Together, these experiments lend credence to our hypothesis that aberrant Ca^{2+}-sensing in PHPT is a product of CaSR-modulating molecules. Understanding the mechanisms of how these molecules interact with and modulate CaSR signaling will be essential to building a complete understanding of the underlying biology of PHPT. The explicit role of ADGRG2 in modulating PTH secretion in primary human cells and the development of PHPT in mice is the precedent for studying CaSR-ADGRG2 crosstalk.

Supplemental Figures

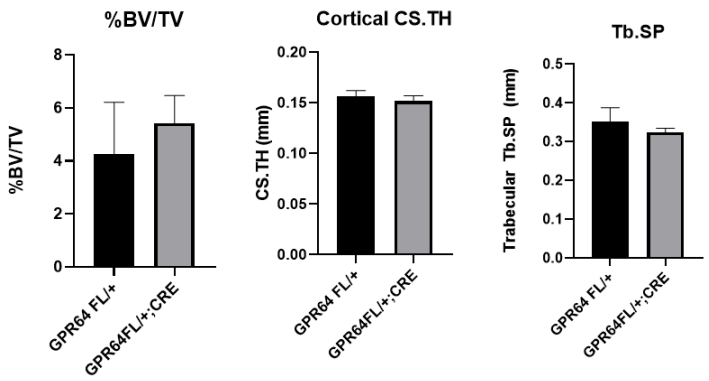

Supplemental Fig 3-1- µCT analysis of *adgrg2* mice showed no significant changes at 7 months.

BV/TV: Bone volume/Trabecular volume

CS.TH: Cross-sectional thickness

Tb.Sp: Trabecular Separation

Chapter 4 - ADGRG2 Modulates Calcium-Sensing Receptor Signaling and Intracellular Trafficking in a Stable HEK293 Cell Model

Abstract

ADGRG2 is an adhesion G protein-coupled receptor (aGPCR) differentially expressed in epididymal and parathyroid tissue. ADGRG2 is overexpressed in parathyroid adenomas, and activation in primary parathyroid cells causes an increase in PTH secretion. Parathyroid adenoma cells express a CaSR that is insensitive to extracellular calcium, leading to an abnormal increase in PTH and serum calcium levels. The mechanisms of CaSR insensitivity are poorly understood. Previous experiments using a transgenic mouse that overexpressed ADGRG2 in the parathyroid glands showed a recapitulation of PHPT. Therefore, we hypothesized that ADGRG2 plays a role in inhibiting CaSR signaling in parathyroid adenomas. We generated a HEK293 cell model which stably expresses ADGRG2 and CaSR to dissect the crosstalk of these two receptors. We found that simultaneous activation of ADGRG2 and CaSR decreased CaSR $G\alpha_q$ and $G\alpha_i$ signaling. SNAP and CLIP tagged ADGRG2 and CaSR constructs were used to monitor the trafficking of these receptors in live cells. We found that the activity of ADGRG2 led to an inhibition of CaSR internalization. These results collectively indicate that ADGRG2 plays an important role in inhibiting CaSR signaling and trafficking and is an essential modulator of CaSR function in parathyroid adenomas.

Introduction

The parathyroid glands are primarily responsible for sensing changes in serum Ca^{2+} concentration and secreting parathyroid hormone (PTH). PTH acts at various organ systems to increase serum Ca^{2+}, acting as a negative feedback mechanism to inhibit further PTH secretion. The CaSR is expressed on parathyroid cells and is primarily responsible for sensing serum calcium levels. In normal or elevated serum Ca^{2+} conditions, CaSR signals through $G\alpha_q$ and $G\alpha_i$ pathways to inhibit PTH release[93]. PHPT patients present with an adenomatous tumor on one or more of their parathyroid glands causing dysregulation of the calcium-PTH feedback loop. Parathyroid tumor cells show a decrease in calcium sensitivity which causes excess PTH secretion and elevated serum calcium levels.

Initially, calcium-insensitivity of parathyroid tumors was thought to be due to decreased overall CaSR expression[30, 302]. We have previously shown, along with other groups, that a subset of PHPT tumors do not show any significant alterations in overall CaSR expression[32, 94]. Our previous data provide strong evidence that CaSR insensitivity is due to other modulatory proteins expressed in parathyroid tumors. In support of this notion, transgenic mice that overexpress the regulator of G protein signaling 5 (RGS5) exclusively in the parathyroid glands develop PHPT phenotypes, including calcium-insensitive tumor formation and decreases in bone density[33].

We identified ADGRG2 using a transcriptome screening approach in parathyroid tissue and confirmed its overexpression in tumors[94]. We also found no significant alterations in CaSR expression compared to normal parathyroid tissue[94]. Stimulating dispersed parathyroid cells with P15, a synthetic peptide agonist for ADGRG2 caused

significant increases in PTH secretion[94]. We also found that the expression of a mutated constitutively active ADGRG2 physically interacts with CaSR in an in-vitro model[94]. Finally, we have successfully recapitulated PHPT phenotypes in transgenic mice that overexpress ADGRG2 in the parathyroid glands (unpublished data). These data point to a significant role of ADGRG2 in PHPT development and diseases progression.

We employ kinetic signaling assays to generate a complete view of ADGRG2 and CaSR signaling and crosstalk (Fig. 4.1A). Our previous studies into the activity of ADGRG2 used a mutated ADGRG2 receptor which showed constitutive activity[5, 7]. When transiently transfecting the wild-type ADGRG2 receptor, we found low activity in response to P15 stimulation. A stable cell line expressing the unaltered ADGRG2 showed a significant response to P15 stimulation. Therefore, we generated a novel stable cell line expressing ADGRG2 and CaSR to dissect their crosstalk in a more representative model.

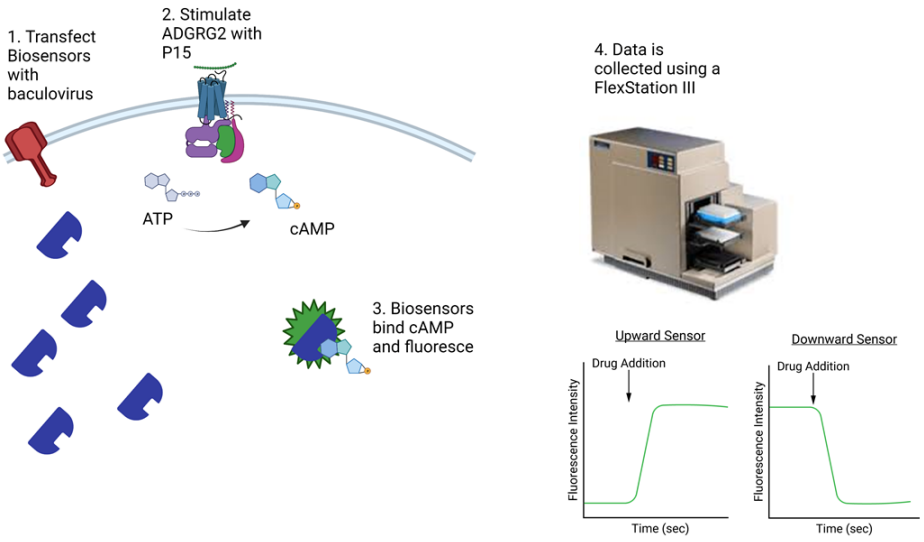

Figure 4-1 Diagram of the kinetic signaling assays used to dissect GPCR signaling. Using a baculovirus, we transduce cells with a cAMP biosensor. This biosensor can increase or decrease fluorescence in response to stimulation, allowing for live monitoring of receptor activity.

Additionally, our previously published results are endpoint assays limited in temporal resolution[6].

The intracellular activity of various GPCRs is an emerging topic in the field, with several receptors showing endosomal signaling activities are necessary for physiological signaling. Several groups have reported sustained CaSR endosomal $G\alpha_q$ signaling as a hallmark for proper activity[303, 304]. Patients who suffer from familial hypocalciuric hypercalcemia (FHH3) present with increased serum Ca^{2+} and PTH, similar to PHPT. FHH3 patients express a mutation in AP2σ, a necessary protein for proper endocytosis of CaSR, leading to decreased CaSR intracellular signaling[303]. The AP2σ mutations are not generally present in PHPT patients, but we hypothesized that ADGRG2 might function to dysregulated proper CaSR trafficking leading to a similar phenotype.

Methods

Cell culture and transfection

Adherent HEK293 cells were purchased from Agilent Technologies (Santa Clara, CA, USA #240085) and cultured in DMEM media (Sigma, St. Louis, MO, USA #D6429) supplemented with 10% FBS, 100 U/mL penicillin, and 100µg/mL streptomycin (Thermo Fisher Scientific, Waltham, MA, USA #15140-122). Cells were transfected with plasmids using lipofectamine 2000 reagent (Thermo Fisher Scientific #11668019) following the manufacturer's instructions. Stable cell lines were cultured in DMEM supplemented with 100 U/mL penicillin, 100 µg/mL streptomycin, and .5 mg/ml hygromycin B or zeocin.

Antibodies

Antibodies were purchased from the following sources: Cell Signaling Technologies (Beverly, MA, USA): rabbit anti-HA (#3724), mouse anti-FLAG (#8146); Sigma: rabbit anti-ß-actin (#A2066)

On-Cell ELISA

Cells were seeded in 96 well plates and allowed to grow to confluency; cells were starved overnight using DMEM (Thermo Fisher Scientific #21068028) supplemented with glutamine and 1.25mM Ca^{2+}. Cells were then fixed with 4% paraformaldehyde for 15 minutes at room temperature. After 3 washes with TBS, cells were blocked for 30 minutes in TBSM (TBS + 3% milk) for surface staining. We then incubated the cells with either rabbit anti-HA (1:2000) or mouse anti-FLAG (1:2000) antibodies in TBS supplemented with 3% bovine serum albumin (BSA) for 2 hours at room temperature. Cells were washed 3 times with TBS then incubated for 1 hour with 1:2000 dilution of either horseradish peroxidase (HRP)-linked horse anti-mouse IgG (Cell Signaling Technologies #7076) or HRP-linked goat anti-rabbit IgG (Cell Signaling Technologies #7074) antibodies in TBSM. After 5 washes with TBS, cells were incubated with 3,3',5,5'-Tetramethylbenzidine (TMB) (Sigma #t0440) for 5 min at room temperature. An equal volume of 1N HCl terminated the reaction. Absorbance at 450nm was measured using a FlexStation III plate reader.

Western blotting

Protein lysates were boiled with reducing sample buffer (Thermo Fisher Scientific #NP0007 and #NP0009) for 10 minutes and loaded on 4-12% Bis-Tris gels (Thermo Fisher

Scientific #NP0336BOX), then transferred to polyvinylidene fluoride (PVDF) membranes. Blots were blocked in TBSTM (TBS + 0.1% Tween-20 + 10% nonfat dry milk) followed by incubation with primary antibodies in TBSTM (1:2000 for HA and FLAG; 1:500 for ß-actin), overnight at 4°C. We incubated PVDF membranes with HRP-linked horse anti-mouse IgG and HRP-linked goat anti-rabbit IgG antibodies (1:5,000) in TBSTM for 2 hours at room temperature. Blots were washed and then developed with ECL SuperSignal™ West Femto substrate (Thermo Fisher Scientific #34095). Blots were imaged separately via an auto-exposure option to avoid image saturation.

Immunofluorescence staining and imaging

Experiments were conducted on a Nikon Ti2E microscope with Nikon analysis software (NIS-Elements AR 5.21.03 64-bit) at room temperature. Fluorescent time-series imaging was initiated for 151 frames in 5 minutes, and images were collected every 2 seconds using a 60X objective. Images were exposed for 500 milliseconds with 2304 x 2304 pixels at a spatial scale of 1.63µm/pixel. Fluorescence intensity analysis was performed in NIS Elements and plotted using GraphPad Prism.

cAMP production assays

Cells were resuspended in DMEM + 10% FBS and were mixed with either Upward or downward Green cADDis cAMP Assay Kit BacMam sensor (Montana Molecular, Bozeman, MT, USA #U0200G), supplemented with 2mM sodium butyrate. Cells were then seeded at 25,000 cells/well in black, clear-bottom, 384-well plates (25µl/well), incubated for 30 min at room temperature in the dark, and then at 37°C for 24 hours. Cells were washed with assay buffer (HBSS; Thermo Fisher Scientific #14065056 supplemented

with 20mM HEPES) and kept in the dark to acclimate to room temperature for 1 hour in 100 µl/well of assay buffer. For upward sensor experiments, cAMP production was recorded for 300 seconds, including 20 seconds of basal measurement of fluorescence (Ex:488nm, Em: 525nm) using the FlexStation III plate reader. For downward sensor experiments, cells were treated with forskolin to increase cytosolic cAMP levels, and after 10 minutes, cells were treated with P15 and Ca^{2+} alone or in combination. 20 seconds of baseline recording were collected (Ex:488nm, Em: 525nm) followed by 10 minutes of FSK treatment and 5 minutes of agonist stimulation. All data were corrected to baseline fluorescence to account for differences in transduction efficiencies across cell lines.

Intracellular calcium mobilization assay

Intracellular Ca^{2+} release was measured using a Flou-4 direct calcium assay kit (Thermo Fisher Scientific, #F10471). Cells were seeded in a black clear-bottom 384-well plate and starved in 12.5µl of DMEM supplemented with L-glutamine and .5mM Ca^{2+} for 6 hours. Cells were then loaded with Flou-4 Direct fluorescent calcium indicator prepared in assay buffer (Hank's balanced salt solution [HBSS] [without Ca^{2+} and Mg^{2+}] + 0.1mM Ca^{2+} + 20 mM HEPES + 2.5 mM probenecid at pH 7.4) for 1 hour at 37°C. P-15, Ca^{2+}, and vehicle controls were prepared at various concentrations in assay buffer. After a 20-seconds baseline reading, P15 was dispensed on a cell plate, and changes in fluorescence intensity were measured for 3 minutes, followed by the addition of Ca^{2+} and 100 seconds of fluorescence measurements in a FlexStation III plate reader (Molecular Devices).

Confocal Live Imaging

All confocal imaging was conducted on an Olympus FV-1000 confocal at a 40x magnification. Images were acquired every 1.6 seconds for a total of 6 minutes. 37 baseline images were collected, followed by the addition of 50ul of either agonists or DMSO control. All images were analyzed in ImageJ.

Results

Generation of a double expressing HEK293-ADGRG2-CaSR Cell Line

To generate a double expressing ADGRG2-CaSR cell line (FL-CaSR), we transfected stable ADGRG2 cell lines with a FLAG-tagged CaSR construct and serially diluted the cells in the appropriate selection markers. Western blot analysis of candidate cell lines confirmed the total expression of both receptors (Fig. 4.3a). We performed on-cell ELISA and immunofluorescence staining to confirm both receptors' surface expression. The surface expression of both receptors was comparable to single-expressing stable cell lines (Fig. 4.3 b,c). To validate the signaling activity of ADGRG2, we conducted a kinetic signaling assay using a genetically encoded cAMP biosensor. We stimulated ADGRG2-FL and FL-CaSR cell lines with 50μM P15, after a 20-second baseline reading, and found the ADGRG2 receptor in the FL-CaSR cell line signals just as robustly as the single-expressing cell line (Fig. 4.3d). To confirm the activity of the CaSR, we conducted an intracellular calcium mobilization assay and found no difference in CaSR activity between single and double-expressing cell lines (Fig. 4.3e). These data confirmed the expression, surface localization, and activity of the FL-CaSR cell line.

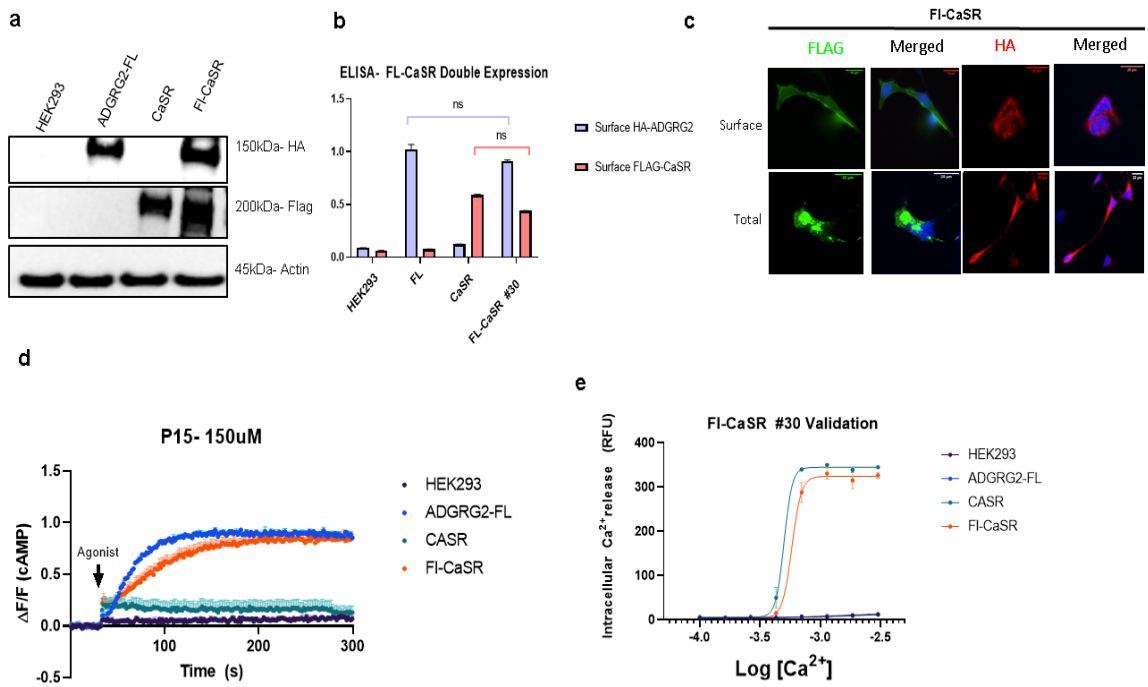

Figure 4-2 Double-expressing HEK-ADGRG2-CaSR cell line recapitulates both surface expression and downstream signaling patterns. A) Representative blots show N-terminal tagged HA and FLAG on ADGRG2 and CaSR, respectively, in total cell lysates. **B)** Cell surface expression of both receptors was determined using ELISA in nonpermeabilized conditions. Data are mean ±S.E.M from a representative experiment of 4 independent experiments performed in triplicate. Data were compared to FL-CaSR#30 using a 2-way ANOVA with Dunnett's test. Ns: not significant. **C)** Immunofluorescence imaging using antibodies against N-terminal tagged FLAG and HA tag in both permeabilized and nonpermeabilized conditions show both total and surface expression of ADGRG2 and CaSR (Counterstaining with DAPI). Representative of images from 3 independent experiments. (Scale bars: 20µm). **D)** To measure the activity of ADGRG2 in a double cell line, cells were transduced with a cAMP biosensor overnight. After 20 seconds of basal fluorescence recoding (Ex: 488nm; Em: 525 nm), cells were activated with 150µM P15 (arrow), and florescence was recorded for 280s. Data is mean of three technical replicates represented as ΔF/F0, Relative fluorescence units (RFUs) divided by the initial fluorescence. **E)** To assess the function of CaSR in a double cell line, cells were seeded in a 384-well plate and loaded with calcium dye. We then stimulated with various concentrations of Ca^{2+} and measured intracellular calcium mobilization in a FlexStation III device. Data is represented as the difference in maximal and basal signal for each concentration of Ca^{2+}.

ADGRG2 activation causes inhibition of CaSR $G\alpha_i$ signaling

To determine the effect of ADGRG2 activity on CaSR $G\alpha_i$ signaling, we transduced various cell lines with a baculovirus expressing a downward $G\alpha_i$ biosensor, which decreases fluorescence in response to increase cAMP production. We confirmed the ability of this biosensor to detect the activity of both ADGRG2 and CaSR signaling

by transducing various cell lines and stimulating them with DMSO, P15, and Ca^{2+} (Supplemental Fig 4.1a-d). We recorded a baseline measurement for 20 seconds followed by forskolin addition, an agonist of adenylyl cyclase to increase cytosolic cAMP, and stimulated varying cell lines with 50µM of P15 and 1.25mM Ca^{2+} simultaneously. We found no response in the HEK293 cells, and the ADGRG2-FL cell line showed a decrease in total cAMP. The CaSR cell line showed a significant fluorescent signal, indicating a decrease in cAMP due to increased $G\alpha_i$ activity. The FL-CaSR cell line showed similar activity to the ADGRG2-FL cell line, representing an ablation of CaSR signaling in response to ADGRG2 activation (Fig. 4.4a). Using the same experimental paradigm, we stimulated FL-CaSR cells with increasing concentrations of P15 conditions; these data show a dose-dependent inhibition of CaSR $G\alpha_i$ signaling in response to ADGRG2 activity (1.25mM: $LogIC_{50}$: -4.362, Hill Slope: -3.216. 2mM: $LogIC_{50}$: -4.283, Hill Slope: -4.838) (Fig. 4.4b). To further confirm these results, we performed a live-imaging analysis of FL-CaSR cells transduced with the $G\alpha_i$ sensor. We collected ten baseline Images followed by the addition of either DMSO or 50µM P15, and images were collected every second for 5 minutes total. Fluorescence intensity plots and images confirm the ablation of CaSR $G\alpha_i$ signaling after ADGRG2 activation with P15 (Fig. 4.4c,d).

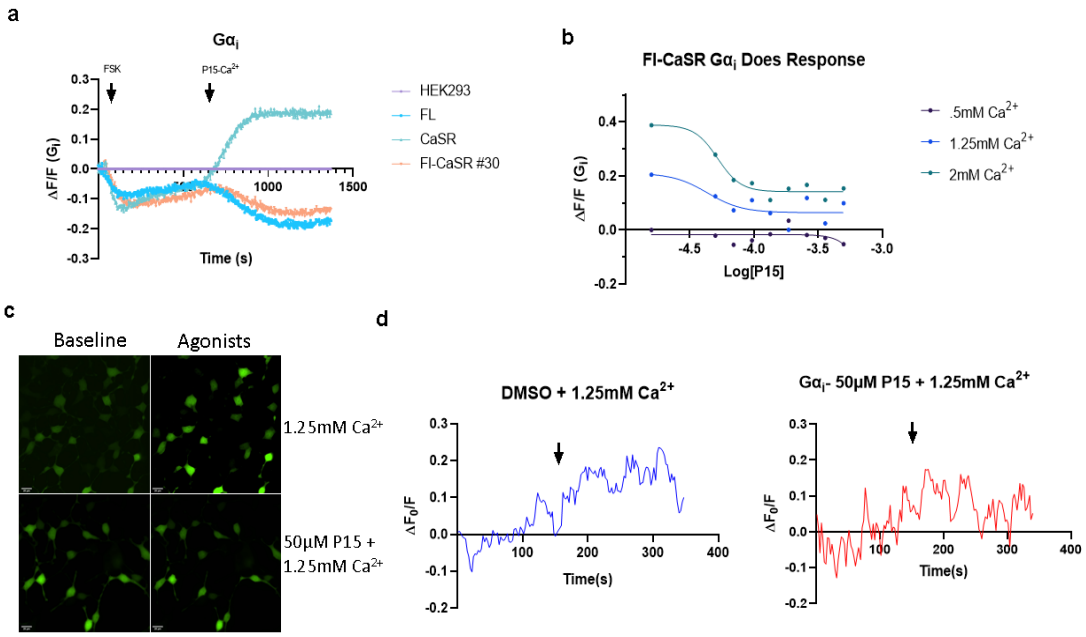

Figure 4-3 ADGRG2 activation modulates CaSR Gi signaling in a dose-dependent manner. A) Various cell lines were transduced with baculovirus containing a downward $G\alpha_i$ biosensor overnight in DMEM supplemented with 10% FBS. After 24 hours cells were treated starved in DMEM supplemented with L-glutamine and .5mM of Ca^{2+} for 6 hours. Media was changed to Hanks Balanced Salt Solution (HBSS) supplemented with .5mM $Ca^{2+}$and HEPES buffer at Ph:7. Cells were treated with 1µM FSK to induce cAMP production. After 10 minutes cells were treated with a mix of 50µM P15 and 2mM Ca^{2+}. CaSR cell lines show an increase in $G\alpha_i$ response, while the double expressing FL-CaSR cell line and the ADGRG2-FL cell line both show a decrease in Gi activity. **B)** FL-CaSR cells were transduced and starved as in A. Cells were treated with varying concentrations of P15 and either .5mM, 1.25mM, and 2mM Ca^{2+}. The activation of both ADGRG2 and CaSR in a single cell line shows dose-dependent inhibition of $G\alpha_i$ activity. Data are mean ± SE from three independent experiments conducted in triplicate. **C)** FL-CaSR cells were transduced as in A and seeded on chambered cover slides. Baseline images were taken followed by the addition of either Ca^{2+} alone or P15 and Ca^{2+}. **D)** Fluorescence intensity was plotted as the change in total fluorescence in NIS elements software and plotted in GraphPad Prism.

ADGRG2 activation causes inhibition of CaSR $G\alpha_q$ signaling

To determine the effect of ADGRG2 activity on CaSR $G\alpha_q$ signaling, we employed a dye-based Ca^{2+} assay. This assay successfully measured intracellular Ca^{2+} mobilization in all cell lines (Supplemental Fig 4.2). We conducted a time course of P15 pre-treatment to determine the optimal time of agonist addition (Supplemental Fig 4.3). We stimulated FL-CaSR cells with varying concentrations of P15 for 3 minutes, followed by the addition of 1.25mM Ca^{2+}. These results show a dose-dependent decrease of

intracellular Ca^{2+} release, a hallmark of $G\alpha_q$ signaling (Log IC_{50}: -4.976, Hill Slope: -5.408) (Fig. 4.5a,b). Live imaging experiments using a calcium dye further confirmed the inhibitory activity of ADGRG2 activation on CaSR $G\alpha_q$ signaling. FL-CaSR cells were loaded with calcium dye, and ten baseline images were collected every second, followed by the addition of either vehicle DMSO or 50μM P15. After 3 minutes, we stimulated the cells with 1.25mM of Ca^{2+} and measured changes in fluorescence for 3 minutes (Fig. 4.5 c,d).

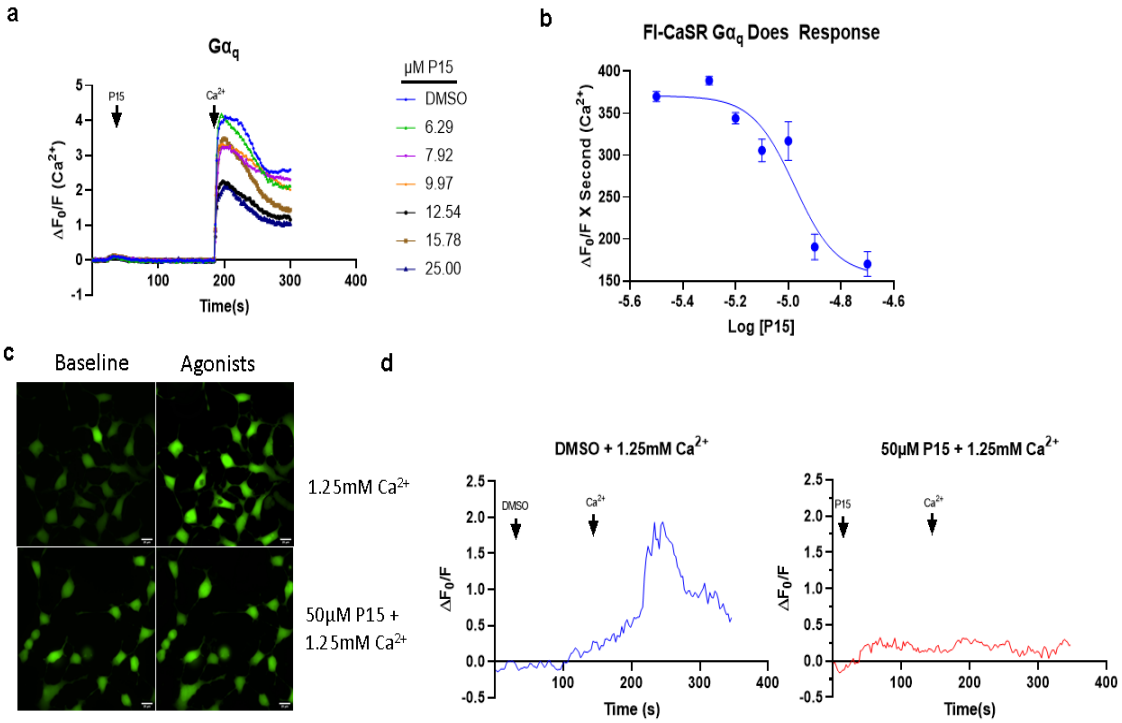

Figure 4-4 ADGRG2 activation modulates CaSR Gi signaling in a dose-dependent manner. A) FL-CaSR cells were seeded in a 384-well plate and allowed to grow to confluency in DMEM supplemented with 10% FBS and 100 U/mL penicillin and 100 μg/mL streptomycin. Cells were starved with DMEM supplemented with glutamine and .5mM Ca^{2+}. Cells were then loaded with Flou-4 Direct Ca^{2+} dye and stimulated with varying concentrations of P15 for 3 minutes followed by 1.25mM Ca^{2+} in a FlexStation III device. **B)** Area under the curve for each concentration of P15 was measured and does response curve plotted. Data are mean ± SE from three independent experiments conducted in triplicate, nonlinear dose-response curve fitting performed in GraphPad Prism. **C)** FL-CaSR cells were loaded with Ca^{2+} indicator and seeded on chambered cover slides. Baseline images were taken followed by addition of either Ca^{2+} alone or P15 and Ca^{2+}. **D)** Fluorescence intensity was plotted as change in total fluorescence in NIS elements software and plotted in GraphPad Prism.

Costimulation of ADGRG2 and CaSR inhibits proper trafficking

Several groups have shown an essential role for endosomal trafficking in the downstream signaling of CaSR[305, 306]. We have previously shown that ADGRG2 both traffics and sustains signaling from the early endosome[78]. Herein we seek to uncover the modulatory effects of ADGRG2 on CaSR intracellular trafficking. We utilized self-labeling SNAP and CLIP protein tags to visualize and track the movement of ADGRG2 and CaSR in a transient cell model. We generated constructs to express an N-terminal

SNAP-tagged ADGRG2 (SNAP-G2) and an N-terminal CLIP-tagged CaSR (CLIP-CaSR) (Fig. 4.6 and 4.7a). An advantage of these protein tags is the ability to bind any substrate, including biotin, fluorescent molecules, FRET/BRET molecules, or affinity tags, using a benzyl linker. Initially, we confirmed protein expression and stability using western blots, HEK293 cells were transfected with the tagged receptors, and whole-cell lysates were collected for analysis. We found that the tagged receptors were expressed at similar quantities and the correct size compared to their non-tagged counterparts (Fig. 4.7b).

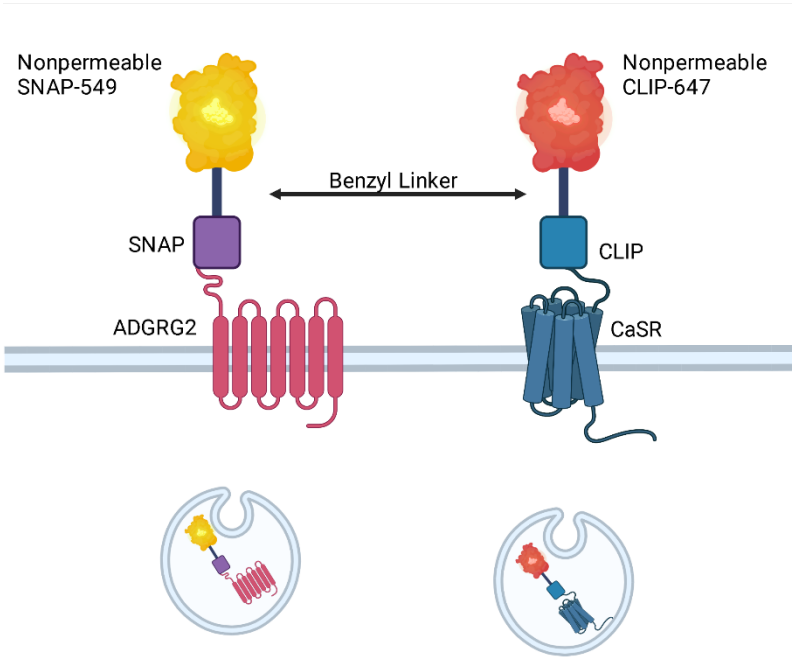

Figure 4-5- Diagram of SNAP and CLIP tag system to monitor receptor trafficking in real-time. ADGRG2 and CaSR were fused to SNAP and CLIP tags respectively via a benzyl linker. The tags were then covalently fused to a fluorescent substrate which is nonpermeable to the cell membrane. Any fluorescence seen within the cytosol is an indication of active endocytosis and not passive diffusion.

We next tested the ability of the SNAP and CLIP tags to bind their fluorescent substrates. We incubated cells expressing both tagged receptors with 50µM of a nonpermeable fluorophore. The SNAP-tag was conjugated to a fluorophore (ex:560, em:575) via a guanine leaving group and a benzyl linker. The CLIP-tag was conjugated

to a fluorophore (ex:660, em:673) using a cytosine leaving group and a benzyl linker. We confirmed the ability of these protein tags to selectively bind their respective substrate on the cell surface (Fig. 4.6c).

To study the effect of ADGRG2 activation on the trafficking of CaSR, we expressed SNAP-G2 and CLIP-CaSR together in a HEK293 cell model. We performed live confocal imaging after one hour of incubation with the nonpermeable SNAP and CLIP fluorescent substrates. Baseline images were collected for 1 minute, followed by the addition of 50μM P15 or 2mM Ca^{2+} alone or in combination. We found that activation of each receptor separately showed expected rapid internalization. When both receptors were simultaneously activated, we saw a complete ablation of receptor trafficking from the cell surface (Fig. 4.7d). This experiment was repeated using cells expressing the SNAP-G2 or CLIP-CaSR alone, and we confirmed the endosomal trafficking of these receptors independent of one another (Supplemental Fig 4.5).

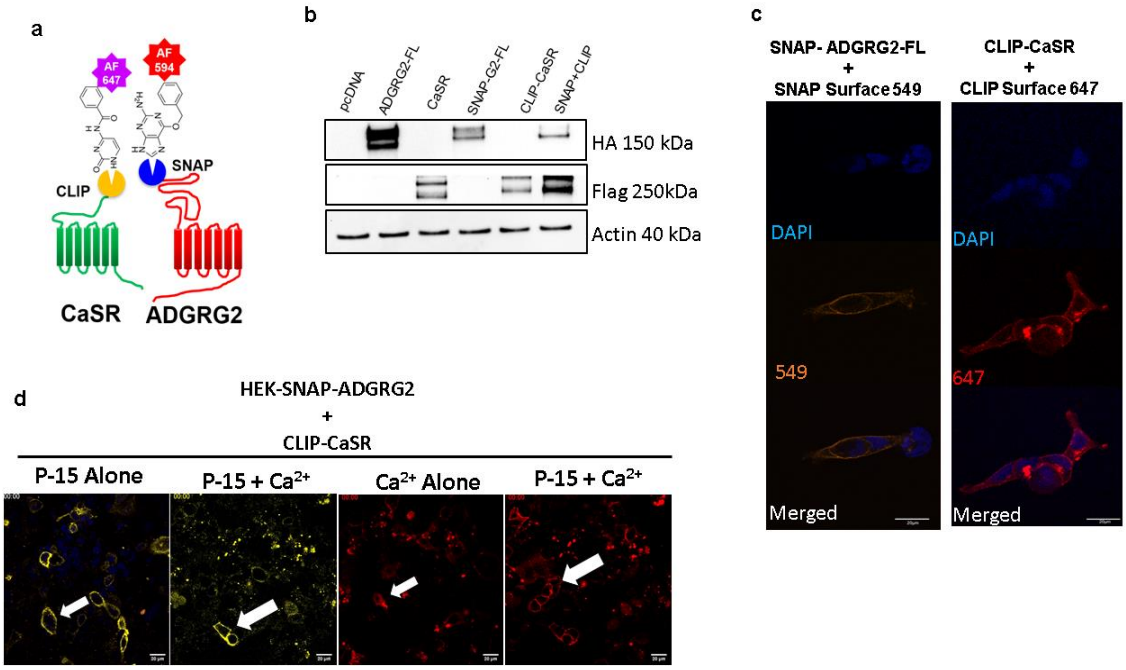

Figure 4-6 Generating SNAP-ADGRG2 and CLIP-CaSR plasmids. A) We generated plasmids that express ADGRG2 and CaSR fused to a SNAP and CLIP tag respectively. These self-labeling tags were then covalently linked with fluorescent tags in order to visualize receptor activity. **B)** HEK293 cells were transfected with PcDNA, HA-tagged ADGRG2-FL, flag-tagged CaSR, and the SNAP-tagged ADGRG2 (SNAP-G2-FL), CLIP-tagged CaSR (CLIP-CaSR), and SNAP-G2-FL plus CLIP-CaSR using lipofectamine 2000 according to manufacturer instructions. After 5 hours cells were incubated in DMEM supplemented with 10% FBS for 24 hours. Protein lysates were collected, and representative blots were probed with HA tag, Flag, and actin antibodies. We found the SNAP and CLIP tags were well expressed at the proper size. **C)** Cells were transfected as in B and seeded on glass coverslips. After 24 hours cells were incubated with 5µM of SNAP-Surface 549 or CLIP-Surface 647 for one hour. All cells were fixed with 4% paraformaldehyde and mounted with ProLong Diamond Antifade Mountant with DAPI for nuclear counterstaining. We confirmed the surface expression of both the SNAP and CLIP tagged receptors and the functionality of the SNAP and CLIP tags. **D)** HEK293 cells were transfected with both SNAP-G2-FL and CLIP-CaSR as in A and seeded on Ibidi µ-Slide 8-well chambered coverslips in DMEM supplemented with 10% FBS. After 24 hours cells were incubated with SNAP-Surface 549 and CLIP-Surface 674 substrates for one hour. Media was aspirated and cells were imaged in 200µl of Hanks Balanced Salt Solution (HBSS) supplemented with .5mM $Ca^{2+}$and HEPES buffer. Baseline video was taken for one minute followed by the addition of 50µM P15, 1.25mM Ca^{2+} alone or in combination. The addition of either agonist alone elicits a movement of receptors into the cell while the addition of both P15 and Ca^{2+} shows no movement of either receptor. Image analysis performed on ImageJ, images, and videos are representative of 3 independent experiments.

Discussion

Our understanding of the pathophysiology of PHPT and parathyroid tumors has dramatically expanded over the past decade. Innovations in surgical resections, molecular biology, pharmacology, and signaling biology, along with novel models and experiments in primary cells, have elucidated much about these cells' dysregulated signaling

pathways. Unfortunately, the primary cause of CaSR insensitivity is a point of contention in the literature. While some studies have shown significant decreases in CaSR expression in tumor samples collected from PHPT patients[30, 92, 307-309], we and others have found that CaSR expression is not altered in a subset of PHPT patient samples[32, 94]. In a recent study, Koh et al. performed ex-vivo analysis on parathyroid tissue samples and found that patients could be grouped based on their cells' ability to sense and respond to changes in extracellular Ca^{2+} levels[32, 94]. While these patients showed varying calcium-sensing capacities, their total expression of Ca^{2+} showed no significant change. These data led to the conclusion that CaSR downregulation is not the obligate underlying mechanism for PHPT pathogenesis.

Our group has previously shown compelling data that dysregulated Ca^{2+}sensing is a function of molecules that modify the activity of CaSR rather than downregulation of CaSR expression[33]. Transgenic mice that overexpress either RGS5 or ADGRG2 exclusively in the parathyroid glands showed biochemical and physical PHPT phenotypes. Parathyroid glands isolated from these transgenic mice showed tumor development and increases in serum PTH levels but no changes in total CaSR expression.

ADGRG2 signals via Gαs to increase cytosolic cAMP, which actively opposes CaSR Gαi-mediated inhibition of adenylyl cyclase. Herein we found ADGRG2 activation caused a significant inhibition of CaSR mediated Gαi signaling. Although the direct mechanism of cAMP-induced PTH secretion is not well defined, studies have shown that $G\alpha_s$-linked GPCRs can induce PTH secretion in the primary culture of bovine parathyroid cells[93, 310]. Several other studies have described detailed mechanisms for cytosolic cAMP in the process of exocytosis and the secretion of various vesicles[311-313]. Given these data,

we can surmise that cAMP is necessary for the proper exocytosis of PTH secretory vesicles, and under physiological conditions, CaSR $G\alpha_i$ activity decreases cytosolic cAMP to inhibit excessive PTH secretion. Based on our results, we conclude that the overexpression of ADGRG2 in PHPT adenomas increases the cytosolic cAMP leading to direct inhibition of CaSR signaling and pathological secretion of PTH.

The stimulation of ADGRG2 before CaSR activation showed inhibition of CaSR $G\alpha_q$ signaling. We found that simultaneous activation of these two receptors showed no change in the activity of CaSR. Pre-treatment with P15 for 3 minutes elicited an inhibitory effect on CaSR-mediated $G\alpha_q$ signaling (Supplemental Fig 4.3). These results are a function of the kinetic properties of the two receptors. Whereas CaSR reaches maximal signal within 10 seconds of agonist addition, ADGRG2 requires approximately 90 seconds to reach maximal response. By pretreating cells with P15 for 3 minutes, we ensured that both receptors reached maximal activity simultaneously.

The mechanism by which ADGRG2 modulates intracellular Ca^{2+} is not fully elucidated. $G\alpha_q$ activity leads to intracellular Ca^{2+} release via activation of inositol 1,4,5-trisphosphate receptors (IP3R) on the endoplasmic reticulum. Parathyroid cells show high expression of the IP3R2 receptor, which contains a PKA phosphorylation site at S937[314, 315]. While the role of the IP3Rs in parathyroid cells has not been directly studied, several studies have found an inhibitory effect of cAMP on IP3R-mediated intracellular Ca^{2+} release in smooth muscle cells and platelets membranes[316, 317]. Further studies are needed to dissect the mechanisms of ADGRG2-mediated inhibition of intracellular Ca^{2+} release and potential downstream IP3R crosstalk.

The importance of intracellular trafficking and the signaling of various GPCRs has emerged as a significant area of research over the last decade. We have previously shown that the mutants of ADGRG2, which lack the NTF, bind ß-arrestin1 and ß-arrestin2, leading to their constitutive internalization in a steady state[78]. To ascertain any crosstalk-mediated modulation of receptor trafficking, we employed SNAP and CLIP tags to monitor ADGRG2 and CaSR, respectively. Our results showed that in a HEK293 model expressing both receptors' internalization was inhibited when stimulated with both P15 and Ca^{2+}. We have previously reported that only the constitutively active ADGRG2 mutant, ΔNTF-G2, shows any physical interaction with CaSR in a co-immunoprecipitation assay[94]. Our live-imaging results recapitulate the necessity of AGDGR2 activation for receptor interaction and provide evidence that the physical interaction leads to an inhibition of CaSR endosomal trafficking, which disrupts its physiological signaling patterns.

The decrease of ADGRG2 trafficking in the double-receptor model does not decrease total $G\alpha_s$ signaling in our kinetic signaling experiments. These results contrast with our previously published data which showed that internalization of ADGRG2 is necessary for maximal cAMP production[78]. We believe these contradictions are due to the transient nature of the SNAP and CLIP tagged receptors. Our unpublished data found that transient transfection of ADGRG2 in HEK293 cells leads to less downstream response when compared to a stably transfected cell line. Furthermore, we found that transiently transfected ADGRG2 did not associate with lipid raft molecules as readily as its stably expressed counterpart. In future experiments, we hope to generate stable cell

lines for SNAP and CLIP tagged ADGRG2 and CaSR more accurately model the trafficking and localization of these receptors *in-vitro.*

ADGRG2 is a surface receptor that makes it a potential therapeutic target for PHPT patients with inoperable adenomas. The effect of ADGRG2 modulation of CaSR signaling and trafficking is quite evident (Fig. 4.8). We hope to test ADGRG2 inhibition in primary PHPT tissues to identify any potential therapeutic benefit of targeting this receptor in future experiments.

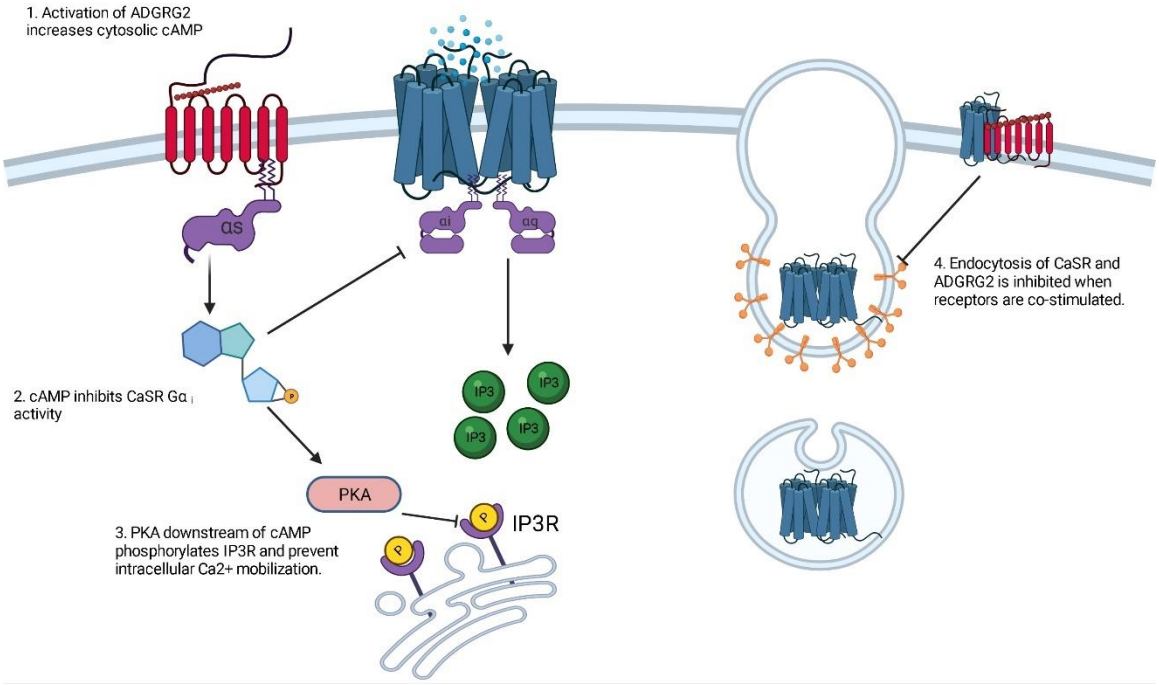

Figure 4-7 Graphical summary of ADGRG2 crosstalk with CaSR. Activation of ADGRG2 with P15 causes the rapid formation of cAMP which actively counteracts CaSR $G\alpha_i$ activity. the cAMP also activates PKA which has been shown to phosphorylate IP3Rs to block intracellular Ca^{2+} release. Finally, the expression of ADGRG2 and CaSR on a single cell led to a halt in intracellular trafficking.

Supplemental Figures

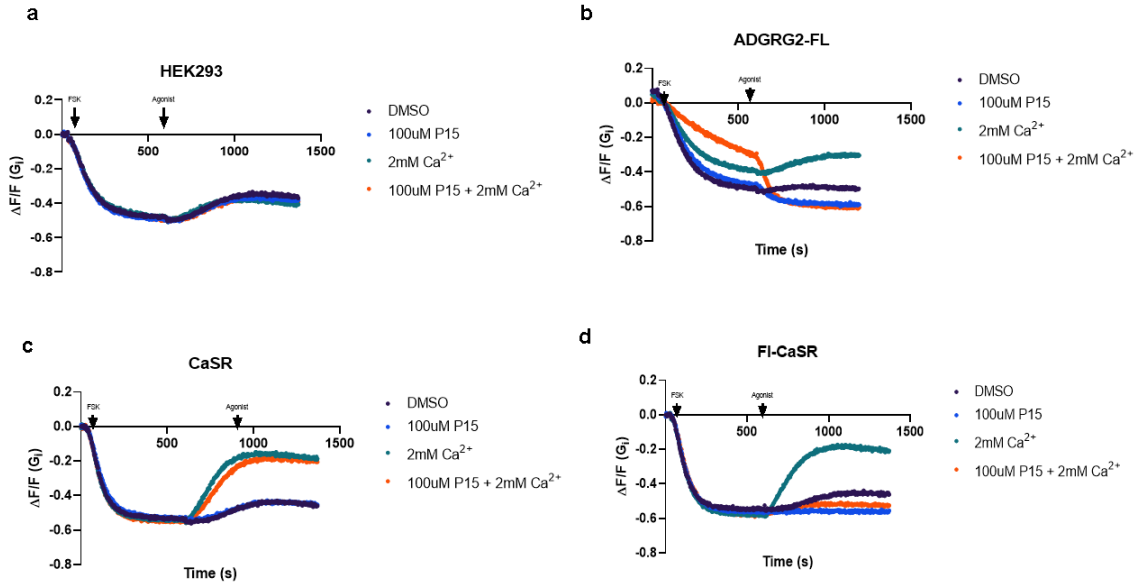

Supplemental Fig 4-1 Biosensors for Gα$_i$ were confirmed in all cell lines. A-D) Various cell lines were transduced with downward Gα$_i$ sensor, as in Fig 4.2a, and treated with DMSO, and P15 or Ca^{2+} alone or in combination. Treatment with FSK increased cytosolic cAMP and seen by the decrease in fluorescence across all cell lines, the increase in fluorescence seen in the CaSR and FL-CaSR line are indicative of CaSR Gα$_i$ activation.

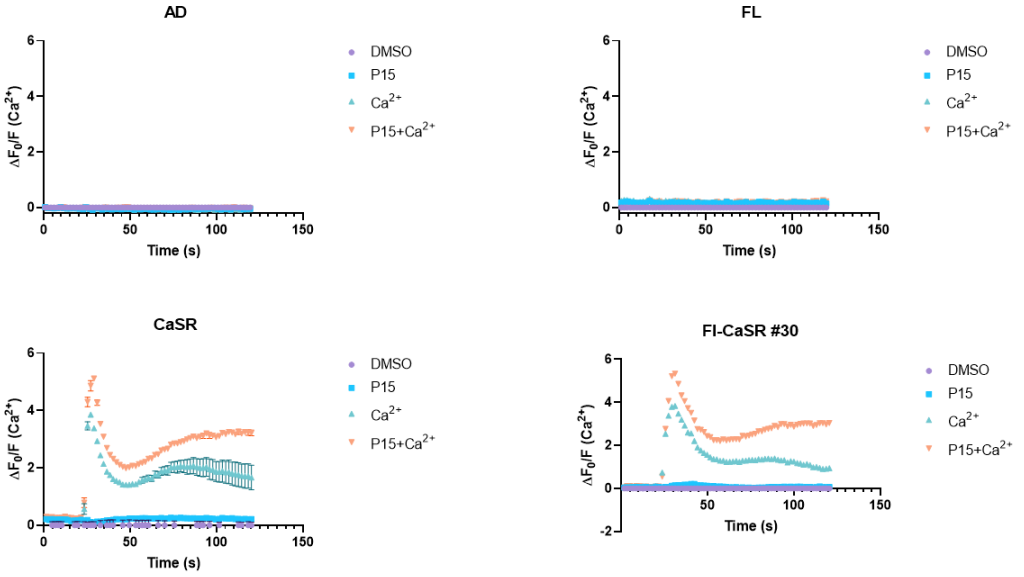

Supplemental Fig 4-2 Intracellular Ca^{2+} mobilization is similar in single and double expressing cell lines. Various cell lines were loaded with a fluorescent Ca^{2+} indicator, as in Fig 4a, and treated with DMSO, and P15 or Ca^{2+} alone or in combination. The Ca^{2+} mobilization assay successfully detected the activity of CaSR in both single and double-expressing cell lines.

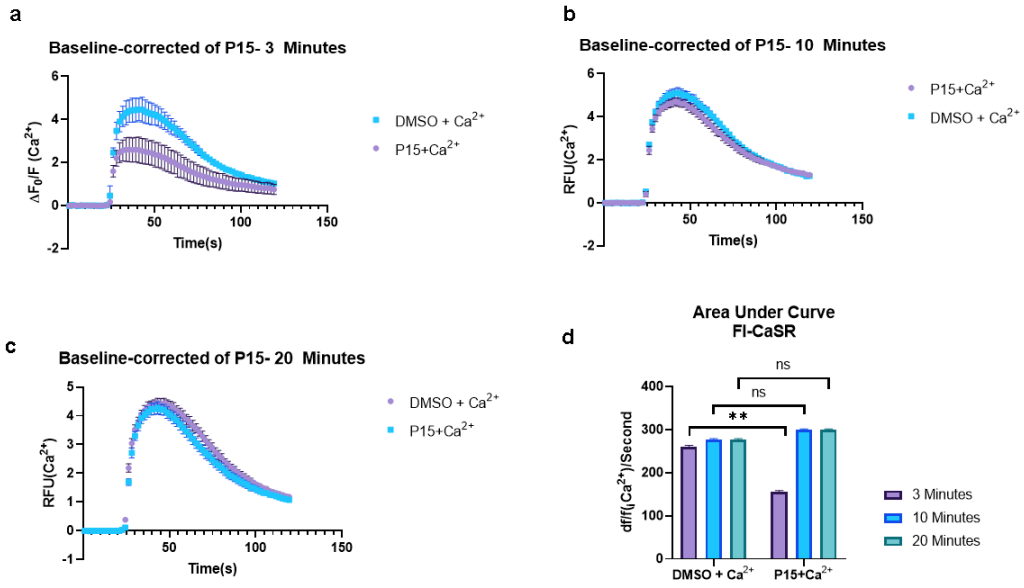

Supplemental Fig 4-3 Pre-incubation with P15 for 3 minutes shows a significant decrease in $G\alpha_q$ activity A-C) In order to determine the optimal time of agonist we employed a Ca^{2+} indicator (Fig.ure. 4a). FL-CaSR cells were pre-treated with P15 for 3, 10, and 20 minutes. We found 3 minutes of pre-incubation showed a sufficient decrease in CaSR-mediated intracellular Ca^{2+} mobilization. **D)** changes in total Ca^{2+} mobilization were calculated as the area under the curve, 2-way ANOVA with multiple comparisons shows a significant (P=.0082) difference between DMSO+Ca^{2+} and P15 +Ca^{2+} only with 3 minutes of pre-incubation. **E)** Area under the curve were calculated for all curves and comparisons were calculated with 2-way ANOVA with multiple comparisons. Data represented as Mean ±SEM.

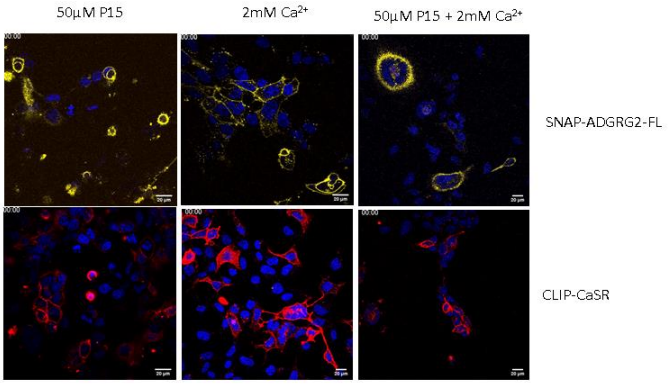

Supplemental Fig 4-4 Trafficking of ADGRG2 and CaSR was confirmed using SNAP and CLIP tags. HEK293 cells expressing SNAP-G2 or CLIP-CaSR alone were treated with P15 or Ca^{2+} alone or in combination. Activation of both receptors caused independent trafficking into the cytosol.

Chapter 5 - Conserved Residues in the Extracellular Loop 2 Regulate Stachel-mediated Activation of ADGRG2.

Abstract

Cleavage and dissociation of a large N-terminal fragment and the consequent unmasking of a short sequence (*Stachel*) remaining on the N-terminus have been proposed as mechanisms of activation of some members of the adhesion G protein-coupled receptor (aGPCR) family. However, the identity of residues that play a role in the activation of aGPCRs by the cognate *Stachel* remains largely unknown. Protein sequence alignments revealed a conserved stretch of residues in the extracellular loop 2 (ECL2) of all 33 members of the aGPCR family. ADGRG2, an orphan aGPCR, plays a major role in male fertility, Ewing sarcoma cell proliferation, and parathyroid cell function. We used ADGRG2 as a model aGPCR and generated mutants of the conserved residues in the ECL2 via site-directed mutagenesis. We show that tryptophan and isoleucine in the ECL2 are essential for receptor stability and surface expression in the HEK293 cells. By adjusting the receptor surface expression levels, we show that mutation of these residues of ECL2 ablates the *Stachel*-mediated activation of multiple signaling pathways of ADGRG2. This study provides a novel understanding of the role of the ECL2 in *Stachel*-mediated signaling and degradation of ADGRG2, which may lay the foundation for the rational design of therapeutics to target aGPCRs.

Introduction

G protein-coupled receptors (GPCRs) play fundamental roles in various cellular processes such as proliferation, metabolism, hormone secretion, contraction, and neurotransmission[318]. The signaling pathways of GPCRs via G proteins and ß-arrestins and their trafficking trajectories have been studied for several decades[319, 320]. This, in combination with recent advances in our understanding of GPCR structures, has formed a strong foundation for rational drug design to target this largest superfamily of surface receptors[321, 322].

Recent genomic and model organism studies have revealed the versatile roles that the adhesion GPCRs (aGPCRs), the second-largest family of GPCRs, play in endocrine, nervous and immune systems[323]. aGPCRs have structural differences with other classes of GPCRs, namely autoproteolysis at a GPCR proteolysis site (GPS) and formation of a two-segmented receptor with a large N-terminal fragment (NTF) and a C-terminal fragment (CTF). The CTF includes the C-terminus, seven-transmembrane helical domains (TM1-7), extracellular loops (ECL1-3), intracellular loops (ICL1-3), and a short extracellular sequence on the N-terminus just before the TM1. Many studies[111, 209, 324, 325], including our recent reports[78, 94], have shown that this short remaining peptide, known as *Stachel* sequence, can activate aGPCRs and might be one of the mechanisms of activation in physiological and pathological states. NTF-dissociating molecular partners can potentially unmask the *Stachel* sequence for its binding to the cognate aGPCR. These studies exploited two main tools to reveal this mechanism: (a) NTF-truncated aGPCRs that show constitutive activation of G proteins; (b) synthetic peptides resembling the *Stachel* sequence that activate aGPCRs[101, 117]. Other mechanisms or modes of aGPCR

activation have been reported as well. For instance, a mutant of ADGRG1 that lacks both NTF and *Stachel* was shown to retain constitutive activation of nuclear factor of activated T cells (NFAT) and recruitment of b-arrestins[117], pointing to dual roles of NTF, shielding the *Stachel* peptide and inhibiting the intrinsic activity of the CTF. Also, a non-cleavable mutant of ADGRD1[261] or non-cleavable wild-type forms of ADGRB1[326] and ADGRG5[112] retain their signaling capabilities. These studies show that aGPCRs use various structural segments, motifs, and the *Stachel* peptide to engage distinct signaling modes[327].

We recently showed that human ADGRG2 (GPR64), an orphan aGPCR, is expressed in human parathyroid glands and regulates the signaling and function of calcium-sensing receptor[94]. We discovered that similar to other aGPCRs (ADGRG1[109], ADGRD1[111], ADGRG6[111]), ADGRG2 is activated by either the endogenous 15-amino acid long *Stachel* (P-15) on the N-terminus of its NTF-truncated mutant (ADGRG2-ΔNTF) or the synthetic P-15[94]. We showed that the deletion of P-15, in addition to the NTF, ablates constitutive activation of G□s and cAMP production in a mutant that starts with the proline 622 (ADGRG2-P622)[78] and elevates receptor response to synthetic P-15. Nevertheless, the binding site of *Stachel* remains unknown among aGPCRs.

Previous studies in other families of GPCRs revealed that some residues in the ECL2 play major roles in ligand access, receptor subtype selectivity, and activity[328-330]. Despite high degrees of diversity in the structure of ECL2 among GPCRs[331], there is a conserved disulfide bond between the cysteines of ECL2 and TM3, which ensures receptor structural integrity. In the Secretin family (class B1), this conserved ECL2 cysteine is followed by a tryptophan residue, forming the CW motif, which is further

followed by an acidic residue (aspartic or glutamic acid). The aGPCR family has the highest homology to the Secretin family. By aligning the ECL2 residues of all 33 human aGPCRs (predicted by either GPCRdb or Uniprot), we show that most of the aGPCRs have an aliphatic residue (leucine or isoleucine) after the CW motif (Fig. 5.1a and Supplemental Fig 5.1). Whether the ECL2 plays a role in the activation of aGPCRs by *Stachel* remains poorly studied.

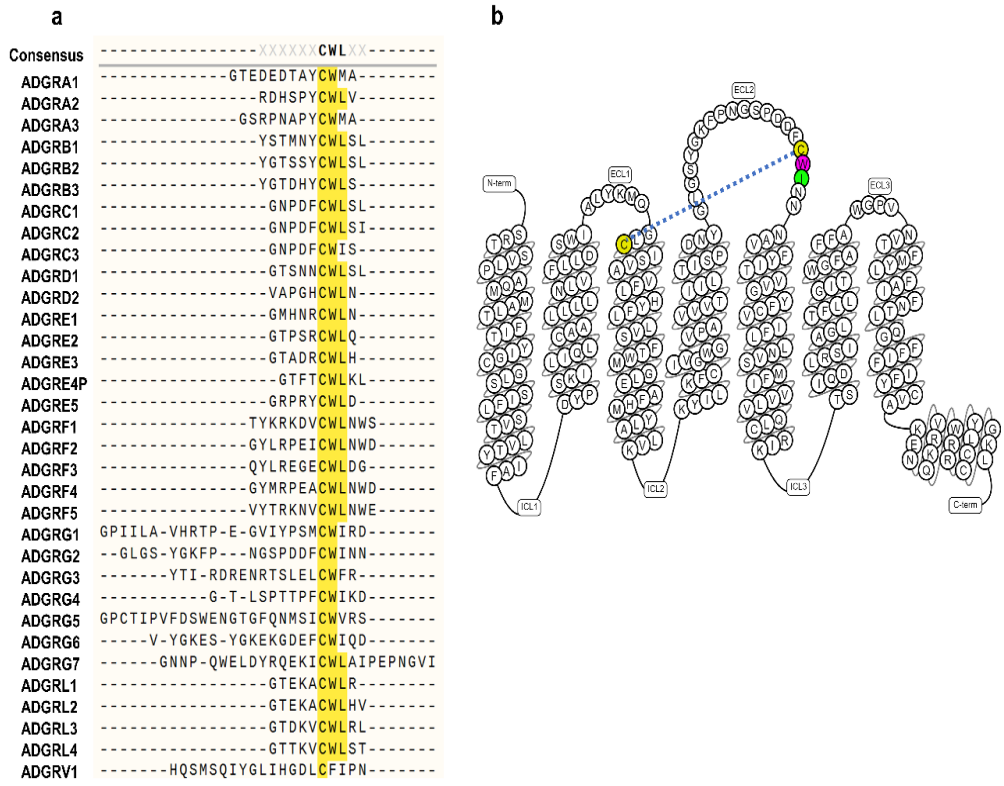

Figure 5-1 Conserved residues in extracellular loop 2 (ECL2) of aGPCRs. A) Multiple alignments of the ECL2 of all 33 members of the aGPCR family. Predicted amino acid sequences of the ECL2 for each aGPCR were derived from GPCRdb. The alignment was conducted in SnapGene software (from Insightful Science; available at www.snapgene.com) using the Clustal Omega algorithm. **B)** Snakeplot of human ADGRG2, exported from www.GPCRdb.org, showing the colored CWI motif in the ECL2. The sequences of the N-terminal fragment and C-terminus are not shown. The dashed line shows the disulfide bond between the cysteines of TM3 and ECL2.

Here, we use ADGRG2 (P622 and ΔNTF) as a model aGPCR to investigate the role of tryptophan and isoleucine of ECL2 (Fig. 5.1b) in receptor activation by the

Stachel. Our study shows that these residues not only regulate receptor activation by P-15 but also control receptor surface expression and degradation.

Methods

Cell culture and transfection

AD-293 (HEK) cells were purchased from Agilent Technologies (Santa Clara, CA, USA #240085) and cultured in DMEM media (Sigma, St. Louis, MO, USA #D6429) supplemented with 10% FBS, 100 U/mL penicillin, and 100µg/mL streptomycin (Thermo Fisher Scientific, Waltham, MA, USA #15140-122). Cells were transfected with plasmids using lipofectamine 2000 reagent (Thermo Fisher Scientific #11668019) following the manufacturer's instructions.

Antibodies

Antibodies were purchased from the following sources: Cell Signaling Technologies (Beverly, MA, USA): rabbit anti-HA (#3724); Thermo Fisher Scientific: mouse anti-V5 (#R960-25); Sigma: rabbit anti-ß-actin (#A2066); Biolegend (San Diego, CA, USA): mouse anti-HA (#901513).

Receptor mutagenesis

We used the Q5 site-directed mutagenesis kit (NEB, Ipswich, MA #E0552S) to generate mutations in the ECL2 of human ADGRG2. Our template for mutations was pcDNA3.1-3xHA-P622-V5 (P622-CWI)[78], a plasmid that expresses an NTF/*Stachel*-truncated ADGRG2 with an N-terminal 3xHA tag and a C-terminal V5 tag. The following primer pairs were used to construct mutants: P622-CWA^{780} (*for*:

CTTCTGCTGGGCCAACAACAATGC; *rev*: TCATCCGGTGAACCATTG), P622-CA^{779}I (*for*: TGACTTCTGCGCCATCAACAACAATGCAGTATTC; *rev*: TCCGGTGAACCATTGGGG), P622-CA^{779}A^{780} (*for*: TGACTTCTGCGCCGCCAACAACAATGCAGTATTCTAC; *rev*: TCCGGTGAACCATTGGGG), P622-$^{G772A/S773A}$ (mutation of G^{772} and S^{773} in the ECL2; *for*: ATTCCCCAATGCTGCTCCGGATGACTTC; *rev*: TTCCCATAGGATCCAAGC). We used the aforementioned primers and pcDNA3.1-3xHA-ΔNTF-V5 (ΔNTF-CWI) as the template to generate mutants of ECL2 of the NTF-truncated ADGRG2. The resulting constructs were verified by sequencing both strands.

On-Cell ELISA

Cells were seeded in 96 well plates and transfected with 50 ng of one of the following plasmids: pcDNA3.1 (empty vector), P622-CWI, P622-CWA, P622-CAI, and P622-CAA. Twenty-four hours after transfections, cells were starved using DMEM (Thermo Fisher Scientific #21068028) supplemented with glutamine and 1.25mM Ca^{2+} overnight. Cells were then fixed with 4% paraformaldehyde for 15 minutes at room temperature. After several washes with TBS, cells were blocked for 30 minutes in TBSM (TBS + 3% milk) for surface staining or TBSM supplemented with 0.2% Triton X-100 for total staining. Cells were then incubated with either rabbit anti-HA (1:2000) or mouse anti-V5 (1:2000) antibodies in TBSB (TBS + 3% BSA) for 2 hours at room temperature. After several washes, cells were incubated for 1 hour with 1:2000 dilution of either horseradish peroxidase (HRP)-linked horse anti-mouse IgG (Cell Signaling Technologies #7076) or HRP-linked goat anti-rabbit IgG (Cell Signaling Technologies #7074) antibodies in TBSM. After 5 washes with TBS, cells were incubated with 3,3',5,5'-Tetramethylbenzidine

(TMB) (Sigma #t0440) for 5 min at room temperature. The reaction was stopped by an equal volume of 1 N HCl. Absorbance at 450nm was measured using a FlexStation III plate reader. In a separate set of experiments, cells were transfected with several amounts of plasmids to determine the doses of mutant plasmids that result in similar surface expression compared to non-mutated P622-CWI or ΔNTF-CWI receptors.

Degradation assay

Cells were transiently transfected with 1 mg of plasmids in 6-well plates, and 24 hours post-starvation were incubated with 100 μg/ml of cycloheximide (Sigma #4859) for indicated time points. In some experiments, transfected cells were pre-incubated with 25 mM chloroquine (Tocris, Minneapolis, MN, USA #4109), 1 mM MG132 (Cell Signaling Technologies #2194), or 10 nM bafilomycin A1 (Tocris #1334) for 16 hours before the 8-hr cycloheximide treatment. Cells were lysed using radioimmunoprecipitation assay (RIPA) lysis buffer (EMD Millipore, Billerica, MA, USA #20-188) supplemented with cocktails of protease (Thermo Fisher Scientific #78429) and phosphatase inhibitors (EMD Millipore #524625). Lysates were then centrifuged at 13,000 rpm for 5 min at 4°C, and supernatants were collected.

Western blotting

Protein lysates were boiled with reducing sample buffer (Thermo Fisher Scientific #NP0007 and #NP0009) for 10 minutes and loaded on 4-12% Bis-Tris gels (Thermo Fisher Scientific #NP0336BOX), then transferred to polyvinylidene fluoride (PVDF) membranes. Blocking was performed in TBSTM (TBS + 0.1% Tween-20 + 10% nonfat dry milk) followed by incubation with primary antibodies in TBSTM (1:2000 for HA and V5; 1:500

for ß-actin), overnight at 4°C. To detect primary antibodies, cells were incubated with HRP-linked horse anti-mouse IgG and HRP-linked goat anti-rabbit IgG antibodies (1:5,000) in TBSTM for 2 hours at room temperature. Blots were washed and then developed with ECL SuperSignal™ West Femto substrate (Thermo Fisher Scientific #34095). Blots were imaged separately via an auto-exposure option that avoided any bands' saturation and then analyzed in iBright™ FL1500 Imaging System (Thermo Fisher Scientific).

Immunofluorescence staining and imaging

HEK cells were transfected with plasmids (either 50 ng or adjusted doses as stated in each figure), seeded on glass coverslips, and serum-starved overnight. Cells were fixed in 4% paraformaldehyde for 10 min and were washed with PBS several times. Cells were blocked with 5% goat serum in PBS for 1 hour and incubated with mouse anti-HA antibody (1:1000) in 1% BSA in PBS for 2 hours at room temperature. After several washing steps with PBS, HA antibody-bound receptors were labeled with Alexa Fluor 594–conjugated goat anti-mouse antibody (1:500) in 1% BSA in PBS for 1 hour. Cells were mounted in ProLong Diamond Antifade Mountant with DAPI (ThermoFisher Scientific #P36971) for nuclear counterstaining. Fluorescence microscopy was conducted by 40x oil objective (1.4 NA) on a Nikon Ti-E microscope equipped with a 16.2 MegaPixels DS-Ri2 camera, and images were analyzed with Nikon NIS-Elements Basic Research software.

Luciferase reporter assays

Luciferase reporter assay was performed as described previously[94], with some modifications. HEK cells were seeded in white clear-bottom 96-well plates (20,000

cells/well) and were transfected with adjusted amounts of receptor plasmids along with 100 ng of either pCRE-Luc or pSRE-Luc reporter plasmids. Cells were then stimulated with increasing concentrations of P-15 or vehicle for 5 hours at 37°C. Using Steadylite reagents (PerkinElmer, Hopkinton, MA, USA, #6066756), the luminescence was measured in a FLEXStation III device.

cAMP production assays

Cells were resuspended in DMEM + 10% FBS and were mixed with Upward Green cADDis cAMP Assay Kit BacMam sensor (Montana Molecular, Bozeman, MT, USA #U0200G), supplemented with 2mM sodium butyrate. Cells were then seeded at 50,000 cells/well in black, clear-bottom, 96-well plates (150µl/well), incubated for 30 min at room temperature in the dark, and then at 37°C for 24 hours. Cells were washed with assay buffer (HBSS; Thermo Fisher Scientific #14065056 supplemented with 20mM HEPES) and kept in the dark to acclimate to room temperature for 1 hour in 100 µl/well of assay buffer. Initial assay development was conducted by transducing with various amounts of the BacMam Gαs sensor followed by stimulation with 10 µM forskolin for 800 seconds (Supplemental Fig 5.4). Considering the speed and amplitude of the signal, we chose 15 µl per well of the sensor as the appropriate volume to monitor cAMP production in HEK cells. After transfection with adjusted doses of plasmids, cells were transduced with 15 µl of the sensor (as described above) and were stimulated with increasing concentrations of P-15 the next day. cAMP production was recorded for 280 seconds after an initial 20 seconds of basal measurement of fluorescence at Excitation 488nm and Emission 525nm using the FLEXStation III plate reader. In a different set of experiments, a previously described homogenous time-resolved FRET (HTRF) assay[78] was used to measure cAMP production

either at basal condition (overnight incubation with 0.5 mM IBMX; Sigma #I5879) or after 2 hours of activation with P-15 in 384-well plates.

Whole-cell label-free impedance assay

Cells were transfected with adjusted amounts of plasmids and were seeded at a density of 50,000 cells per well in 100 µl of DMEM (Thermo Fisher Scientific #21068028) supplemented with glutamine and 1.25mM Ca^{2+} in CytoView-Z 96-well plates (Axion BioSystems, Atlanta, GA, USA #Z96-IMP-96B) overnight. After 45 minutes of baseline recording of impedance in the Maestro Z device (Axion BioSystems) cells were activated with 100 mM P-15 or vehicle (DMSO). Impedance against 1kHz voltage frequency was recorded for several hours at 37°C, 5% CO2 in a humidified environment in the Maestro Z machine. Data normalization to vehicle and analyses were performed in AxIS Z software.

Statistical analysis

Statistical analyses were conducted using t-test, one-Way or two-Way ANOVA with Dunnett's or Holm-Sidak multiple comparison tests in GraphPad Prism 9.0 software; $P < 0.05$ was considered significant.

Results

Mutations in ECL2 alter the expression of ADGRG2

We transiently expressed the ADGRG2-P622 (P622-CWI) and its ECL2 mutants, P622-CWA, P622-CAI, and P622-CAA, in HEK cells and used a cell-based ELISA assay to determine their surface expression via their N-terminal HA-tag. We noticed that all ECL2-mutants show significantly reduced expression on the surface in comparison to the

P622-CWI receptor (Fig. 5.2a). This lower surface expression was confirmed by immunofluorescence imaging of receptors on the cell surface (Fig. 5.2b). Measuring the total expression via the V5-tag at the C-terminus by ELISA revealed that all three mutants are expressed at reduced levels compared to the P622-CWI receptor (Fig. 5.2c). Western blot analyses of the whole-cell lysates confirmed the reduced expression of mutants (Fig. 5.2d).

We have previously shown that the P622 receptor lacks the constitutive activity of the NTF-truncated (ΔNTF) ADGRG2. We observed a similar reduction of expression in mutants of the CWI motif in ΔNTF receptor (ΔNTF-CWA, ΔNTF-CAI, ΔNTF-CAA) compared with the ΔNTF-CWI receptor (Supplemental Fig 5.2). Interestingly, mutation of P622 on residues other than the CWI motif, glycine^{772} and serine^{773}, to alanine (P622-$^{G772A/S773A}$) did not alter the total or surface expression level of the receptor (Supplemental Fig 5.3 a&b).

Together, these data suggest that ADGRG2 expression is controlled by tryptophan and isoleucine in the CWI motif of the ECL2, irrespective of the activation state of the receptor.

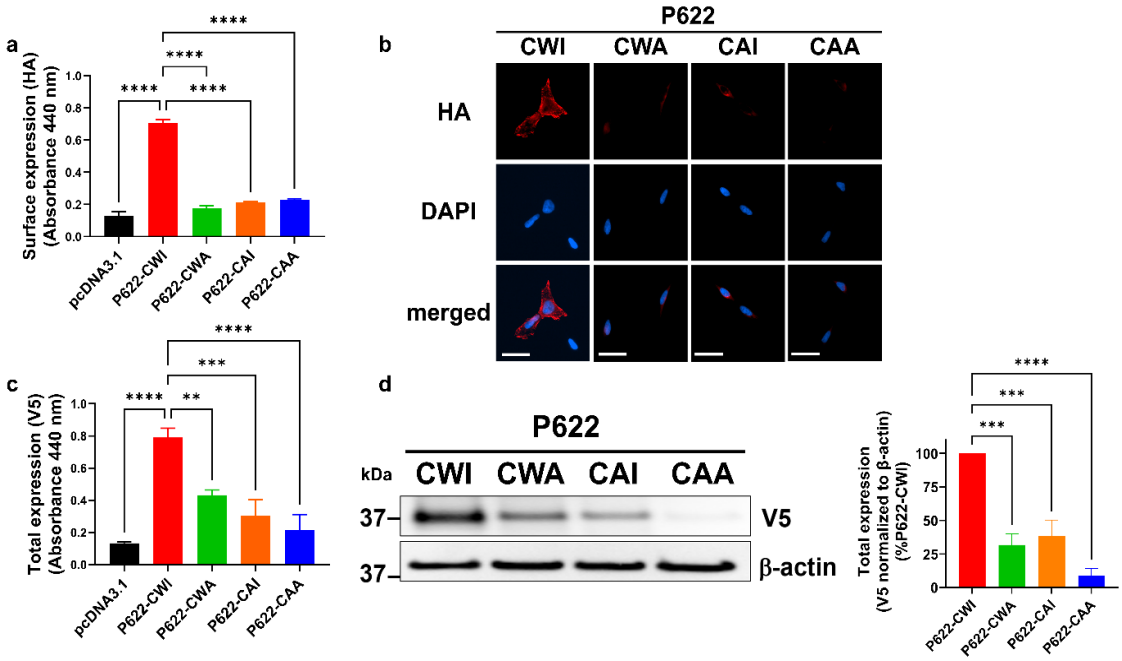

Figure 5-2- Expression of ADGRG2-P622 is regulated by the residues in the CWI motif in the ECL2.HEK cells were transfected with the same dose (50 ng for a, b, and c; 1 mg for d) of plasmids expressing P622-CWI or mutants. Cell surface expression of receptors was determined by **A)** ELISA and **B)** immunofluorescence imaging using an antibody against the N-terminal HA-tag in non-permeabilized conditions. Nuclear counterstaining with DAPI (scale bars: 20 mm). **C)** ELISA was used to measure the total expression by using an antibody against the C-terminal V5 tag in permeabilized conditions. **D)** Representative blots show C-terminal V5-tagged P622-CWI and mutant receptors in total cell lysates. Densitometry data were used to normalize V5 expression to b-actin for each plasmid and are shown as a percentage of P622-CWI. Data are mean ± S.E.M from a representative experiment out of 4 (for a and c, performed in quadruplicate) independent experiments. Images (b and d) are representative of 3 independent experiments. One-Way ANOVA with Dunnett's multiple comparison test was used for statistical analyses. (*:P<0.05; **:P<0.01; ***:P<0.001; ****:P<0.0001.)

ECL2-mutations accelerate ADGRG2 degradation

To determine if the reduced expression is due to possible degradation of ECL2 mutants of P622, we isolated cell lysates at several time points post-incubation with a protein translation inhibitor, cycloheximide. The expression of the receptor with intact CWI motif remained substantially unchanged up to 8 hours post-inhibition of translation. However, the protein level of all P622-CWA, P622-CAI, and P622-CAA was significantly reduced starting at 2 hours post-inhibition and continued to diminish continuously up to 8 hours (Fig. 5.3).

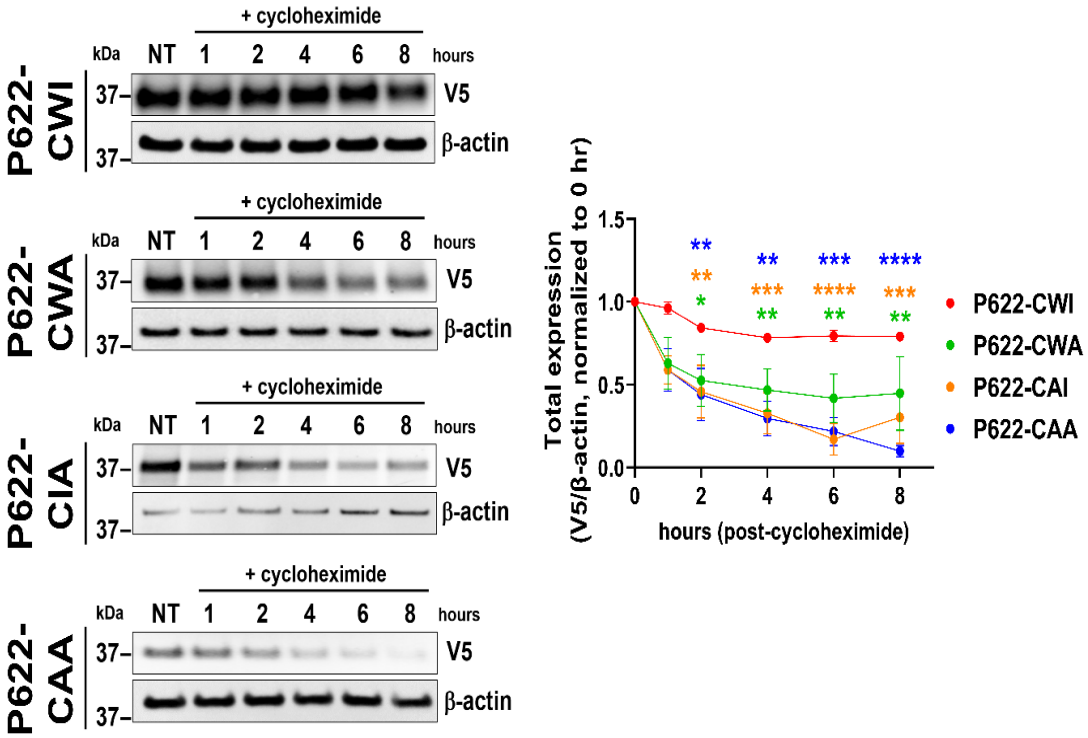

Figure 5-3 Degradation of ADGRG2-P622 is regulated by the residues in the CWI motif in the ECL2.A) HEK cells were transfected with the same dose of plasmids (1µg) expressing P622-CWI or mutants. Cells were then incubated with cycloheximide (100 µg/ml) for up to 8 hours and total cell lysates were run on SDS-PAGE, transferred to PVDF membranes, and probed with V5 and ß-actin antibodies. Differential exposure time in the iBright Imaging system was used to make the mutants visible to facilitate the band density quantification. Representative blots show a reduction of mutant receptor levels over time. **B)** Density values of V5 were normalized to that of ß-actin for each plasmid at NT (0 hours). Densitometry analyses are shown on the right. Data are mean ± S.E.M from 4 independent experiments. Two-Way ANOVA with Dunnett's multiple test was used to compare protein levels at each time point to that of basal expression (NT) of respective receptors. *:P<0.05; **:P<0.01; ***:P<0.001; ****:P<0.0001.

GPCR degradation can occur at various stages, including lysosomes and proteasomes[332]. We used inhibitors of several proteolytic processes, chloroquine (lysosomal acidification inhibitor), MG-132 (proteasomal inhibitor), and bafilomycin A1 (inhibitor of v-ATPase, endosomal acidification, and late-stage vesicle maturation) to determine the underlying mechanism of degradation of ECL2 mutants of P622. Western blotting analyses show that the expression of ECL2 mutants remained unchanged in the presence of either chloroquine or bafilomycin, and cycloheximide further decreased the receptor levels (Fig. 5.4). However, inhibition of proteasomal degradation by MG-132 substantially increased the receptor levels, though the 8-hour translation inhibition by cycloheximide in the presence of MG-132 reduced the expression to basal levels (Fig. 5.4).

This set of data reveals that mutation of conserved residues in the ECL2 of ADGRG2 induces receptor degradation via an unidentified mechanism, in addition to a proteasomal pathway.

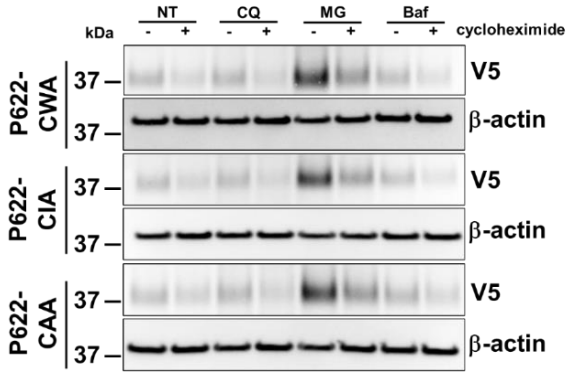

Figure 5-4 Proteasomal but not endosomal or lysosomal pathways control degradation of ECL2 mutants.(a) HEK cells were transfected with the same dose of plasmids (1 µg) expressing P622-CWA, P622-CAI, and P622-CAA. Cells were then pre-incubated with chloroquine (CQ; lysosomal acidification inhibitor, 25 µM), MG-132 (MG; proteasomal inhibitor, 1 µM), and bafilomycin A1 (Baf; inhibitor of v-ATPase, endosomal acidification, and late-stage vesicle maturation, 10 nM) overnight, followed by 8-h incubation with cycloheximide (100 µg/ml). Total cell lysates were run on SDS-PAGE, transferred to PVDF membranes, and probed with V5 and β-actin antibodies. Representative blots from 3 independent experiments are shown.

Mutation of tryptophan and isoleucine in ECL2 ablates ADGRG2-mediated induction of transcription factors

We have previously shown that the synthetic P-15 induces cAMP-response element-binding protein (CRE) transcription factor in a luciferase reporter assay. To test whether ECL2 mutations affect receptor activation by the *Stachel* peptide despite their reduced surface expression, we adjusted the dose of the transfected plasmids so that the mutants and P622-CWI receptor reach similar surface expression levels (Fig. 5.5a). This was further confirmed by immunofluorescence imaging (Fig. 5.5b). Thereafter, for all signaling assays, we adjusted the doses of mutant and P622-CWI plasmids and supplemented the total plasmid dose with empty backbone pcDNA3.1 plasmid.

Using the CRE and SRE reporter assays, we stimulated cells expressing comparable surface levels of P622-CWI and mutant receptors with increasing concentrations of P-15 or vehicle for 5 hours. The basal CRE and SRE activity was similar among P622-CWI and mutant receptors. Concentration-response curves revealed that while the P622-CWI receptor responds in a concentration-dependent manner to P-15, none of the mutants are activated by this synthetic peptide (Fig. 5.5c and d). Although the mutation of $G^{772}S^{773}$ to alanine in the ECL2 did not affect the expression level, the CRE and SRE response to P-15 was reduced by 30% and 40%, respectively (Supplemental Fig. 5 c&d).

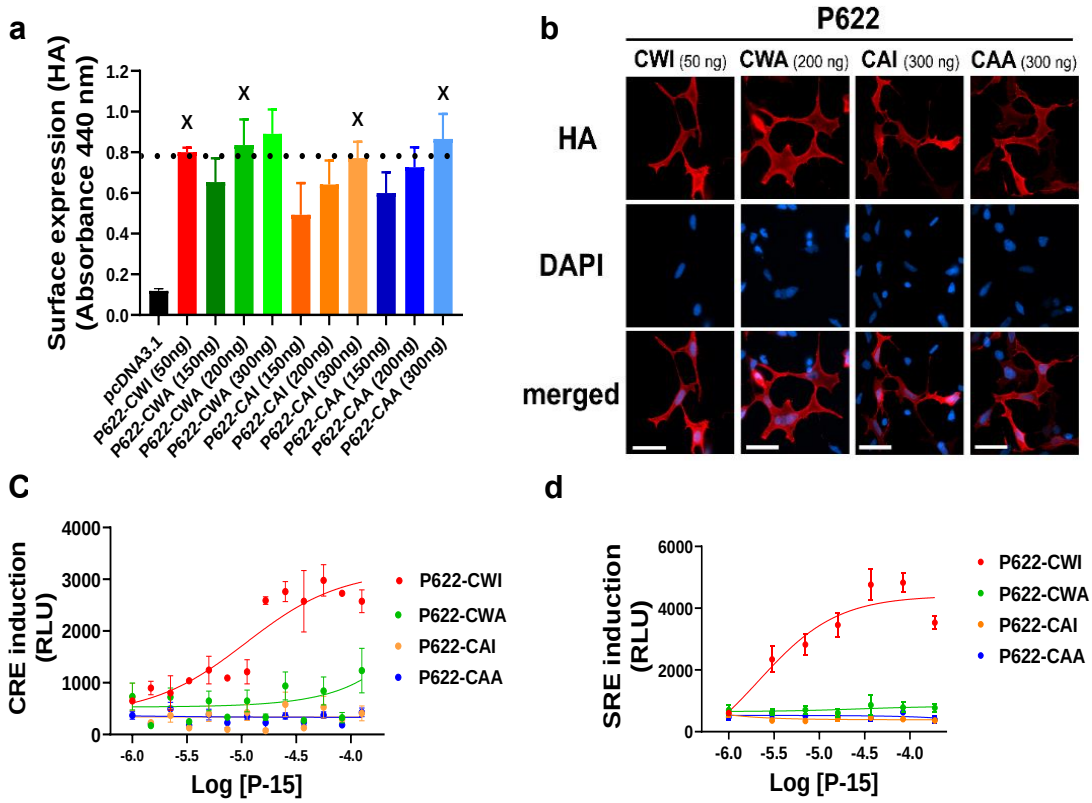

Figure 5-5 ECL2 plays a major role in ADGRG2 activation by synthetic *Stachel* peptide. **A)** HEK cells were transfected with one dose of P622-CWI (50 ng) and different doses of mutant P622 plasmids. Cell surface expression of receptors was determined by ELISA using an antibody against the N-terminal HA-tag in non-permeabilized conditions. X denotes the amount of mutant plasmids that resulted in comparable surface expression as 50 ng P622-CWI plasmid. Data are mean ± S.E.M from a representative experiment out of 3 independent experiments performed in quadruplicate. **B)** Cell surface expression of receptors, after transfection with the adjusted doses of plasmids, was determined by immunofluorescence imaging using an antibody against the N-terminal HA-tag in non-permeabilized conditions. Nuclear counterstaining with DAPI. Representative images from 3 independent experiments are shown (scale bars: 20 µm). **C-D)** Cells were transfected with adjusted doses of either P622-CWI or mutant plasmids along with either CRE-Luc **C)** or SRE-Luc **D)** plasmids. After an overnight of serum starvation, cells were activated with increasing concentrations of P-15 for 5 h. Luciferase induction was measured in a luminescence-based assay. Relative light units (RLU) recorded in a luminometer are representative from 3 independent experiments performed in triplicate and are presented as mean ± S.E.M.

We also used adjusted doses of ΔNTF-CWA, ΔNTF-CAI, ΔNTF-CAA plasmids, which resulted in similar surface expression compared with ΔNTF-CWI (Fig. 5.6a-b). Using a homogenous time-resolved FRET (HTRF) assay in the presence of IBMX, an inhibitor of phosphodiesterases, we measured the basal cAMP production and found that while ΔNTF-CWI-expressing cells show high cAMP levels, this basal activity is absent

in ECL2-mutated ΔNTF receptors (Fig. 5.6c). Also, stimulation with synthetic P-15 increased the CRE luciferase activity only in the ΔNTF-CWI expressing cells (Fig. 5.6d).

These data suggest that an intact CWI motif is essential for activation of ADGRG2 via either the self-activating *Stachel* (in ΔNTF) or the synthetic peptide. Also, residues other than CWI in the ECL2 may play a role in the activation of ADGRG2 by P-15.

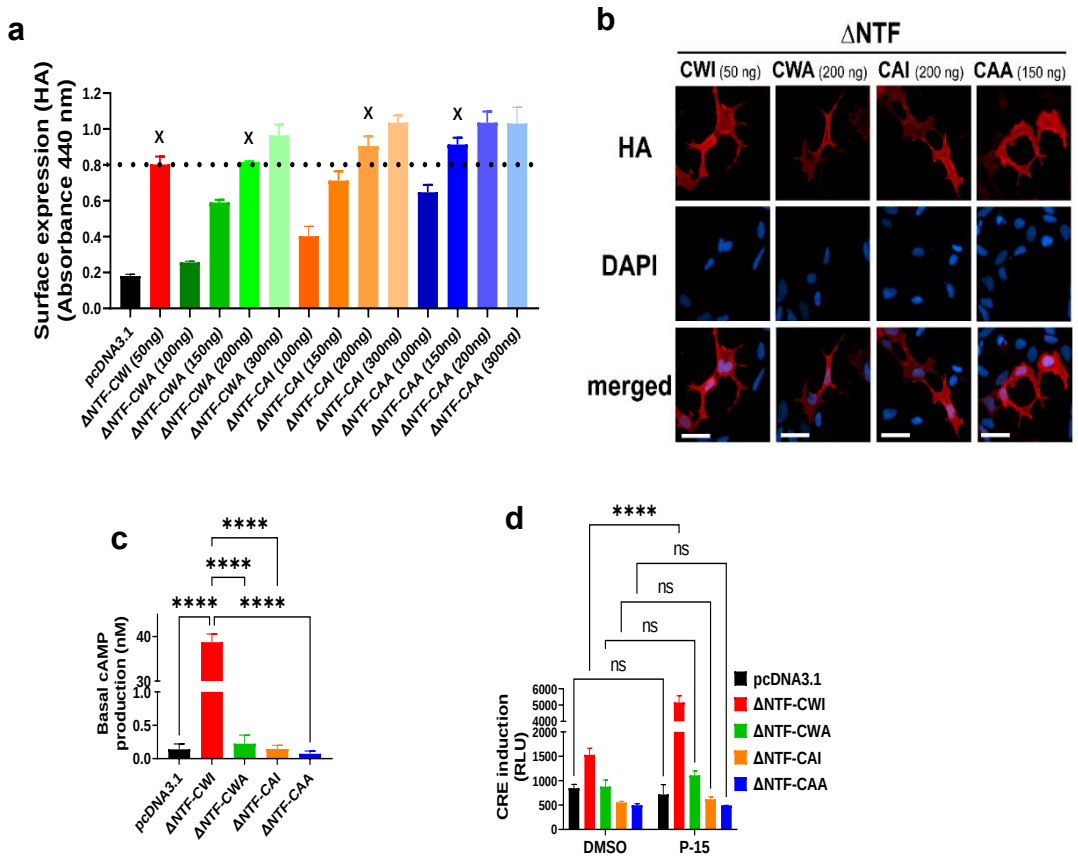

Figure 5-6 ECL2 is essential for the constitutive activity of NTF-truncated ADGRG2. A) HEK cells were transfected with one dose of ΔNTF-CWI (50 ng) and different doses of mutant ΔNTF plasmids. Cell surface expression of receptors was determined by ELISA using an antibody against the N-terminal HA-tag in non-permeabilized conditions. X denotes the amount of mutant plasmids that resulted in comparable surface expression as 50 ng ΔNTF-CWI plasmid. Data are mean ± S.E.M from a representative experiment out of 3 independent experiments performed in triplicate. **B**) Cell surface expression of receptors, after transfection with the adjusted doses of plasmids, was determined by immunofluorescence imaging using an antibody against the N-terminal HA-tag in non-permeabilized conditions. Nuclear counterstaining with DAPI. Representative images from 3 independent experiments are shown (scale bars: 20 µm). **C)** Cells were transfected with adjusted doses of either ΔNTF-CWI or mutant plasmids and pcDNA3.1 as control. Basal cAMP production was measured after overnight incubation with 0.5 mM IBMX in starvation media in an HTRF assay. cAMP production in nM is presented as mean ± S.E.M from a representative experiment out of 3 independent experiments performed in duplicate. Data were compared with ΔNTF-CWI with one-Way ANOVA with Dunnett's test. ****$P < 0.0001$. **D**) Cells were transfected with adjusted doses of either ΔNTF-CWI or mutant plasmids along with CRE-Luc plasmid. After an overnight of serum starvation, cells were activated with either vehicle (DMSO) or 100 µM of P-15 for 5 h. Luciferase induction was measured in a luminescence-based assay. Relative light units (RLU) recorded in a luminometer are mean ± S.E.M from a representative experiment from 3 independent experiments performed in triplicate. Data were compared between vehicle and P-15 for each plasmid with two-Way ANOVA with Sidak's multiple comparison test. ****$P < 0.0001$; ns: not significant.

Gαs pathway activation by the Stachel is controlled by the ECL2

We have previously used an endpoint HTRF assay to measure cAMP production downstream of ADGRG2-P622-Gαs pathway[78]. To monitor the production of cAMP in kinetic mode, we developed a new cAMP production assay by using a genetically-encoded biosensor[333]. We induced cAMP production by forskolin, an activator of adenylyl cyclase, and optimized the amount of sensor needed to reach a robust adenylyl cyclase response (Supplemental Fig 5a&b). A 20-second baseline measurement was followed by stimulation with increasing concentrations of P-15 in cells that were transfected with adjusted doses of P622-CWI and ECL2-mutated receptors (Fig. 5.7a-d). While the P622-CWI receptor responded to P-15 in a concentration-dependent manner, the mutants showed no response, except for the P622-CWA mutant that responded marginally to the highest P-15 concentration. To ensure that increased doses of transfected plasmids did not alter the responsiveness of the adenylyl cyclase-cAMP axis, we compared the forskolin-induced cAMP production. Our data show that despite increased doses of transfected mutant plasmids, cells respond similarly to the forskolin (Fig. 5.7e).

We accumulated cAMP production overnight in the presence of IBMX, and using an HTRF assay, we found that the basal levels of cAMP are comparable among receptors (Fig. 5.7f). A 2-hour stimulation with P-15 resulted in a concentration-dependent production of cAMP by the P622-CWI receptor (Fig. 5.7g) and a modest response by the P622-CWA mutant.

Together, these data show that induction of the Gαs-adenylyl cyclase-cAMP pathway by *Stachel* is dependent on the presence of an intact ECL2.

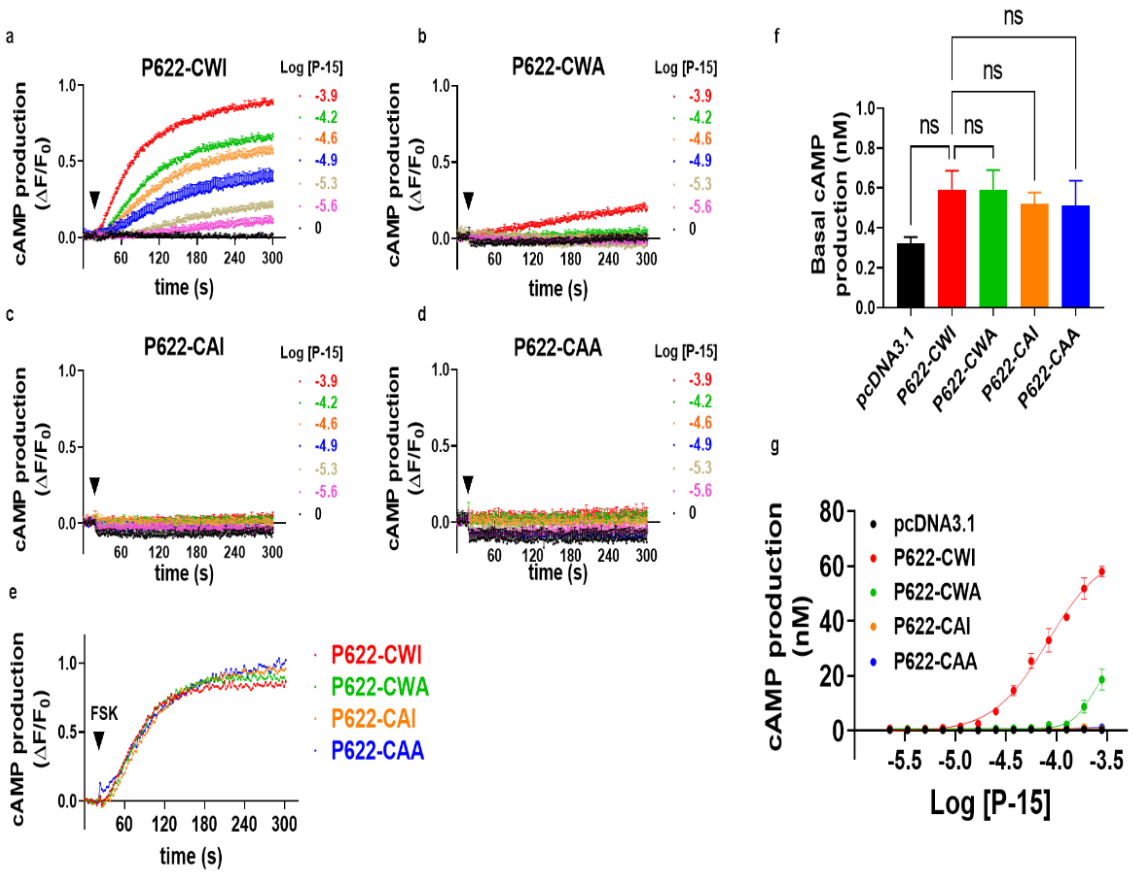

Figure 5-7 ECL2-mutated ADGRG2-P622 receptors are not activated by P-15. (**A**–**D**) Cells were transfected with adjusted doses of P622-CWI and mutant plasmids and were transduced with a cAMP biosensor overnight. After a 20-s basal recording of fluorescence (Ex: 488 nm; Em: 525 nm), cells were activated with increasing concentrations of P-15 (arrowheads), and fluorescence was recorded for another 280 s. Relative fluorescence unit (RFU) data were analyzed in GraphPad Prism and are presented as change in RFU divided by the initial RFU (ΔF/F0). **E)** Cells transfected with adjusted doses of plasmids and biosensor were stimulated with 1 µM forskolin (FSK). Data are mean ± S.E.M and are representative of 3 independent experiments performed in triplicate. **F)** Basal cAMP production was measured after overnight incubation with 0.5 mM IBMX in starvation media in an HTRF assay. cAMP production in nM is presented as mean ± S.E.M from a representative experiment out of 3 independent experiments performed in triplicate. Data were compared with P622-CWI with one-Way ANOVA with Dunnett's test. ns: not significant. **G)** Cells were stimulated with increasing concentrations of P-15 for 2 h and cAMP production in nM was measured in an HTRF assay. Data are mean ± S.E.M from a representative experiment from three independent experiments performed in duplicate.

ECL2 mutations derail the whole-cell response to P-15

We and others have shown that ADGRG2 couples to multiple signaling pathways including $G\alpha_q$, $G\alpha_s$, and $G\alpha_{13}$[78, 108, 287, 324]. Considering that measuring the production of either a single second messenger (e.g. cAMP) or induction of a couple of transcription factors (e.g., CRE and SRE) cannot detect the 'overall' response of cells to GPCR ligands, whole-cell label-free assays have been developed (Fig. 5.8A)[334-337]. To investigate if the overall response of cells to synthetic P-15 is regulated by the ECL2 conserved residues, we developed a new non-invasive whole-cell label-free impedance assay. Activation of P622-CWI-transfected cells with P-15 resulted in a rapid decrease in cell monolayer impedance to 1kHZ frequency of electrical field voltage (Fig. 5.8B). However, neither empty plasmid nor ECL2-mutated receptors responded to the P-15 stimulation.

This data confirms the lack of receptor activation by *Stachel* peptide in the absence of ECL2 conserved tryptophan and isoleucine residues.

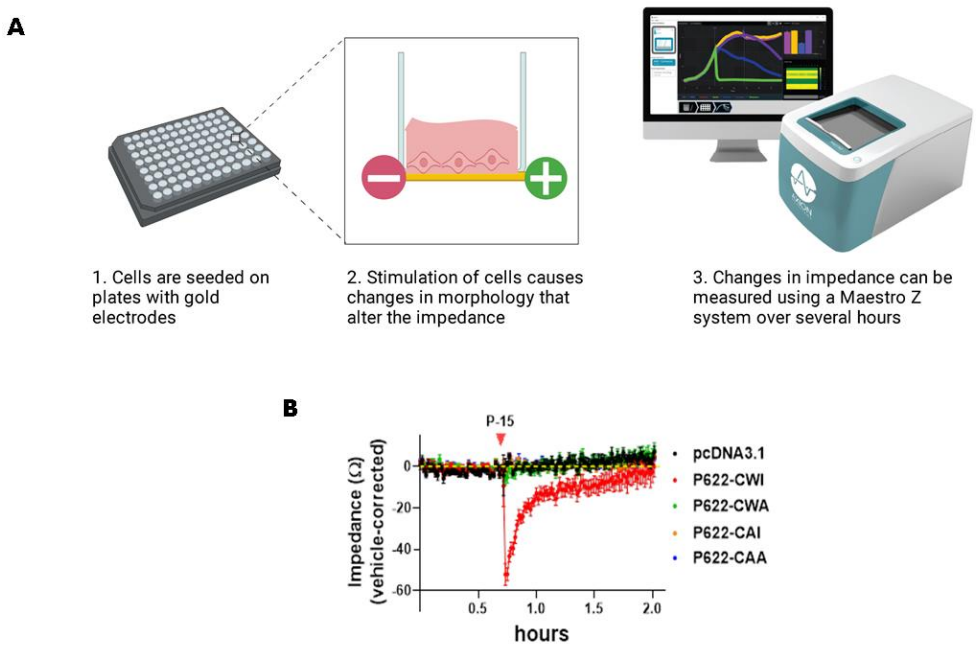

Figure 5-8 Whole-cell impedance assay shows a lack of activation of the ECL2-mutated ADGRG2 receptor by the Stachel peptide. Cells were transfected with adjusted doses of WT and mutant plasmids and were then seeded in plates that have electrodes at the bottom of each well to apply various frequencies of electric voltages. Serum-starved cells, at monolayer confluency, were kept in the Maestro Z device until the recorded impedance (Ω) reached a steady state. Cells were stimulated with either vehicle (DMSO) or 100 µM P-15 and impedance was recorded for up to 2 h. Data are corrected to that of the vehicle for each plasmid and are mean ± S.E.M from a representative experiment out of 3 independent experiments conducted in quadruplicate.

Discussion

Our understanding of the mechanisms of activation of aGPCRs has substantially increased over the last decade. This progress was made possible due to basic pharmacology and cell biology studies in various cellular backgrounds and model organisms[100, 111, 210, 290, 325]. Now we know that binding of an extracellular molecular partner to the NTF of ADGRG1 dissociates it from the CTF and unmasks a *Stachel* sequence, which subsequently activates ADGRG1[109, 117, 338]. Similar mechanisms of activation exist for a few other aGPCRs[112, 324]. A comprehensive mutational analysis of ADGRL1 revealed that several residues in the transmembrane domains regulate the constitutive activity of this

aGPCR[128]. The same study also predicted a non-conserved tyrosine at the end of ECL2, which regulates *Stachel*-mediated signaling of ADGRL1. However, the binding site of the *Stachel* on a majority of aGPCRs remains largely unknown. Structural similarities of class B1 GPCRs to aGPCRs (formerly class B2) and the fact that class B1 receptors bind to peptide hormones provides hints on the possible binding site of the *Stachel*. Specifically, the ECL2 forms an orthosteric binding pocket for peptide hormones in PTH 1 receptor (PTH1R)[339] and corticotropin-releasing factor 1 receptor (CRFR1)[340]. In the current study, we tested the role of conserved residues in and around the CW motif of the ECL2 in the activation of an NTF/*Stachel*- or NTF-truncated ADGRG2 (P622 and ΔNTF) by its *Stachel*, P-15 (Fig. 4.9). Our results provide evidence that the lack of isoleucine and/or tryptophan in the ECL2 not only completely abolishes the signaling pathways of ADGRG2 but also dysregulates receptor stability in HEK293 cells (Fig. 5.3).

We focused on the ADGRG2-P622 receptor in this study because we had previously shown that ADGRG2-P622 responds significantly more to the synthetic P-15 in comparison to the full-length receptor (ADGRG2-FL) in a battery of assays[78]. This maximal response by ADGRG2-P622 is presumably due to the availability of the binding site for P-15, which might be masked by the NTF in ADGRG2-FL. The lack of constitutive activity in cells that express ADGRG2-P622 in the current study confirms the role of endogenous *Stachel* in the activation of ADGRG2.

Here, we used several readouts to assess receptor response to the synthetic peptide. The use of kinetic and endpoint cAMP production assays allowed us to measure the Gαs signaling of ADGRG2. Genetically encoded biosensor and HTRF assays showed a lack of activation of ECL2 mutants either in the short-term (minutes) or long-term (2 hours). We

supplemented these assays with CRE and SRE reporter assays, in which cells are activated for 5 hours. Both assays showed that ECL2 mutants are not activated by P-15, suggesting that the coupling of both $G\alpha_s$ and $G\alpha_{13}$ proteins to ADGRG2 is ablated in the absence of either tryptophan or isoleucine or both. To assess other possible but unknown signaling pathways that may originate from ADGRG2, we developed a whole-cell label-free impedance assay. We have previously used similar label-free assays to study GPR55 and cannabinoid 2 receptor[341, 342]. This method allowed us to measure the overall response, rather than a singular signaling pathway, from a monolayer of cells upon activation with P-15 in kinetic mode. Using this readout, we observed a strong, fast *Stachel*-specific reduction of impedance from WT receptor-expressing cells, indicating possible movement of cells and consequent disruption of cell-cell contact in the monolayer. This response was transient, and impedance was mostly restored in 15 min. Nevertheless, we did not detect a response from cells expressing any of the ECL2 mutated receptors, further confirming the lack of activation by P-15.

It is noteworthy that mutant receptors were degraded in the absence of either endogenous or synthetic *Stachel* peptides. Do the ECL2 mutations induce constitutive activity followed by sustained internalization and degradation? This does not seem to be plausible because we did not detect any altered basal activity of P622, either in CRE reporter assay or cAMP production assays. We observed a similar pattern of degradation in ECL2-mutated ΔNTF receptors; however, those mutants lacked the constitutive activity of ΔNTF, further suggesting that: 1) ECL2 plays a role in the activation of ADGRG2 and 2) degradation of ECL2 mutants is not due to constitutive activity or presence of the *Stachel*. The P622-$^{G772A/S773A}$ mutant, in which the CWI motif is intact but glycine^{772} and

serine[773] of the ECL2 are mutated, however, was not degraded. This mutant showed only a 30-40% reduction in signaling to CRE and SRE, which is a much smaller effect than the mutations in the CWI motif (~100% reduction). This suggests that while residues of the CWI motif regulate both receptor stability and signaling, other non-conserved residues of the ECL2 contribute to ADGRG2 response to synthetic P-15, and this effect is independent of receptor stability.

Do the ECL2 mutations hinder receptor transport and incorporation into the plasma membrane? Our western blotting, ELISA, and immunofluorescence imaging data suggest that the diminished surface expression of mutants is likely to be due to the fast degradation of receptors upon translation. We have previously shown that ADGRG2-ΔNTF gets ubiquitinated but is expressed on the plasma membrane at levels comparable to that of the full-length ADGRG2[78, 94]. Our current data show that the degradation of P622 mutants is mediated in part by proteasomal pathways but not via endosomal or lysosomal pathways. Further detailed studies are needed to unravel how the isoleucine and tryptophan of ECL2 impact these degradation mechanisms and whether the transport of ECL2 mutants via Golgi apparatus is impaired. Interestingly, a previous study showed that many of the mutants of ADGRL1 with blunted activity have significantly reduced surface expression[128], although the underlying cause(s) for such reduction was not explored.

Irrespective of the underlying reason for diminished receptor levels and degradation, we adjusted the surface expression levels by increasing the dose of the transfected plasmids and conducted our signaling assays in this condition. Nevertheless, comparable surface expression of ECL2-mutated and P622 or ΔNTF receptors did not rescue their response to P-15, supporting the role of ECL2 in *Stachel*-mediated activation

of ADGRG2. Whether the ECL2 of other aGPCRs play similar roles in receptor stability and activation by *Stachel* peptides warrants further studies.

While finalizing this manuscript, we noticed that a separate group reported that several residues, including the tryptophan and isoleucine of the ECL2, participate in the binding of *Stachel* peptide to ADGRG2[343]. Although this study corroborates some of our findings, differences exist between the two studies. We used 'human' ADGRG2-P622 that lacks the NTF and the *Stachel* sequence to prevent interaction of the endogenous P-15 on the N-terminus of the receptor with the receptor in addition to ADGRG2-ΔNTF. Sun et al., however, determined the binding of a 'mouse' P-15 that was modified at several residues to the 'mouse' ADGRG2 ortholog. This modified P-15 showed higher potency compared to natural P-15 and is potentially a new pharmacological tool for future ADGRG2 studies. However, its application remains to be validated by testing whether it shows affinity or activity towards other aGPCRs that share similar *Stachel* sequence and ECL2 motifs as ADGRG2. Another major difference between these two studies is that while we observed a significant alteration of ECL2-mutated receptor stability and cell surface expression, Sun et al. did not report such changes.

Lack of activation of P622 or ΔNTF by the *Stachel* could be due to either impaired binding of the peptide to the ECL2 or impaired signaling of receptor irrespective of peptide binding. Although we did not directly examine the binding affinity of the P-15 to the ECL2 mutants, authors of the recent paper[343] showed that mutations in TM6 and ECL2 abolish the binding of a modified *Stachel* to the ADGRG2.

ADGRG2 plays various physiological and pathological roles. For instance, mutations or truncations in ADGRG2 are associated with different forms of male

infertility[344, 345], and male *adgrg2*-null mice are infertile[301]. ADGRG2 also promotes proliferation and metastasis of Ewing sarcoma cells both *in vitro* and *in vivo*[171]. We have previously shown that ADGRG2 is enriched in parathyroid glands, is upregulated in parathyroid adenomas from patients with primary hyperparathyroidism, and its activation by P-15 elevates PTH secretion[94]. Although ADGRG2 is still an orphan aGPCR, our findings on the role of ECL2 in receptor stability and *Stachel*-mediated activation provide a foundation for future targeting of this receptor via small molecules or biologics (Fig.. 5.9).

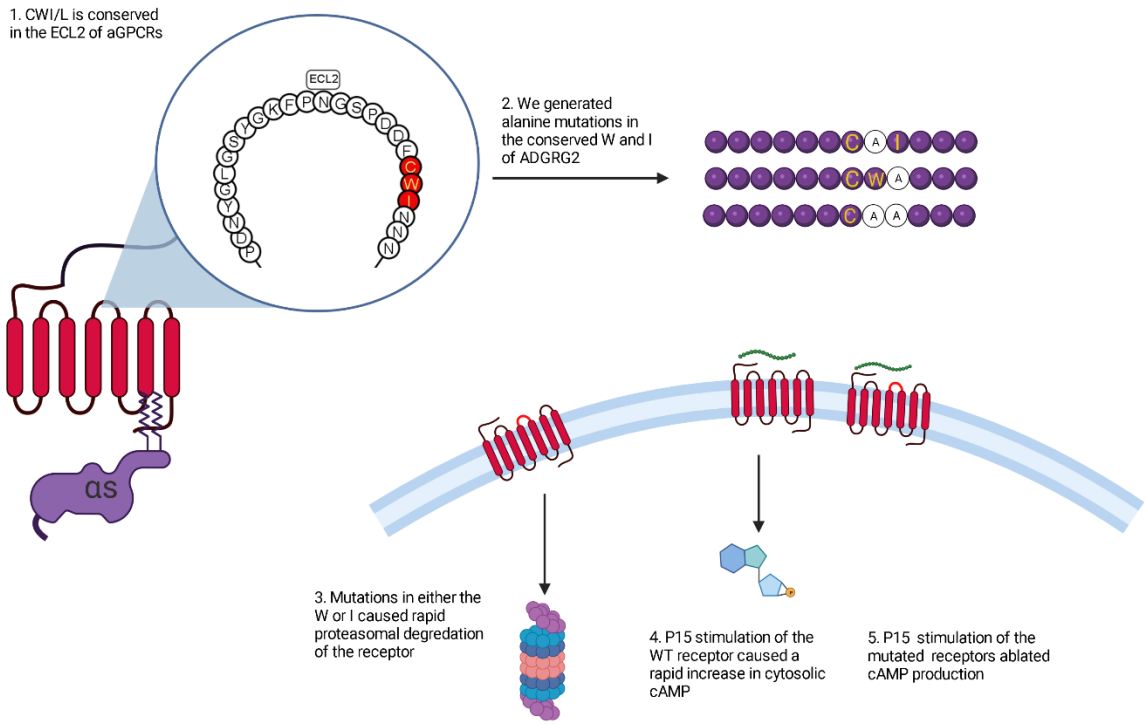

Figure 5-9 Graphical summary of the effect of ECL2 mutations on ADGRG2 expression, stability and signaling. We found a conserved CWI/L motif among most aGPCRs. Alanine mutations in the conserved W and I of ADGRG2 led to decreased receptor expression, due to rapid proteasomal degradation. Furthermore, stimulation with P15 showed no effect on the ECL2 mutated receptors which indicates a necessary role for this motif in ADGRG2 signaling.

Supplemental Figures

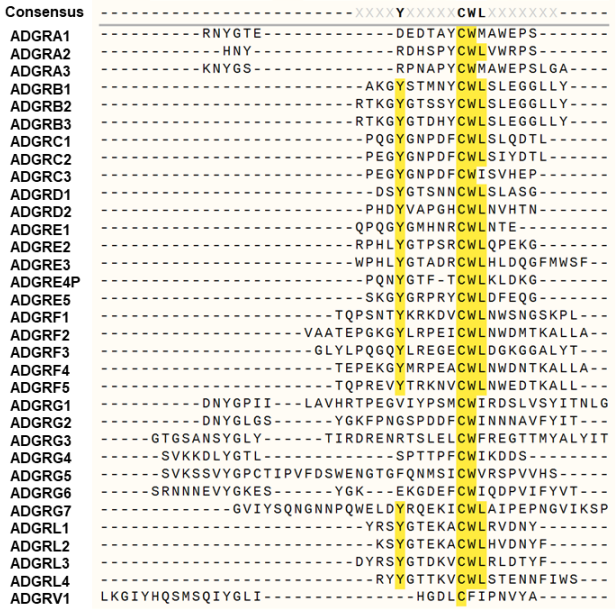

Supplemental Fig 5-1 Multiple alignments of the ECL2 of all 33 members of the aGPCR family. Predicted amino acid sequences of the ECL2 for each aGPCR were derived from Uniprot. The alignment was conducted in SnapGene software (from Insightful Science; available at www.snapgene.com) using the Clustal Omega algorithm.

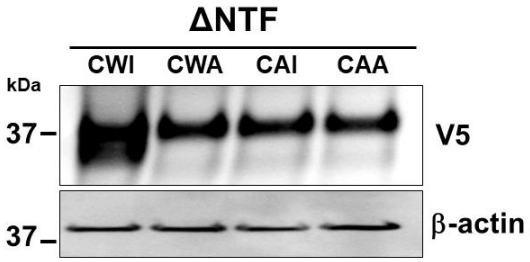

Supplemental Fig 5-2 HEK cells were transfected with the same dose of plasmids (1 μg) expressing ΔNTF-CWI or mutants. Total cell lysates were run on SDS-PAGE, transferred to PVDF membranes, and probed with V5 and β-actin antibodies. Representative blots (from 3 independent experiments) show differential levels of mutant receptors compared with ΔNTF-CWI.

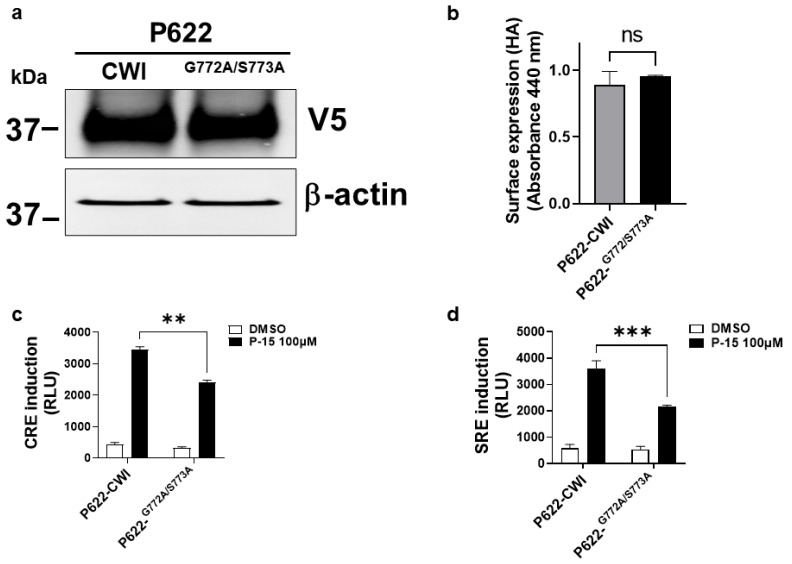

Supplemental Figure 5-3 A) HEK cells were transfected with the same dose of plasmids (1 µg) expressing P622-CWI (G772S773) or mutant (P622- G772A/S773A). Total cell lysates were run on SDSPAGE, transferred to PVDF membranes, and probed with V5 and β-actin antibodies. Representative blots (from 3 independent experiments) show similar levels of receptors. **B)** HEK cells were transfected with the same dose (50 ng) of plasmids expressing P622-CWI (G772S773) or mutant (P622- G772A/S773A). Cell surface expression of receptors was determined by ELISA using an antibody against the N-terminal HA-tag in non-permeabilized conditions. Data are mean ± S.E.M from a representative experiment out of 3 independent experiments performed in triplicate. t-test was used for statistical analyses; ns: not significant. **C-D)** Cells were transfected with 50 ng of either P622-CWI (G772S773) or mutant (P622- G772A/S773A) plasmids along with either CRE-Luc or SRE-Luc plasmids. After an overnight of serum starvation, cells were activated with either DMSO or 100 µM of P-15 for 5 hours. Luciferase induction was measured in a luminescence-based assay. Relative light units 40 (RLU) recorded in a luminometer are mean ± S.E.M from a representative experiment from 3 independent experiments performed in duplicate. Data were compared with P622-CWI with two Way ANOVA with Sidak's multiple comparison test. **:P<0.001.

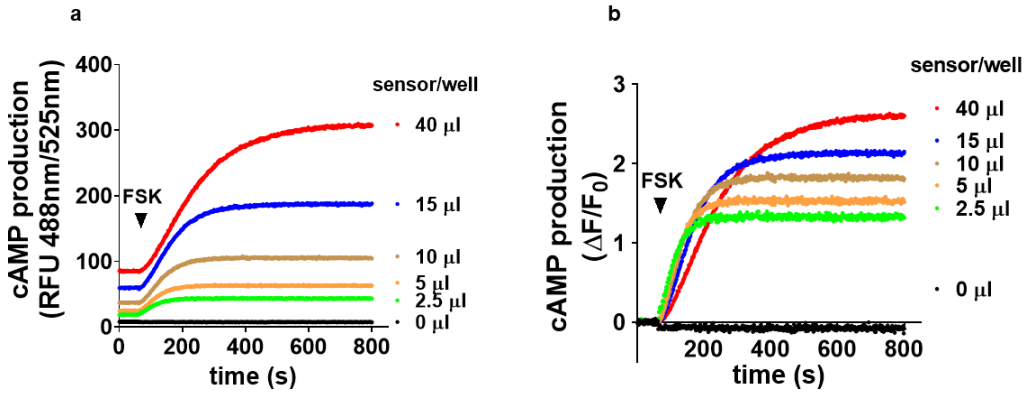

Supplemental Figure 5-4 Characterization of a fluorescent genetically encoded cAMP sensor. HEK cells were transduced with various amounts of Upward Green cADDis cAMP sensor in 96-well plates overnight. Cells were washed with assay buffer and then the fluorescence (Excitation at 488 nm/Emission at 525 nm) was recorded for 1 min before and 12 min after addition of 10 µM FSK. **A)** Raw data showing the relative fluorescence units (RFU) for each amount of sensor. **B)** Data were analyzed in GraphPad Prism and are presented as change in RFU divided by the initial RFU (ΔF/F0).

Chapter 6 - Future Directions

Summary

PHPT is a common and important disease with a hallmark feature of abnormal Ca^{2+} sensing by parathyroid CaSR. The medical and surgical advancements in PHPT treatment have significantly increased the quality of life for PHPT patients, but they fall short in addressing the root cause of the disease. Cinacalcet is a calcimimetic drug that allosterically binds to the CaSR to increase its sensitivity to serum Ca^{2+} and reduce PTH secretion. Unfortunately, cinacalcet does not affect the bone symptoms of PHPT; therefore, some patients require combination therapy with bisphosphonates to preserve bone density. Nevertheless, its efficacy suggests that understanding CaSR signaling will be important to both understanding and treatment of this disease.

Several genetic abnormalities have been identified in parathyroid adenomas, including heritable syndromes and sporadic mutations. While these abnormalities have been essential in our understanding of parathyroid tumor pathogenesis, they are not ubiquitous in PHPT patients. To develop more broadly applicable therapeutics, they must correct abnormalities seen across all parathyroid tumor diseases. The common factor among all PHPT patients is an inability of the parathyroid glands to inhibit PTH secretion in response to serum Ca^{2+} levels. The mechanisms of Ca^{2+} insensitivity are a topic of dispute in the literature. While some groups have found that CaSR is downregulated in parathyroid tumors, we have seen no alterations in CaSR expression. Therefore, we hypothesized that the dysregulation of CaSR is not inherent to the receptor but a result of interacting molecules which dampen the CaSR response to Ca^{2+}.

We performed an RNA transcriptome screen to identify modifiers of CaSR function. RGS5, a GAP protein was differentially expressed in parathyroid adenomas compared to normal parathyroid glands. Therefore, we hypothesized that RGS5 might function to inhibit the signaling of CaSR. Transgenic mice that overexpress RGS5 in the parathyroid glands develop PHPT symptoms. RGS5 overexpression caused decreased bone density, hyperparathyroidism, and hypercalcemia in transgenic RGS5 mice. These results supported our central hypothesis that CaSR-modifying proteins are responsible for the dysregulation of PTH secretion and CaSR dysfunction in PHPT. Recapitulating PHPT phenotypes by overexpressing RGS5 was the precedent for studying other potential modifiers of CaSR function.

ADGRG2 is an aGPCR, the second largest family of GPCRs, and while these receptors have diverse functions in many diseases and physiological functions, they are understudied relative to other GPCR families. We identified ADGRG2 in a transcriptome microarray in 2015; at the time, this protein had no known function and was previously thought to be expressed only in epididymal tissue. We found that ADGRG2 was differentially expressed in parathyroid tissues and overexpressed in parathyroid tumors. We hypothesized that, like RGS5, ADGRG2 might play an essential role in parathyroid tumor biology and CaSR dysregulation.

We developed a transgenic mouse model with parathyroid-restricted overexpression of ADGRG2. These mice were aged for seven months, followed by an interrogation of their biochemical profiles, bone histomorphometry, and histological assessment of their parathyroid glands. Parathyroid overexpression of ADGRG2 caused the development of stereotypical PHPT phenotypes, including adenomatosis,

hypercalcemia, and hyperparathyroidism. Bone histomorphometry showed no significant alterations at the seven months time point. The recapitulation of PHPT phenotypes in this mouse led us to design a battery of *in-vitro* studies to identify any crosstalk between CaSR and ADGRG2.

Our early *in-vitro* reports, using transient models, found that ADGRG2 showed no downstream signaling activity in response to P15. Previously published data was collected using constitutively active mutated receptors. To gain a more biologically accurate view of ADGRG2 activity, we developed stable HEK293 models which stably express ADGRG2 and CaSR, alone or in combination. The stable cell lines responded to P15 stimulation and provided the tools necessary for studying the mechanisms of ADGRG2-CaSR crosstalk.

CaSR signals via two well-defined signaling pathways, the $G\alpha_i$ and $G\alpha_{q,}$ which inhibit cAMP and increase intracellular Ca^{2+} release, respectively. CaSR responds to extracellular $Ca^{2+,}$ and its activity inhibits PTH secretion. When extracellular Ca^{2+} levels decrease, CaSR is inactive, and PTH is released to increase serum $Ca^{2+,}$ which functions as a negative feedback mechanism to activate CaSR. We tested the ability of ADGRG2 to modulate both the $G\alpha_i$ and $G\alpha_q$ pathways using kinetic signaling assays. Using a biosensor for Gai activity, we found that the activation of ADGRG2 completely inhibited CaSR Gai activation. We also utilized a dye-based intracellular Ca^{2+} mobilization assay to assess CaSR $G\alpha_q$ activity. Co-stimulation of ADGRG2 and CaSR with both P15 and Ca^{2+} caused a decrease in intracellular Ca^{2+} mobilization. These results indicate that ADGRG2 counteracts both canonical CaSR signaling pathways.

There is increasing evidence of the importance of intracellular trafficking for proper GPCR function. CaSR is known to maintain signaling within the early endosome, and the inability of CaSR to traffic into the endosome is a hallmark of FHH3, a disease with a similar presentation to PHPT[304]. We have also shown that ADGRG2 maintains $G\alpha_s$ signaling from the early endosome[78]. To test whether the co-stimulation of ADGRG2 and CaSR affected proper intracellular trafficking, we conducted live confocal imaging using SNAP and CLIP tags. These tags were covalently linked to nonpermeable fluorescent substrates, which allowed us to monitor the movement of these receptors in real time. We found that co-stimulation with Ca^{2+} and P15 caused the receptors to maintain surface expression and inhibited trafficking into the cytosol. These results confirm our previous report that ADGRG2 and CaSR physically interact only in an active state, and we now know that this interaction disrupts proper trafficking.

Our results show that ADGRG2 is actively opposing the functionality of CaSR, and it is a surface receptor with a limited expression profile. These results indicate that ADGRG2 may serve as a target for future therapeutic development. To identify targetable regions of ADGRG2, we aligned all 33 members of the aGPCR family and found a highly conserved CWI/L motif in the ECL2. The ECL2 of other receptors is known to play an important role in receptor activity; therefore, we hypothesized that the conserved CWI of ADGRG2 may be an essential motif for its function. We created mutations in the W and I of ADGRG2 and expressed these mutants in HEK293 cells. Stimulating ADGRG2 ECL2 mutants with P15 showed complete ablation of signal both in endpoint (luciferase and HTRF) and kinetic (Upward $G\alpha_s$ biosensor) assays. Using an impedance assay, we measured the whole-cell response of ADGRG2 mutants

to P15 stimulation, and we confirmed the ablation of response to P15 in ECL2 mutants. We also found that mutations in either conserved residues disrupt receptor stability and cause rapid proteasomal degradation.

Our studies on ECL2 may have broad implications beyond PHPT. Interestingly, other groups have confirmed an essential role of this conserved CWI/L motif in other aGPCRs[346-348]. Given the variety of aGPCR functions and expression across human physiology and pathology, these studies could represent the first step in aGPCR therapeutics for several other disease states.

Limitations

HEK293 cells are a robust system for studying receptors and signaling pathways, but they are extremely limited in their capacity to produce functional data. Our HEK293 cell lines all recapitulate the signaling pathways of CaSR and ADGRG2, but without the ability to secrete PTH, we can only make inferences about the cross-talk of these receptors in parathyroid cells. Although several attempts have been made, there are currently no human parathyroid cell lines, making mechanistic studies extremely difficult. Therefore, we were limited to using HEK293 cells, which we modified to express receptors of interest and primary cells.

Culture and manipulation of primary parathyroid cells present complications. After dispersion, primary cells rapidly lose viability, limiting the number of experiments performed. We made several attempts to knock-down ADGRG2 using lentiviral shRNA, but the cells did not remain viable long enough for the protein to turnover. Furthermore, the tissue size collected is minimal and often would not provide enough cells to do

relevant experiments. More research into the development of parathyroid cell lines and primary cell culture methods is needed to overcome these hurdles.

To have a more biologically relevant model system, we generated a transgenic mouse that overexpresses ADGRG2 in the parathyroid glands. We performed these experiments with heterozygous mice due to embryonic lethality of homozygous expressing animals. Due to time constraints, we could only conduct a small pilot experiment using ten transgenic mice. Each animal requires a minimum of seven months for the onset of symptoms and potentially one year for bone phenotypes to appear. To fully characterize these transgenic mice, these experiments will be repeated with older mice, at least one year to allow for complete symptom development.

The unique signaling mechanism of aGPCRs limited our abilities to stimulate ADGRG2 in a biologically relevant manner. aGPCRs express a large NTF which shields a bound agonist known as the *Stachel* peptide. The endogenous ligand of an aGPCR binds to the NTF and causes its dissociation, allowing the *Stachel* peptide to interact with the receptor and activate downstream signaling. Most aGPCRs are orphan receptors, and to exogenously activate these receptors, a synthetic *Stachel* peptide must be employed. Unfortunately, without the endogenous ligand, we do not see the dissociation of the NTF, which may be dampening the overall receptor signal.

The lack of an endogenous ligand also limits our ability to understand the role of ADGRG2 in parathyroid biology. While we identified its role in parathyroid adenomas and its crosstalk with CaSR, ADGRG2 has no known function in normal glands. Deorphanization of the aGPCRs is a significant focus for many groups, and several receptors have been deorphanized in the past few years. Uncovering the endogenous

ligand for ADGRG2 would provide a more relevant agonist for *in-vitro* and *ex-vivo* experiments. It would also elucidate the physiologic role of ADGRG2 in normal parathyroid glands.

Trafficking of GPCRs is a growing area of research, and our results provide a preliminary glimpse into the complex trafficking patterns of ADGRG2 and CaSR. SNAP and CLIP tags are incredibly versatile tags, but we can only definitively state that the receptors are trafficking in response to stimulation, but the specific localization is not yet clear. Furthermore, the SNAP and CLIP substrates are nonpermeable to the cell membrane and do not allow us to visualize the trafficking from the ER to the cell surface. Based on our knowledge of GPCR trafficking in the literature and our data, we can surmise that the receptors localize to the endosome, but further experimentation will be needed to confirm these results.

Conclusion & Future Directions

Ca^{2+} sensing and PTH dysregulation is a hallmark of all parathyroid tumors, but the exact mechanisms of these pathologies have not been identified. Based on our results, we identified ADGRG2 as a potential modifier of the CaSR function. To fully elucidate the functional action of ADGRG2, these experiments must be confirmed in primary human parathyroid cells. Our previous attempts at knocking down ADGRG2 in parathyroid cells failed due to the reduced viability of primary cells. As the field of primary cell culture evolves, we may identify new methods for parathyroid cell culture or immortalization; this would provide us with the tools to better test the role of ADGRG2 in human cells. To test the therapeutic potential of ADGRG2 inhibition, we are currently

developing an ADGRG2 knock-out mouse that would provide us with the most biologically relevant yet feasible model system.

The discovery of ECL2 as an essential motif for P15-mediated ADGRG2 activity provides a novel mechanism for receptor inhibition. We are currently exploring therapeutic development methods, particularly biologics that block the conserved CWI motif in the ECL2. By blocking the CWI motif with an antibody, we could successfully blunt the action of ADGRG2 while avoiding the viability issues seen with lentiviral transduction of primary cells. This biologic would also serve as the first step in potential therapeutic development. By dosing ADGRG2 overexpressing mice with an ECL2-CWI blocking antibody, we should see a decrease in hyperparathyroidism, hypercalcemia, and adenoma development.

The trafficking alterations identified in our SNAP and CLIP experiments require further experimentation. One of the significant limitations of using these tags is their transient nature. Our data have shown that transient expression of ADGRG2 leads to much weaker overall signaling output when compared to stable cell lines. Therefore, to better employ the SNAP and CLIP tag system, we will generate stable cell lines of SNAP-G2 and CLIP-CaSR to be more biologically accurate. We also plan to combine these tags with markers for various organelles, particularly the endosome and membrane, to understand better where these receptors traffick upon stimulation. Finally, to better quantitate the effect of trafficking on cell signaling, we plan to recapitulate these experiments in a plate assay. By treating our double expressing cell line with Dyngo, a dynamin inhibitor, we can inhibit endocytosis and measure the downstream signaling

partners of ADGRG2 and CaSR. These experiments will help uncover the role of trafficking in the downstream signaling of both receptors.

We do not have live-cell data of ADGRG2 and CaSR interacting; those data were collected using transiently expressed receptors in a Co-IP assay. We will employ a Nano-Glo luciferase assay system to confirm protein-protein interaction in live cells. This assay uses a nanoluciferase molecule split into two units independently fused to proteins of interest. By expressing two nanoluciferase-bound molecules in a single cell, the cleaved nanoluciferase should reassemble and produce a luminescent signal if the molecules are proximal to one another. We have fused ADGRG2 and CaSR with the cleaved nanoluciferase molecules and are currently optimizing this system to determine protein-protein interaction in live cells.

We have defined a novel role for ADGRG2 in PHPT, but we believe this work expands far beyond parathyroid biology. ADGRG2 is typically restricted to epididymal or parathyroid tissue, but several groups have recently reported its overexpression in various cancer modalities. Specifically, ADGRG2 is overexpressed in Ewing's sarcoma and breast cancer cells. In the future, we hope to use what we have learned about ADGRG2 and aGPCRs as a whole and interrogate their function and therapeutic potential in other diseases. If we successfully develop antibodies against the CWI motif of ADGRG2, we hope to use it as a tool to understand better the role of ADGRG2 in these more aggressive diseases.

The current literature surrounding ADGRG2 does not focus on parathyroid biology but its role in epididymal biology. ADGRG2 is expressed in the efferent ducts and the proximal epididymis. Studies have identified that mutations of ADGRG2 can

cause male infertility. ADGRG2-null mice have decreased sperm motility and altered sperm morphology[349]. The rate of male infertility has dramatically increased continuously in the past years; therefore, developing novel fertility therapeutics is of the utmost importance. Developing an ADGRG2 ECL2 blocking antibody could be the foundation of ADGRG2-targeted male contraception and fertility treatment.

The field of aGPCR research is rapidly growing, and advances in cell biology techniques have significantly increased our ability to interrogate this novel class of receptors. The opportunities for aGPCRs to serve as diagnostic, prognostic, and therapeutic targets is an essential avenue for future investigation.

References

1. Taterra, D. *et al.* The prevalence and anatomy of parathyroid glands: a meta-analysis with implications for parathyroid surgery. *Langenbecks Arch Surg* **404**, 63-70 (2019).

2. Talmage, R.V. & Kraintz, F.W. Progressive changes in renal phosphate and calcium excretion in rats following parathyroidectomy or parathyroid administration. *Proc Soc Exp Biol Med* **87**, 263-267 (1954).

3. Cha, S.K., Wu, T. & Huang, C.L. Protein kinase C inhibits caveolae-mediated endocytosis of TRPV5. *Am J Physiol Renal Physiol* **294**, F1212-1221 (2008).

4. van Abel, M. *et al.* Coordinated control of renal Ca(2+) transport proteins by parathyroid hormone. *Kidney Int* **68**, 1708-1721 (2005).

5. Fu, Q., Jilka, R.L., Manolagas, S.C. & O'Brien, C.A. Parathyroid hormone stimulates receptor activator of NFkappa B ligand and inhibits osteoprotegerin expression via protein kinase A activation of cAMP-response element-binding protein. *J Biol Chem* **277**, 48868-48875 (2002).

6. Xing, L., Schwarz, E.M. & Boyce, B.F. Osteoclast precursors, RANKL/RANK, and immunology. *Immunol Rev* **208**, 19-29 (2005).

7. Wallig, M.A. Chapter 20 - Endocrine System, in *Fundamentals of Toxicologic Pathology (Third Edition)*. (eds. M.A. Wallig, W.M. Haschek, C.G. Rousseaux & B. Bolon) 565-624 (Academic Press, 2018).

8. Baloch, Z.W. & Livolsi, V.A. Chapter 1 - Parathyroids: Morphology and Pathology, in *The Parathyroids (Third Edition)*. (ed. J.P. Bilezikian) 23-36 (Academic Press, San Diego; 2015).

9. Haschek, W.M., Rousseaux, C.G. & Wallig, M.A. Chapter 17 - Endocrine System, in *Fundamentals of Toxicologic Pathology (Second Edition)*. (eds. W.M. Haschek, C.G. Rousseaux & M.A. Wallig) 513-551 (Academic Press, San Diego; 2010).

10. Nowak, F.V. & Mooradian, A.D. Endocrine Function and Dysfunction, in *Encyclopedia of Gerontology (Second Edition)*. (ed. J.E. Birren) 480-494 (Elsevier, New York; 2007).

11. Rottembourg, J. & Menegaux, F. Are oxyphil cells responsible for the ineffectiveness of cinacalcet hydrochloride in haemodialysis patients? *Clin Kidney J* **12**, 433-436 (2019).

12. Guilmette, J. & Sadow, P.M. Parathyroid Pathology. *Surg Pathol Clin* **12**, 1007-1019 (2019).

13. Muppidi, V., Meegada, S.R. & Rehman, A. Secondary Hyperparathyroidism, in *StatPearls* (Treasure Island (FL); 2021).

14. Palumbo, V.D. *et al.* Tertiary hyperparathyroidism: a review. *Clin Ter* **172**, 241-246 (2021).

15. Yeh, M.W. *et al.* Incidence and prevalence of primary hyperparathyroidism in a racially mixed population. *J Clin Endocrinol Metab* **98**, 1122-1129 (2013).

16. DeLellis, R.A. Parathyroid tumors and related disorders. *Mod Pathol* **24 Suppl 2**, S78-93 (2011).

17. Shaha, A.R. & Shah, J.P. Parathyroid carcinoma: a diagnostic and therapeutic challenge. *Cancer* **86**, 378-380 (1999).

18. Thakker, R.V. Genetics of parathyroid tumours. *J Intern Med* **280**, 574-583 (2016).

19. Brewer, K., Costa-Guda, J. & Arnold, A. Molecular genetic insights into sporadic primary hyperparathyroidism. *Endocr Relat Cancer* **26**, R53-R72 (2019).

20. Farnebo, F. *et al.* Alterations of the MEN1 gene in sporadic parathyroid tumors. *J Clin Endocrinol Metab* **83**, 2627-2630 (1998).

21. Lemos, M.C. & Thakker, R.V. Multiple endocrine neoplasia type 1 (MEN1): analysis of 1336 mutations reported in the first decade following identification of the gene. *Hum Mutat* **29**, 22-32 (2008).

22. Thakker, R.V. *et al.* Clinical practice guidelines for multiple endocrine neoplasia type 1 (MEN1). *The Journal of clinical endocrinology and metabolism* **97**, 2990-3011 (2012).

23. Occhi, G. *et al.* A novel mutation in the upstream open reading frame of the CDKN1B gene causes a MEN4 phenotype. *PLoS Genet* **9**, e1003350 (2013).

24. Bricaire, L. *et al.* Frequent large germline HRPT2 deletions in a French National cohort of patients with primary hyperparathyroidism. *J Clin Endocrinol Metab* **98**, E403-408 (2013).

25. Carpten, J.D. *et al.* HRPT2, encoding parafibromin, is mutated in hyperparathyroidism-jaw tumor syndrome. *Nat Genet* **32**, 676-680 (2002).

26. Silverberg, S.J., Lewiecki, E.M., Mosekilde, L., Peacock, M. & Rubin, M.R. Presentation of asymptomatic primary hyperparathyroidism: proceedings of the third international workshop. *J Clin Endocrinol Metab* **94**, 351-365 (2009).

27. Lundgren, E., Rastad, J., Thrufjell, E., Akerstrom, G. & Ljunghall, S. Population-based screening for primary hyperparathyroidism with serum calcium and parathyroid hormone values in menopausal women. *Surgery* **121**, 287-294 (1997).

28. Tordjman, K.M., Greenman, Y., Osher, E., Shenkerman, G. & Stern, N. Characterization of normocalcemic primary hyperparathyroidism. *Am J Med* **117**, 861-863 (2004).

29. Schini, M. *et al.* Normocalcemic Hyperparathyroidism: Study of its Prevalence and Natural History. *J Clin Endocrinol Metab* **105** (2020).

30. Agarwal, S. *et al.* CaSR expression in normal parathyroid and PHPT: new insights into pathogenesis from an autopsy-based study. *J Endocrinol Invest* (2021).

31. Yano, S. *et al.* Decrease in vitamin D receptor and calcium-sensing receptor in highly proliferative parathyroid adenomas. *Eur J Endocrinol* **148**, 403-411 (2003).

32. Koh, J. *et al.* Ex Vivo Intact Tissue Analysis Reveals Alternative Calcium-sensing Behaviors in Parathyroid Adenomas. *J Clin Endocrinol Metab* **106**, 3168-3183 (2021).

33. Balenga, N. *et al.* Parathyroid-Targeted Overexpression of Regulator of G-Protein Signaling 5 (RGS5) Causes Hyperparathyroidism in Transgenic Mice. *J Bone Miner Res* **34**, 955-963 (2019).

34. Ng, C.H. *et al.* Cinacalcet and primary hyperparathyroidism: systematic review and meta regression. *Endocr Connect* **9**, 724-735 (2020).

35. Peacock, M. *et al.* Cinacalcet hydrochloride maintains long-term normocalcemia in patients with primary hyperparathyroidism. *J Clin Endocrinol Metab* **90**, 135-141 (2005).

36. Rostoker, G., Bellamy, J. & Janklewicz, P. Cinacalcet to prevent parathyrotoxic crises in hypercalcaemic patients awaiting parathyroidectomy. *BMJ Case Rep* **2011** (2011).

37. Marcocci, C. *et al.* Cinacalcet reduces serum calcium concentrations in patients with intractable primary hyperparathyroidism. *J Clin Endocrinol Metab* **94**, 2766-2772 (2009).

38. Marcocci, C. *et al.* Parathyroid carcinoma. *J Bone Miner Res* **23**, 1869-1880 (2008).

39. Silverberg, S.J. *et al.* Cinacalcet hydrochloride reduces the serum calcium concentration in inoperable parathyroid carcinoma. *J Clin Endocrinol Metab* **92**, 3803-3808 (2007).

40. Khan, A.A. *et al.* Alendronate in primary hyperparathyroidism: a double-blind, randomized, placebo-controlled trial. *J Clin Endocrinol Metab* **89**, 3319-3325 (2004).

41. Faggiano, A. *et al.* Cinacalcet hydrochloride in combination with alendronate normalizes hypercalcemia and improves bone mineral density in patients with primary hyperparathyroidism. *Endocrine* **39**, 283-287 (2011).

42. Monassier, L. [Claude Bernard and nicotinic receptors: from the neuromuscular junction to tobacco weaning]. *Biol Aujourdhui* **211**, 169-172 (2017).

43. Langley, J.N. On the reaction of cells and of nerve-endings to certain poisons, chiefly as regards the reaction of striated muscle to nicotine and to curari. *J Physiol* **33**, 374-413 (1905).

44. Kent, R.S., De Lean, A. & Lefkowitz, R.J. A quantitative analysis of beta-adrenergic receptor interactions: resolution of high and low affinity states of the receptor by computer modeling of ligand binding data. *Mol Pharmacol* **17**, 14-23 (1980).

45. Dohlman, H.G., Thorner, J., Caron, M.G. & Lefkowitz, R.J. Model systems for the study of seven-transmembrane-segment receptors. *Annu Rev Biochem* **60**, 653-688 (1991).

46. Cerione, R.A. *et al.* Reconstitution of a hormone-sensitive adenylate cyclase system. The pure beta-adrenergic receptor and guanine nucleotide regulatory protein confer hormone responsiveness on the resolved catalytic unit. *J Biol Chem* **259**, 9979-9982 (1984).

47. Dixon, R.A. *et al.* Cloning of the gene and cDNA for mammalian beta-adrenergic receptor and homology with rhodopsin. *Nature* **321**, 75-79 (1986).

48. Schioth, H.B. & Fredriksson, R. The GRAFS classification system of G-protein coupled receptors in comparative perspective. *Gen Comp Endocrinol* **142**, 94-101 (2005).

49. Oldham, W.M. & Hamm, H.E. Heterotrimeric G protein activation by G-protein-coupled receptors. *Nat Rev Mol Cell Biol* **9**, 60-71 (2008).

50. Khan, S.M. *et al.* The expanding roles of Gbetagamma subunits in G protein-coupled receptor signaling and drug action. *Pharmacol Rev* **65**, 545-577 (2013).

51. Brinkerhoff, C.J., Traynor, J.R. & Linderman, J.J. Collision coupling, crosstalk, and compartmentalization in G-protein coupled receptor systems: can a single model explain disparate results? *J Theor Biol* **255**, 278-286 (2008).

52. Navarro, G. *et al.* Evidence for functional pre-coupled complexes of receptor heteromers and adenylyl cyclase. *Nat Commun* **9**, 1242 (2018).

53. Sprang, S. GEFs: master regulators of G-protein activation. *Trends Biochem Sci* **26**, 266-267 (2001).

54. Harden, T.K., Waldo, G.L., Hicks, S.N. & Sondek, J. Mechanism of activation and inactivation of Gq/phospholipase C-beta signaling nodes. *Chem Rev* **111**, 6120-6129 (2011).

55. Gohla, A., Schultz, G. & Offermanns, S. Role for G(12)/G(13) in agonist-induced vascular smooth muscle cell contraction. *Circ Res* **87**, 221-227 (2000).

56. Suzuki, N., Hajicek, N. & Kozasa, T. Regulation and physiological functions of G12/13-mediated signaling pathways. *Neurosignals* **17**, 55-70 (2009).

57. Rojas, R.J. *et al.* Galphaq directly activates p63RhoGEF and Trio via a conserved extension of the Dbl homology-associated pleckstrin homology domain. *J Biol Chem* **282**, 29201-29210 (2007).

58. Vogt, S., Grosse, R., Schultz, G. & Offermanns, S. Receptor-dependent RhoA activation in G12/G13-deficient cells: genetic evidence for an involvement of Gq/G11. *J Biol Chem* **278**, 28743-28749 (2003).

59. Strathmann, M.P. & Simon, M.I. G alpha 12 and G alpha 13 subunits define a fourth class of G protein alpha subunits. *Proceedings of the National Academy of Sciences of the United States of America* **88**, 5582-5586 (1991).

60. Riobo, N.A. & Manning, D.R. Receptors coupled to heterotrimeric G proteins of the G12 family. *Trends Pharmacol Sci* **26**, 146-154 (2005).

61. Hodge, R.G. & Ridley, A.J. Regulating Rho GTPases and their regulators. *Nat Rev Mol Cell Biol* **17**, 496-510 (2016).

62. He, W., Cowan, C.W. & Wensel, T.G. RGS9, a GTPase accelerator for phototransduction. *Neuron* **20**, 95-102 (1998).

63. Xie, G.X. & Palmer, P.P. How regulators of G protein signaling achieve selective regulation. *J Mol Biol* **366**, 349-365 (2007).

64. Ishii, M., Fujita, S., Yamada, M., Hosaka, Y. & Kurachi, Y. Phosphatidylinositol 3,4,5-trisphosphate and Ca2+/calmodulin competitively bind to the regulators of G-protein-signalling (RGS) domain of RGS4 and reciprocally regulate its action. *Biochem J* **385**, 65-73 (2005).

65. Palczewski, K., Buczylko, J., Kaplan, M.W., Polans, A.S. & Crabb, J.W. Mechanism of rhodopsin kinase activation. *J Biol Chem* **266**, 12949-12955 (1991).

66. Dean, K.R. & Akhtar, M. Novel mechanism for the activation of rhodopsin kinase: implications for other G protein-coupled receptor kinases (GRK's). *Biochemistry* **35**, 6164-6172 (1996).

67. Chen, C.Y., Dion, S.B., Kim, C.M. & Benovic, J.L. Beta-adrenergic receptor kinase. Agonist-dependent receptor binding promotes kinase activation. *J Biol Chem* **268**, 7825-7831 (1993).

68. Kuhn, H. Light-regulated binding of rhodopsin kinase and other proteins to cattle photoreceptor membranes. *Biochemistry* **17**, 4389-4395 (1978).

69. van Gastel, J. *et al.* beta-Arrestin Based Receptor Signaling Paradigms: Potential Therapeutic Targets for Complex Age-Related Disorders. *Front Pharmacol* **9**, 1369 (2018).

70. Ferguson, S.S. *et al.* Role of beta-arrestin in mediating agonist-promoted G protein-coupled receptor internalization. *Science* **271**, 363-366 (1996).

71. Shenoy, S.K. & Lefkowitz, R.J. beta-Arrestin-mediated receptor trafficking and signal transduction. *Trends Pharmacol Sci* **32**, 521-533 (2011).

72. Reiter, E., Ahn, S., Shukla, A.K. & Lefkowitz, R.J. Molecular mechanism of beta-arrestin-biased agonism at seven-transmembrane receptors. *Annu Rev Pharmacol Toxicol* **52**, 179-197 (2012).

73. Thomsen, A.R.B. *et al.* GPCR-G Protein-beta-Arrestin Super-Complex Mediates Sustained G Protein Signaling. *Cell* **166**, 907-919 (2016).

74. Jean-Charles, P.Y., Kaur, S. & Shenoy, S.K. G Protein-Coupled Receptor Signaling Through beta-Arrestin-Dependent Mechanisms. *J Cardiovasc Pharmacol* **70**, 142-158 (2017).

75. Feinstein, T.N. *et al.* Noncanonical control of vasopressin receptor type 2 signaling by retromer and arrestin. *The Journal of biological chemistry* **288**, 27849-27860 (2013).

76. Ferrandon, S. *et al.* Sustained cyclic AMP production by parathyroid hormone receptor endocytosis. *Nat Chem Biol* **5**, 734-742 (2009).

77. Calebiro, D. *et al.* Persistent cAMP-signals triggered by internalized G-protein-coupled receptors. *PLoS Biol* **7**, e1000172 (2009).

78. Azimzadeh, P., Talamantez-Lyburn, S.C., Chang, K.T., Inoue, A. & Balenga, N. Spatial regulation of GPR64/ADGRG2 signaling by beta-arrestins and GPCR kinases. *Annals of the New York Academy of Sciences* **1456**, 26-43 (2019).

79. Luttrell, L.M. & Miller, W.E. Arrestins as regulators of kinases and phosphatases. *Prog Mol Biol Transl Sci* **118**, 115-147 (2013).

80. Wang, P., Jiang, Y., Wang, Y., Shyy, J.Y. & DeFea, K.A. Beta-arrestin inhibits CAMKKbeta-dependent AMPK activation downstream of protease-activated-receptor-2. *BMC Biochem* **11**, 36 (2010).

81. Cheung, R. *et al.* An arrestin-dependent multi-kinase signaling complex mediates MIP-1beta/CCL4 signaling and chemotaxis of primary human macrophages. *J Leukoc Biol* **86**, 833-845 (2009).

82. Bock, A. & Bermudez, M. Allosteric coupling and biased agonism in G protein-coupled receptors. *FEBS J* **288**, 2513-2528 (2021).

83. Wootten, D., Christopoulos, A., Marti-Solano, M., Babu, M.M. & Sexton, P.M. Mechanisms of signalling and biased agonism in G protein-coupled receptors. *Nat Rev Mol Cell Biol* **19**, 638-653 (2018).

84. Su, M. *et al.* Structural Basis of the Activation of Heterotrimeric Gs-Protein by Isoproterenol-Bound beta1-Adrenergic Receptor. *Mol Cell* **80**, 59-71 e54 (2020).

85. Maeda, S., Qu, Q., Robertson, M.J., Skiniotis, G. & Kobilka, B.K. Structures of the M1 and M2 muscarinic acetylcholine receptor/G-protein complexes. *Science* **364**, 552-557 (2019).

86. Geng, Y. *et al.* Structural mechanism of ligand activation in human calcium-sensing receptor. *Elife* **5** (2016).

87. Ray, K., Clapp, P., Goldsmith, P.K. & Spiegel, A.M. Identification of the sites of N-linked glycosylation on the human calcium receptor and assessment of their role in cell surface expression and signal transduction. *J Biol Chem* **273**, 34558-34567 (1998).

88. Leach, K. *et al.* International Union of Basic and Clinical Pharmacology. CVIII. Calcium-Sensing Receptor Nomenclature, Pharmacology, and Function. *Pharmacol Rev* **72**, 558-604 (2020).

89. Clarke, B.L., Hassager, C. & Fitzpatrick, L.A. Regulation of parathyroid hormone release by protein kinase-C is dependent on extracellular calcium in bovine parathyroid cells. *Endocrinology* **132**, 1168-1175 (1993).

90. Moallem, E., Silver, J. & Naveh-Many, T. Regulation of parathyroid hormone messenger RNA levels by protein kinase A and C in bovine parathyroid cells. *J Bone Miner Res* **10**, 447-452 (1995).

91. Huang, K.P. The mechanism of protein kinase C activation. *Trends Neurosci* **12**, 425-432 (1989).

92. Chen, R.A. & Goodman, W.G. Role of the calcium-sensing receptor in parathyroid gland physiology. *Am J Physiol Renal Physiol* **286**, F1005-1011 (2004).

93. Conigrave, A.D. The Calcium-Sensing Receptor and the Parathyroid: Past, Present, Future. *Front Physiol* **7**, 563 (2016).

94. Balenga, N. *et al.* Orphan Adhesion GPCR GPR64/ADGRG2 Is Overexpressed in Parathyroid Tumors and Attenuates Calcium-Sensing Receptor-Mediated Signaling. *J Bone Miner Res* **32**, 654-666 (2017).

95. Koh, J. *et al.* Ex vivo intact tissue analysis reveals alternative calcium-sensing behaviors in parathyroid adenomas. *J Clin Endocrinol Metab* (2021).

96. Quinn, S.J., Kifor, O., Kifor, I., Butters, R.R., Jr. & Brown, E.M. Role of the cytoskeleton in extracellular calcium-regulated PTH release. *Biochemical and biophysical research communications* **354**, 8-13 (2007).

97. Davies, S.L., Gibbons, C.E., Vizard, T. & Ward, D.T. Ca2+-sensing receptor induces Rho kinase-mediated actin stress fiber assembly and altered cell morphology, but not in response to aromatic amino acids. *Am J Physiol Cell Physiol* **290**, C1543-1551 (2006).

98. Wang, T. *et al.* CD97, an adhesion receptor on inflammatory cells, stimulates angiogenesis through binding integrin counterreceptors on endothelial cells. *Blood* **105**, 2836-2844 (2005).

99. Luo, R. *et al.* G protein-coupled receptor 56 and collagen III, a receptor-ligand pair, regulates cortical development and lamination. *Proceedings of the National Academy of Sciences of the United States of America* **108**, 12925-12930 (2011).

100. Paavola, K.J., Sidik, H., Zuchero, J.B., Eckart, M. & Talbot, W.S. Type IV collagen is an activating ligand for the adhesion G protein-coupled receptor GPR126. *Sci Signal* **7**, ra76 (2014).

101. Hamann, J. *et al.* International Union of Basic and Clinical Pharmacology. XCIV. Adhesion G protein-coupled receptors. *Pharmacological reviews* **67**, 338-367 (2015).

102. Arac, D. *et al.* A novel evolutionarily conserved domain of cell-adhesion GPCRs mediates autoproteolysis. *EMBO J* **31**, 1364-1378 (2012).

103. Langenhan, T., Aust, G. & Hamann, J. Sticky signaling--adhesion class G protein-coupled receptors take the stage. *Sci Signal* **6**, re3 (2013).

104. Purcell, R.H. & Hall, R.A. Adhesion G Protein-Coupled Receptors as Drug Targets. *Annu Rev Pharmacol Toxicol* **58**, 429-449 (2018).

105. Okajima, D., Kudo, G. & Yokota, H. Brain-specific angiogenesis inhibitor 2 (BAI2) may be activated by proteolytic processing. *J Recept Signal Transduct Res* **30**, 143-153 (2010).

106. Paavola, K.J., Stephenson, J.R., Ritter, S.L., Alter, S.P. & Hall, R.A. The N terminus of the adhesion G protein-coupled receptor GPR56 controls receptor signaling activity. *J Biol Chem* **286**, 28914-28921 (2011).

107. Azimzadeh, P., Talamantez-Lyburn, S.C., Chang, K.T., Inoue, A. & Balenga, N. Spatial regulation of GPR64/ADGRG2 signaling by beta-arrestins and GPCR kinases. *Annals of the New York Academy of Sciences* (2019).

108. Demberg, L.M., Rothemund, S., Schoneberg, T. & Liebscher, I. Identification of the tethered peptide agonist of the adhesion G protein-coupled receptor GPR64/ADGRG2. *Biochem Biophys Res Commun* **464**, 743-747 (2015).

109. Stoveken, H.M., Hajduczok, A.G., Xu, L. & Tall, G.G. Adhesion G protein-coupled receptors are activated by exposure of a cryptic tethered agonist. *Proceedings of the National Academy of Sciences of the United States of America* **112**, 6194-6199 (2015).

110. Ward, Y. *et al.* LPA receptor heterodimerizes with CD97 to amplify LPA-initiated RHO-dependent signaling and invasion in prostate cancer cells. *Cancer Res* **71**, 7301-7311 (2011).

111. Liebscher, I. *et al.* A tethered agonist within the ectodomain activates the adhesion G protein-coupled receptors GPR126 and GPR133. *Cell reports* **9**, 2018-2026 (2014).

112. Wilde, C. *et al.* The constitutive activity of the adhesion GPCR GPR114/ADGRG5 is mediated by its tethered agonist. *FASEB J* **30**, 666-673 (2016).

113. Shima, Y., Kengaku, M., Hirano, T., Takeichi, M. & Uemura, T. Regulation of dendritic maintenance and growth by a mammalian 7-pass transmembrane cadherin. *Dev Cell* **7**, 205-216 (2004).

114. Gray, J.X. *et al.* CD97 is a processed, seven-transmembrane, heterodimeric receptor associated with inflammation. *Journal of immunology* **157**, 5438-5447 (1996).

115. Krasnoperov, V. *et al.* Dissociation of the subunits of the calcium-independent receptor of alpha-latrotoxin as a result of two-step proteolysis. *Biochemistry* **48**, 3230-3238 (2009).

116. Kaur, B., Brat, D.J., Devi, N.S. & Van Meir, E.G. Vasculostatin, a proteolytic fragment of brain angiogenesis inhibitor 1, is an antiangiogenic and antitumorigenic factor. *Oncogene* **24**, 3632-3642 (2005).

117. Kishore, A., Purcell, R.H., Nassiri-Toosi, Z. & Hall, R.A. Stalk-dependent and Stalk-independent Signaling by the Adhesion G Protein-coupled Receptors GPR56 (ADGRG1) and BAI1 (ADGRB1). *J Biol Chem* **291**, 3385-3394 (2016).

118. Dai, S., Wang, X., Li, X. & Cao, Y. MicroRNA-139-5p acts as a tumor suppressor by targeting ELTD1 and regulating cell cycle in glioblastoma multiforme. *Biochem Biophys Res Commun* **467**, 204-210 (2015).

119. Serban, F. *et al.* Silencing of epidermal growth factor, latrophilin and seven transmembrane domain-containing protein 1 (ELTD1) via siRNA-induced cell death in glioblastoma. *J Immunoassay Immunochem* **38**, 21-33 (2017).

120. Ji, B. *et al.* GPR56 promotes proliferation of colorectal cancer cells and enhances metastasis via epithelialmesenchymal transition through PI3K/AKT signaling activation. *Oncol Rep* **40**, 1885-1896 (2018).

121. Yang, L. *et al.* GPR56 Regulates VEGF production and angiogenesis during melanoma progression. *Cancer research* **71**, 5558-5568 (2011).

122. Millar, M.W., Corson, N. & Xu, L. The Adhesion G-Protein-Coupled Receptor, GPR56/ADGRG1, Inhibits Cell-Extracellular Matrix Signaling to Prevent Metastatic Melanoma Growth. *Front Oncol* **8**, 8 (2018).

123. Chiang, N.Y. *et al.* GPR56/ADGRG1 Activation Promotes Melanoma Cell Migration via NTF Dissociation and CTF-Mediated Galpha12/13/RhoA Signaling. *The Journal of investigative dermatology* **137**, 727-736 (2017).

124. Hatanaka, H. *et al.* Vascularization is decreased in pulmonary adenocarcinoma expressing brain-specific angiogenesis inhibitor 1 (BAI1). *International journal of molecular medicine* **5**, 181-183 (2000).

125. Kaur, B., Brat, D.J., Calkins, C.C. & Van Meir, E.G. Brain angiogenesis inhibitor 1 is differentially expressed in normal brain and glioblastoma independently of p53 expression. *Am J Pathol* **162**, 19-27 (2003).

126. Fukushima, Y. *et al.* Brain-specific angiogenesis inhibitor 1 expression is inversely correlated with vascularity and distant metastasis of colorectal cancer. *International journal of oncology* **13**, 967-970 (1998).

127. Wang, W. *et al.* Expression of brain-specific angiogenesis inhibitor 1 is inversely correlated with pathological grade, angiogenesis and peritumoral brain edema in human astrocytomas. *Oncol Lett* **5**, 1513-1518 (2013).

128. Nazarko, O. *et al.* A Comprehensive Mutagenesis Screen of the Adhesion GPCR Latrophilin-1/ADGRL1. *iScience* **3**, 264-278 (2018).

129. Fund, W.C.R. in Global cancer statistics for the most common cancers, Vol. 2019 (2018).

130. Bray, F. *et al.* Global cancer statistics 2018: GLOBOCAN estimates of incidence and mortality worldwide for 36 cancers in 185 countries. *CA Cancer J Clin* **68**, 394-424 (2018).

131. Kan, Z. *et al.* Diverse somatic mutation patterns and pathway alterations in human cancers. *Nature* **466**, 869-873 (2010).

132. Kang, X. *et al.* Antiangiogenic activity of BAI1 in vivo: implications for gene therapy of human glioblastomas. *Cancer Gene Ther* **13**, 385-392 (2006).

133. Jeong, B.C. *et al.* Brain-specific angiogenesis inhibitor 2 regulates VEGF through GABP that acts as a transcriptional repressor. *FEBS Lett* **580**, 669-676 (2006).

134. Bari, M.F. *et al.* BAI3, CDX2 and VIL1: a panel of three antibodies to distinguish small cell from large cell neuroendocrine lung carcinomas. *Histopathology* **64**, 547-556 (2014).

135. Lee, D.K. *et al.* Agonist-independent nuclear localization of the Apelin, angiotensin AT1, and bradykinin B2 receptors. *J Biol Chem* **279**, 7901-7908 (2004).

136. Kumar, V., Jong, Y.J. & O'Malley, K.L. Activated nuclear metabotropic glutamate receptor mGlu5 couples to nuclear Gq/11 proteins to generate inositol 1,4,5-trisphosphate-mediated nuclear Ca2+ release. *The Journal of biological chemistry* **283**, 14072-14083 (2008).

137. Shenoy, S.K. *et al.* beta-arrestin1 mediates metastatic growth of breast cancer cells by facilitating HIF-1-dependent VEGF expression. *Oncogene* **31**, 282-292 (2012).

138. Cianfrocca, R. *et al.* Nuclear beta-arrestin1 is a critical cofactor of hypoxia-inducible factor-1alpha signaling in endothelin-1-induced ovarian tumor progression. *Oncotarget* **7**, 17790-17804 (2016).

139. Hamoud, N. *et al.* Spatiotemporal regulation of the GPCR activity of BAI3 by C1qL4 and Stabilin-2 controls myoblast fusion. *Nat Commun* **9**, 4470 (2018).

140. Peng, Y. & Croce, C.M. The role of MicroRNAs in human cancer. *Signal Transduct Target Ther* **1**, 15004 (2016).

141. Gao, Y. *et al.* miR-138-5p reverses gefitinib resistance in non-small cell lung cancer cells via negatively regulating G protein-coupled receptor 124. *Biochem Biophys Res Commun* **446**, 179-186 (2014).

142. Wheeler, D.L., Dunn, E.F. & Harari, P.M. Understanding resistance to EGFR inhibitors-impact on future treatment strategies. *Nat Rev Clin Oncol* **7**, 493-507 (2010).

143. Anderson, K.D. *et al.* Angiogenic sprouting into neural tissue requires Gpr124, an orphan G protein-coupled receptor. *Proceedings of the National Academy of Sciences of the United States of America* **108**, 2807-2812 (2011).

144. Cho, C., Smallwood, P.M. & Nathans, J. Reck and Gpr124 Are Essential Receptor Cofactors for Wnt7a/Wnt7b-Specific Signaling in Mammalian CNS Angiogenesis and Blood-Brain Barrier Regulation. *Neuron* **95**, 1056-1073 e1055 (2017).

145. Feliciano, A. *et al.* miR-99a reveals two novel oncogenic proteins E2F2 and EMR2 and represses stemness in lung cancer. *Cell Death Dis* **8**, e3141 (2017).

146. Nguyen, D.X. *et al.* WNT/TCF signaling through LEF1 and HOXB9 mediates lung adenocarcinoma metastasis. *Cell* **138**, 51-62 (2009).

147. Stacey, M. *et al.* The epidermal growth factor-like domains of the human EMR2 receptor mediate cell attachment through chondroitin sulfate glycosaminoglycans. *Blood* **102**, 2916-2924 (2003).

148. Shannon, J.M. *et al.* Chondroitin sulfate proteoglycans are required for lung growth and morphogenesis in vitro. *American journal of physiology. Lung cellular and molecular physiology* **285**, L1323-1336 (2003).

149. Li, G. *et al.* Glycosaminoglycans and glycolipids as potential biomarkers in lung cancer. *Glycoconj J* **34**, 661-669 (2017).

150. Gupte, J. *et al.* Signaling property study of adhesion G-protein-coupled receptors. *FEBS Lett* **586**, 1214-1219 (2012).

151. Ranzani, M., Annunziato, S., Adams, D.J. & Montini, E. Cancer gene discovery: exploiting insertional mutagenesis. *Mol Cancer Res* **11**, 1141-1158 (2013).

152. Lum, A.M. *et al.* Orphan receptor GPR110, an oncogene overexpressed in lung and prostate cancer. *BMC cancer* **10**, 40 (2010).

153. Akagi, K., Suzuki, T., Stephens, R.M., Jenkins, N.A. & Copeland, N.G. RTCGD: retroviral tagged cancer gene database. *Nucleic Acids Res* **32**, D523-527 (2004).

154. Uren, A.G. *et al.* Large-scale mutagenesis in p19(ARF)- and p53-deficient mice identifies cancer genes and their collaborative networks. *Cell* **133**, 727-741 (2008).

155. Bhat, R.R. *et al.* GPCRs profiling and identification of GPR110 as a potential new target in HER2+ breast cancer. *Breast cancer research and treatment* **170**, 279-292 (2018).

156. Huang, H. *et al.* Aberrant expression of novel and previously described cell membrane markers in human breast cancer cell lines and tumors. *Clinical cancer research : an official journal of the American Association for Cancer Research* **11**, 4357-4364 (2005).

157. Jiang, L. *et al.* Differential cellular localization of CELSR2 and ING4 and correlations with hormone receptor status in breast cancer. *Histology and histopathology* **33**, 835-842 (2018).

158. Tian, H. *et al.* Effects of targeted CD97 immune epitopes small interference RNA on cellular biological behaviors in MDA-MB231 malignant breast cancer cell line. *Am J Transl Res* **9**, 4640-4651 (2017).

159. Wilson, K.S., Roberts, H., Leek, R., Harris, A.L. & Geradts, J. Differential gene expression patterns in HER2/neu-positive and -negative breast cancer cell lines and tissues. *Am J Pathol* **161**, 1171-1185 (2002).

160. Ashaie, M.A. & Chowdhury, E.H. Cadherins: The Superfamily Critically Involved in Breast Cancer. *Curr Pharm Des* **22**, 616-638 (2016).

161. Usui, T. *et al.* Flamingo, a seven-pass transmembrane cadherin, regulates planar cell polarity under the control of Frizzled. *Cell* **98**, 585-595 (1999).

162. Katoh, Y. & Katoh, M. Comparative integromics on FAT1, FAT2, FAT3 and FAT4. *International journal of molecular medicine* **18**, 523-528 (2006).

163. Davies, J.Q. *et al.* Leukocyte adhesion-GPCR EMR2 is aberrantly expressed in human breast carcinomas and is associated with patient survival. *Oncol Rep* **25**, 619-627 (2011).

164. Meisen, W.H. *et al.* Changes in BAI1 and nestin expression are prognostic indicators for survival and metastases in breast cancer and provide opportunities for dual targeted therapies. *Mol Cancer Ther* **14**, 307-314 (2015).

165. Volpert, O.V. *et al.* Inducer-stimulated Fas targets activated endothelium for destruction by anti-angiogenic thrombospondin-1 and pigment epithelium-derived factor. *Nat Med* **8**, 349-357 (2002).

166. Maubant, S. *et al.* Blockade of alpha v beta3 and alpha v beta5 integrins by RGD mimetics induces anoikis and not integrin-mediated death in human endothelial cells. *Blood* **108**, 3035-3044 (2006).

167. Kotecki, N., Lefranc, F., Devriendt, D. & Awada, A. Therapy of breast cancer brain metastases: challenges, emerging treatments and perspectives. *Ther Adv Med Oncol* **10**, 1758835918780312 (2018).

168. Madjd, Z. *et al.* Loss of CD55 is associated with aggressive breast tumors. *Clinical cancer research : an official journal of the American Association for Cancer Research* **10**, 2797-2803 (2004).

169. Ikeda, J. *et al.* Prognostic significance of CD55 expression in breast cancer. *Clinical cancer research : an official journal of the American Association for Cancer Research* **14**, 4780-4786 (2008).

170. Tang, X. *et al.* GPR116, an adhesion G-protein-coupled receptor, promotes breast cancer metastasis via the Galphaq-p63RhoGEF-Rho GTPase pathway. *Cancer research* **73**, 6206-6218 (2013).

171. Richter, G.H. *et al.* G-Protein coupled receptor 64 promotes invasiveness and metastasis in Ewing sarcomas through PGF and MMP1. *J Pathol* **230**, 70-81 (2013).

172. Peeters, M.C. *et al.* The adhesion G protein-coupled receptor G2 (ADGRG2/GPR64) constitutively activates SRE and NFkappaB and is involved in cell adhesion and migration. *Cell Signal* **27**, 2579-2588 (2015).

173. Holch, J., Stintzing, S. & Heinemann, V. Treatment of Metastatic Colorectal Cancer: Standard of Care and Future Perspectives. *Visc Med* **32**, 178-183 (2016).

174. Morkel, M., Riemer, P., Blaker, H. & Sers, C. Similar but different: distinct roles for KRAS and BRAF oncogenes in colorectal cancer development and therapy resistance. *Oncotarget* **6**, 20785-20800 (2015).

175. Yoshida, Y. *et al.* Expression of angiostatic factors in colorectal cancer. *International journal of oncology* **15**, 1221-1225 (1999).

176. Bader, J.E. *et al.* Macrophage depletion using clodronate liposomes decreases tumorigenesis and alters gut microbiota in the AOM/DSS mouse model of colon cancer. *American journal of physiology. Gastrointestinal and liver physiology* **314**, G22-g31 (2018).

177. Wang, Y. *et al.* Gene expression profiles and molecular markers to predict recurrence of Dukes' B colon cancer. *J Clin Oncol* **22**, 1564-1571 (2004).

178. Grone, J. *et al.* Molecular profiles and clinical outcome of stage UICC II colon cancer patients. *International journal of colorectal disease* **26**, 847-858 (2011).

179. Wu, Y. *et al.* Elevated G-Protein Receptor 125 (GPR125) Expression Predicts Good Outcomes in Colorectal Cancer and Inhibits Wnt/beta-Catenin Signaling Pathway. *Medical science monitor : international medical journal of experimental and clinical research* **24**, 6608-6616 (2018).

180. Fearon, E.R. & Vogelstein, B. A genetic model for colorectal tumorigenesis. *Cell* **61**, 759-767 (1990).

181. Zhan, T., Rindtorff, N. & Boutros, M. Wnt signaling in cancer. *Oncogene* **36**, 1461-1473 (2017).

182. Lemieux, E., Cagnol, S., Beaudry, K., Carrier, J. & Rivard, N. Oncogenic KRAS signalling promotes the Wnt/beta-catenin pathway through LRP6 in colorectal cancer. *Oncogene* **34**, 4914-4927 (2015).

183. Wobus, M., Huber, O., Hamann, J. & Aust, G. CD97 overexpression in tumor cells at the invasion front in colorectal cancer (CC) is independently regulated of the canonical Wnt pathway. *Mol Carcinog* **45**, 881-886 (2006).

184. Steinert, M. *et al.* Expression and regulation of CD97 in colorectal carcinoma cell lines and tumor tissues. *Am J Pathol* **161**, 1657-1667 (2002).

185. Eichler, W. CD97 isoform expression in leukocytes. *J Leukoc Biol* **68**, 561-567 (2000).

186. Yin, Y. *et al.* CD97 Promotes Tumor Aggressiveness Through the Traditional G Protein-Coupled Receptor-Mediated Signaling in Hepatocellular Carcinoma. *Hepatology* **68**, 1865-1878 (2018).

187. Huang, L.C. & Hueng, D.Y. CD97 and glioma invasion. *J Neurosurg* **120**, 579-580 (2014).

188. Liu, D. *et al.* The invasion and metastasis promotion role of CD97 small isoform in gastric carcinoma. *PLoS One* **7**, e39989 (2012).

189. Hilbig, D. *et al.* The Interaction of CD97/ADGRE5 With beta-Catenin in Adherens Junctions Is Lost During Colorectal Carcinogenesis. *Front Oncol* **8**, 182 (2018).

190. Han, S.L. *et al.* The impact of expressions of CD97 and its ligand CD55 at the invasion front on prognosis of rectal adenocarcinoma. *International journal of colorectal disease* **25**, 695-702 (2010).

191. Yang, L. *et al.* High expression of GPR116 indicates poor survival outcome and promotes tumor progression in colorectal carcinoma. *Oncotarget* **8**, 47943-47956 (2017).

192. Wang, C., Fan, H.Q. & Zhang, Y.W. MiR-511-5p functions as a tumor suppressor and a predictive of prognosis in colorectal cancer by directly targeting GPR116. *European review for medical and pharmacological sciences* **23**, 6119-6130 (2019).

193. Sewda, K. *et al.* Cell-surface markers for colon adenoma and adenocarcinoma. *Oncotarget* **7**, 17773-17789 (2016).

194. Jin, G. *et al.* The G-protein coupled receptor 56, expressed in colonic stem and cancer cells, binds progastrin to promote proliferation and carcinogenesis. *Oncotarget* **8**, 40606-40619 (2017).

195. Dockray, G.J., Varro, A., Dimaline, R. & Wang, T. The gastrins: their production and biological activities. *Annu Rev Physiol* **63**, 119-139 (2001).

196. Chou, R. *et al.* Screening for prostate cancer: a review of the evidence for the U.S. Preventive Services Task Force. *Ann Intern Med* **155**, 762-771 (2011).

197. Iguchi, T. *et al.* Orphan G protein-coupled receptor GPR56 regulates neural progenitor cell migration via a G alpha 12/13 and Rho pathway. *J Biol Chem* **283**, 14469-14478 (2008).

198. Guo, R. *et al.* Expression and function of lysophosphatidic acid LPA1 receptor in prostate cancer cells. *Endocrinology* **147**, 4883-4892 (2006).

199. Scarlett, K.A. *et al.* Agonist-induced CXCR4 and CB2 Heterodimerization Inhibits Galpha13/RhoA-mediated Migration. *Mol Cancer Res* **16**, 728-739 (2018).

200. Coke, C.J. *et al.* Simultaneous Activation of Induced Heterodimerization between CXCR4 Chemokine Receptor and Cannabinoid Receptor 2 (CB2) Reveals a Mechanism for Regulation of Tumor Progression. *The Journal of biological chemistry* **291**, 9991-10005 (2016).

201. Moreno, E. *et al.* Targeting CB2-GPR55 receptor heteromers modulates cancer cell signaling. *The Journal of biological chemistry* **289**, 21960-21972 (2014).

202. Aust, G. *et al.* CD97, but not its closely related EGF-TM7 family member EMR2, is expressed on gastric, pancreatic, and esophageal carcinomas. *Am J Clin Pathol* **118**, 699-707 (2002).

203. Liu, D. *et al.* Role of CD97 isoforms in gastric carcinoma. *International journal of oncology* **36**, 1401-1408 (2010).

204. Li, C. *et al.* CD97 promotes gastric cancer cell proliferation and invasion through exosome-mediated MAPK signaling pathway. *World J Gastroenterol* **21**, 6215-6228 (2015).

205. Liu, D. *et al.* CD97 promotion of gastric carcinoma lymphatic metastasis is exosome dependent. *Gastric cancer : official journal of the International Gastric Cancer Association and the Japanese Gastric Cancer Association* **19**, 754-766 (2016).

206. Zhu, X., Huang, G. & Jin, P. Clinicopathological and prognostic significance of aberrant G protein-couple receptor 110 (GPR110) expression in gastric cancer. *Pathology, research and practice* **215**, 539-545 (2019).

207. Lee, J.W. *et al.* Orphan GPR110 (ADGRF1) targeted by N-docosahexaenoylethanolamine in development of neurons and cognitive function. *Nat Commun* **7**, 13123 (2016).

208. Stoveken, H.M. *et al.* Dihydromunduletone Is a Small-Molecule Selective Adhesion G Protein-Coupled Receptor Antagonist. *Molecular pharmacology* **90**, 214-224 (2016).

209. Salzman, G.S. *et al.* Stachel-independent modulation of GPR56/ADGRG1 signaling by synthetic ligands directed to its extracellular region. *Proceedings of the National Academy of Sciences of the United States of America* **114**, 10095-10100 (2017).

210. Zhu, B. *et al.* GAIN domain-mediated cleavage is required for activation of G protein-coupled receptor 56 (GPR56) by its natural ligands and a small-molecule agonist. *The Journal of biological chemistry* (2019).

211. Chan, H.C.S., McCarthy, D., Li, J., Palczewski, K. & Yuan, S. Designing Safer Analgesics via mu-Opioid Receptor Pathways. *Trends Pharmacol Sci* (2017).

212. DeWire, S.M. *et al.* A G protein-biased ligand at the mu-opioid receptor is potently analgesic with reduced gastrointestinal and respiratory dysfunction compared with morphine. *J Pharmacol Exp Ther* **344**, 708-717 (2013).

213. Rajagopal, S., Rajagopal, K. & Lefkowitz, R.J. Teaching old receptors new tricks: biasing seven-transmembrane receptors. *Nat Rev Drug Discov* **9**, 373-386 (2010).

214. Chandler, C., Liu, T., Buckanovich, R. & Coffman, L.G. The double edge sword of fibrosis in cancer. *Transl Res* **209**, 55-67 (2019).

215. Knierim, A.B. *et al.* Genetic basis of functional variability in adhesion G protein-coupled receptors. *Scientific reports* **9**, 11036 (2019).

216. Sugita, S., Ichtchenko, K., Khvotchev, M. & Sudhof, T.C. alpha-Latrotoxin receptor CIRL/latrophilin 1 (CL1) defines an unusual family of ubiquitous G-protein-linked receptors. G-protein coupling not required for triggering exocytosis. *The Journal of biological chemistry* **273**, 32715-32724 (1998).

217. Silva, J.P. *et al.* Latrophilin 1 and its endogenous ligand Lasso/teneurin-2 form a high-affinity transsynaptic receptor pair with signaling capabilities. *Proceedings of the National Academy of Sciences of the United States of America* **108**, 12113-12118 (2011).

218. Boucard, A.A., Maxeiner, S. & Sudhof, T.C. Latrophilins function as heterophilic cell-adhesion molecules by binding to teneurins: regulation by alternative splicing. *J Biol Chem* **289**, 387-402 (2014).

219. O'Sullivan, M.L. *et al.* FLRT proteins are endogenous latrophilin ligands and regulate excitatory synapse development. *Neuron* **73**, 903-910 (2012).

220. Boucard, A.A., Ko, J. & Sudhof, T.C. High affinity neurexin binding to cell adhesion G-protein-coupled receptor CIRL1/latrophilin-1 produces an intercellular adhesion complex. *The Journal of biological chemistry* **287**, 9399-9413 (2012).

221. Meza-Aguilar, D.G. & Boucard, A.A. Latrophilins updated. *Biomol Concepts* **5**, 457-478 (2014).

222. Lelianova, V.G. *et al.* Alpha-latrotoxin receptor, latrophilin, is a novel member of the secretin family of G protein-coupled receptors. *J Biol Chem* **272**, 21504-21508 (1997).

223. Kocibalova, Z., Guzyova, M., Imrichova, D., Sulova, Z. & Breier, A. Overexpression of the ABCB1 drug transporter in acute myeloid leukemia cells is associated with downregulation of latrophilin-1. *Gen Physiol Biophys* **37**, 353-357 (2018).

224. Yasinska, I.M. *et al.* The Tim-3-Galectin-9 Pathway and Its Regulatory Mechanisms in Human Breast Cancer. *Frontiers in immunology* **10**, 1594 (2019).

225. Zheng, C.X. *et al.* Whole-exome sequencing to identify novel somatic mutations in squamous cell lung cancers. *International journal of oncology* **43**, 755-764 (2013).

226. Lu, Y.C. *et al.* Structural Basis of Latrophilin-FLRT-UNC5 Interaction in Cell Adhesion. *Structure* **23**, 1678-1691 (2015).

227. Kotepui, M., Thawornkuno, C., Chavalitshewinkoon-Petmitr, P., Punyarit, P. & Petmitr, S. Quantitative real-time RT-PCR of ITGA7, SVEP1, TNS1, LPHN3, SEMA3G, KLB and MMP13 mRNA expression in breast cancer. *Asian Pac J Cancer Prev* **13**, 5879-5882 (2012).

228. Favara, D.M., Banham, A.H. & Harris, A.L. A review of ELTD1, a pro-angiogenic adhesion GPCR. *Biochem Soc Trans* **42**, 1658-1664 (2014).

229. Gordon, S., Hamann, J., Lin, H.H. & Stacey, M. F4/80 and the related adhesion-GPCRs. *Eur J Immunol* **41**, 2472-2476 (2011).

230. Maiga, A. *et al.* Transcriptome analysis of G protein-coupled receptors in distinct genetic subgroups of acute myeloid leukemia: identification of potential disease-specific targets. *Blood Cancer J* **6**, e431 (2016).

231. I, K.Y. *et al.* Activation of Adhesion GPCR EMR2/ADGRE2 Induces Macrophage Differentiation and Inflammatory Responses via Galpha16/Akt/MAPK/NF-kappaB Signaling Pathways. *Frontiers in immunology* **8**, 373 (2017).

232. Ivan, M.E. *et al.* Epidermal growth factor-like module containing mucin-like hormone receptor 2 expression in gliomas. *J Neurooncol* **121**, 53-61 (2015).

233. Archer, K.J., Mas, V.R., Maluf, D.G. & Fisher, R.A. High-throughput assessment of CpG site methylation for distinguishing between HCV-cirrhosis and HCV-associated hepatocellular carcinoma. *Mol Genet Genomics* **283**, 341-349 (2010).

234. Kane, A.J., Sughrue, M.E., Rutkowski, M.J., Phillips, J.J. & Parsa, A.T. EMR-3: a potential mediator of invasive phenotypic variation in glioblastoma and novel therapeutic target. *Neuroreport* **21**, 1018-1022 (2010).

235. Hamann, J., Vogel, B., van Schijndel, G.M. & van Lier, R.A. The seven-span transmembrane receptor CD97 has a cellular ligand (CD55, DAF). *J Exp Med* **184**, 1185-1189 (1996).

236. Wandel, E., Saalbach, A., Sittig, D., Gebhardt, C. & Aust, G. Thy-1 (CD90) is an interacting partner for CD97 on activated endothelial cells. *J Immunol* **188**, 1442-1450 (2012).

237. Tjong, W.Y. & Lin, H.H. The RGD motif is involved in CD97/ADGRE5-promoted cell adhesion and viability of HT1080 cells. *Sci Rep* **9**, 1517 (2019).

238. Eichler, W., Hamann, J. & Aust, G. Expression characteristics of the human CD97 antigen. *Tissue Antigens* **50**, 429-438 (1997).

239. He, Z., Wu, H., Jiao, Y. & Zheng, J. Expression and prognostic value of CD97 and its ligand CD55 in pancreatic cancer. *Oncol Lett* **9**, 793-797 (2015).

240. Meng, Z.W., Liu, M.C., Hong, H.J., Du, Q. & Chen, Y.L. Expression and prognostic value of soluble CD97 and its ligand CD55 in intrahepatic cholangiocarcinoma. *Tumour Biol* **39**, 1010428317694319 (2017).

241. Singh, V. *et al.* Esophageal Cancer Epigenomics and Integrome Analysis of Genome-Wide Methylation and Expression in High Risk Northeast Indian Population. *OMICS* **19**, 688-699 (2015).

242. Park, G.B. & Kim, D. MicroRNA-503-5p Inhibits the CD97-Mediated JAK2/STAT3 Pathway in Metastatic or Paclitaxel-Resistant Ovarian Cancer Cells. *Neoplasia* **21**, 206-215 (2019).

243. Wu, J., Lei, L., Wang, S., Gu, D. & Zhang, J. Immunohistochemical expression and prognostic value of CD97 and its ligand CD55 in primary gallbladder carcinoma. *J Biomed Biotechnol* **2012**, 587672 (2012).

244. Wobus, M. *et al.* Association of the EGF-TM7 receptor CD97 expression with FLT3-ITD in acute myeloid leukemia. *Oncotarget* **6**, 38804-38815 (2015).

245. Vaikari, V.P., Yang, J., Wu, S. & Alachkar, H. CD97 expression is associated with poor overall survival in acute myeloid leukemia. *Exp Hematol* **75**, 64-73 e64 (2019).

246. Mustafa, T. *et al.* Expression of the epidermal growth factor seven-transmembrane member CD97 correlates with grading and staging in human oral squamous cell carcinomas. *Cancer Epidemiol Biomarkers Prev* **14**, 108-119 (2005).

247. Hoang-Vu, C. *et al.* Regulation of CD97 protein in thyroid carcinoma. *J Clin Endocrinol Metab* **84**, 1104-1109 (1999).

248. Safaee, M. *et al.* Proportional upregulation of CD97 isoforms in glioblastoma and glioblastoma-derived brain tumor initiating cells. *PLoS One* **10**, e0111532 (2015).

249. Aust, G., Hamann, J., Schilling, N. & Wobus, M. Detection of alternatively spliced EMR2 mRNAs in colorectal tumor cell lines but rare expression of the molecule in colorectal adenocarcinomas. *Virchows Arch* **443**, 32-37 (2003).

250. Vallon, M. & Essler, M. Proteolytically processed soluble tumor endothelial marker (TEM) 5 mediates endothelial cell survival during angiogenesis by linking integrin alpha(v)beta3 to glycosaminoglycans. *J Biol Chem* **281**, 34179-34188 (2006).

251. Posokhova, E. *et al.* GPR124 functions as a WNT7-specific coactivator of canonical beta-catenin signaling. *Cell Rep* **10**, 123-130 (2015).

252. Cherry, A.E. *et al.* GPR124 regulates microtubule assembly, mitotic progression, and glioblastoma cell proliferation. *Glia* **67**, 1558-1570 (2019).

253. Wang, Z., Li, Y., Zhou, F., Piao, Z. & Hao, J. beta-elemene enhances anticancer bone neoplasms efficacy of paclitaxel through regulation of GPR124 in bone neoplasms cells. *Oncol Lett* **16**, 2143-2150 (2018).

254. Williams, S.V. *et al.* High-resolution analysis of genomic alteration on chromosome arm 8p in urothelial carcinoma. *Genes, chromosomes & cancer* **49**, 642-659 (2010).

255. Wang, Y., Cho, S.G., Wu, X., Siwko, S. & Liu, M. G-protein coupled receptor 124 (GPR124) in endothelial cells regulates vascular endothelial growth factor (VEGF)-induced tumor angiogenesis. *Curr Mol Med* **14**, 543-554 (2014).

256. Yates, L.L. *et al.* The PCP genes Celsr1 and Vangl2 are required for normal lung branching morphogenesis. *Hum Mol Genet* **19**, 2251-2267 (2010).

257. Shima, Y. *et al.* Opposing roles in neurite growth control by two seven-pass transmembrane cadherins. *Nat Neurosci* **10**, 963-969 (2007).

258. Khor, G.H., Froemming, G.R., Zain, R.B., Abraham, T.M. & Lin, T.K. Involvement of CELSR3 Hypermethylation in Primary Oral Squamous Cell Carcinoma. *Asian Pac J Cancer Prev* **17**, 219-223 (2016).

259. Gu, X. *et al.* CELSR3 mRNA expression is increased in hepatocellular carcinoma and indicates poor prognosis. *PeerJ* **7**, e7816 (2019).

260. Pan, Y., Liu, G., Wang, D. & Li, Y. Analysis of lncRNA-Mediated ceRNA Crosstalk and Identification of Prognostic Signature in Head and Neck Squamous Cell Carcinoma. *Front Pharmacol* **10**, 150 (2019).

261. Bohnekamp, J. & Schoneberg, T. Cell adhesion receptor GPR133 couples to Gs protein. *J Biol Chem* **286**, 41912-41916 (2011).

262. Bayin, N.S. *et al.* GPR133 (ADGRD1), an adhesion G-protein-coupled receptor, is necessary for glioblastoma growth. *Oncogenesis* **5**, e263 (2016).

263. Yang, J., Wu, S. & Alachkar, H. Characterization of upregulated adhesion GPCRs in acute myeloid leukemia. *Transl Res* **212**, 26-35 (2019).

264. Zhou, L.L. *et al.* Differentially expressed long noncoding RNAs and regulatory mechanism of LINC02407 in human gastric adenocarcinoma. *World journal of gastroenterology* **25**, 5973-5990 (2019).

265. Yu, X.J. *et al.* Characterization of Somatic Mutations in Air Pollution-Related Lung Cancer. *EBioMedicine* **2**, 583-590 (2015).

266. Xie, K. *et al.* Polymorphisms in genes related to epithelial-mesenchymal transition and risk of non-small cell lung cancer. *Carcinogenesis* **38**, 1029-1035 (2017).

267. Hasan, A.N., Ahmad, M.W., Madar, I.H., Grace, B.L. & Hasan, T.N. An in silico analytical study of lung cancer and smokers datasets from gene expression omnibus (GEO) for prediction of differentially expressed genes. *Bioinformation* **11**, 229-235 (2015).

268. Sadras, T. *et al.* Differential expression of MUC4, GPR110 and IL2RA defines two groups of CRLF2-rearranged acute lymphoblastic leukemia patients with distinct secondary lesions. *Cancer Lett* **408**, 92-101 (2017).

269. Liu, Z., Zhang, G., Zhao, C. & Li, J. Clinical Significance of G Protein-Coupled Receptor 110 (GPR110) as a Novel Prognostic Biomarker in Osteosarcoma. *Medical science monitor : international medical journal of experimental and clinical research* **24**, 5216-5224 (2018).

270. Ma, B. *et al.* Gpr110 deficiency decelerates carcinogen-induced hepatocarcinogenesis via activation of the IL-6/STAT3 pathway. *Am J Cancer Res* **7**, 433-447 (2017).

271. Espinal-Enriquez, J. *et al.* Genome-wide expression analysis suggests a crucial role of dysregulation of matrix metalloproteinases pathway in undifferentiated thyroid carcinoma. *BMC Genomics* **16**, 207 (2015).

272. Carr, J.C. *et al.* Overexpression of membrane proteins in primary and metastatic gastrointestinal neuroendocrine tumors. *Ann Surg Oncol* **20 Suppl 3**, S739-S746 (2013).

273. Sherman, S.K. *et al.* GIPR expression in gastric and duodenal neuroendocrine tumors. *J Surg Res* **190**, 587-593 (2014).

274. Zhang, W. *et al.* TRIM58/cg26157385 methylation is associated with eight prognostic genes in lung squamous cell carcinoma. *Oncol Rep* **40**, 206-216 (2018).

275. Fukuzawa, T. *et al.* Lung surfactant levels are regulated by Ig-Hepta/GPR116 by monitoring surfactant protein D. *PLoS One* **8**, e69451 (2013).

276. Kang, G. *et al.* Exome sequencing identifies early gastric carcinoma as an early stage of advanced gastric cancer. *PLoS One* **8**, e82770 (2013).

277. Park, D. *et al.* BAI1 is an engulfment receptor for apoptotic cells upstream of the ELMO/Dock180/Rac module. *Nature* **450**, 430-434 (2007).

278. Cork, S.M. *et al.* A proprotein convertase/MMP-14 proteolytic cascade releases a novel 40 kDa vasculostatin from tumor suppressor BAI1. *Oncogene* **31**, 5144-5152 (2012).

279. Zencir, S. *et al.* Identification of brain-specific angiogenesis inhibitor 2 as an interaction partner of glutaminase interacting protein. *Biochem Biophys Res Commun* **411**, 792-797 (2011).

280. Kim, J.C. *et al.* Gene expression profiling: canonical molecular changes and clinicopathological features in sporadic colorectal cancers. *World journal of gastroenterology* **14**, 6662-6672 (2008).

281. Bolliger, M.F., Martinelli, D.C. & Sudhof, T.C. The cell-adhesion G protein-coupled receptor BAI3 is a high-affinity receptor for C1q-like proteins.

Proceedings of the National Academy of Sciences of the United States of America **108**, 2534-2539 (2011).

282. Kee, H.J. *et al.* Expression of brain-specific angiogenesis inhibitor 3 (BAI3) in normal brain and implications for BAI3 in ischemia-induced brain angiogenesis and malignant glioma. *FEBS Lett* **569**, 307-316 (2004).

283. Xu, L., Begum, S., Hearn, J.D. & Hynes, R.O. GPR56, an atypical G protein-coupled receptor, binds tissue transglutaminase, TG2, and inhibits melanoma tumor growth and metastasis. *Proceedings of the National Academy of Sciences of the United States of America* **103**, 9023-9028 (2006).

284. Little, K.D., Hemler, M.E. & Stipp, C.S. Dynamic regulation of a GPCR-tetraspanin-G protein complex on intact cells: central role of CD81 in facilitating GPR56-Galpha q/11 association. *Mol Biol Cell* **15**, 2375-2387 (2004).

285. Xu, L. *et al.* GPR56 plays varying roles in endogenous cancer progression. *Clinical & experimental metastasis* **27**, 241-249 (2010).

286. Daga, S. *et al.* High GPR56 surface expression correlates with a leukemic stem cell gene signature in CD34-positive AML. *Cancer Med* **8**, 1771-1778 (2019).

287. Zhang, D.L. *et al.* Gq activity- and beta-arrestin-1 scaffolding-mediated ADGRG2/CFTR coupling are required for male fertility. *Elife* **7** (2018).

288. Ahn, J.I. *et al.* G-protein coupled receptor 64 (GPR64) acts as a tumor suppressor in endometrial cancer. *BMC Cancer* **19**, 810 (2019).

289. Leja, J. *et al.* Novel markers for enterochromaffin cells and gastrointestinal neuroendocrine carcinomas. *Mod Pathol* **22**, 261-272 (2009).

290. Petersen, S.C. *et al.* The adhesion GPCR GPR126 has distinct, domain-dependent functions in Schwann cell development mediated by interaction with laminin-211. *Neuron* **85**, 755-769 (2015).

291. Garinet, S. *et al.* High Prevalence of a Hotspot of Noncoding Somatic Mutations in Intron 6 of GPR126 in Bladder Cancer. *Mol Cancer Res* **17**, 469-475 (2019).

292. Chase, A. *et al.* TFG, a target of chromosome translocations in lymphoma and soft tissue tumors, fuses to GPR128 in healthy individuals. *Haematologica* **95**, 20-26 (2010).

293. Hu, Q.X. *et al.* Constitutive Galphai coupling activity of very large G protein-coupled receptor 1 (VLGR1) and its regulation by PDZD7 protein. *J Biol Chem* **289**, 24215-24225 (2014).

294. Shin, D., Lin, S.T., Fu, Y.H. & Ptacek, L.J. Very large G protein-coupled receptor 1 regulates myelin-associated glycoprotein via Galphas/Galphaq-mediated protein kinases A/C. *Proceedings of the National Academy of Sciences of the United States of America* **110**, 19101-19106 (2013).

295. Fu, Q. *et al.* [MiR-145 inhibits drug resistance to Oxaliplatin in colorectal cancer cells through regulating G protein coupled receptor 98]. *Zhonghua wei chang wai ke za zhi = Chinese journal of gastrointestinal surgery* **20**, 566-570 (2017).

296. Park, J.W. *et al.* Troglitazone, the peroxisome proliferator-activated receptor-gamma agonist, induces antiproliferation and redifferentiation in human thyroid cancer cell lines. *Thyroid* **15**, 222-231 (2005).

297. Saikia, S., Bordoloi, M. & Sarmah, R. Established and In-trial GPCR Families in Clinical Trials: A Review for Target Selection. *Curr Drug Targets* **20**, 522-539 (2019).

298. Liang, Y. *et al.* Identification of a novel alternative splicing variant of RGS5 mRNA in human ocular tissues. *FEBS J* **272**, 791-799 (2005).

299. Koh, J. *et al.* Regulator of G protein signaling 5 is highly expressed in parathyroid tumors and inhibits signaling by the calcium-sensing receptor. *Molecular endocrinology* **25**, 867-876 (2011).

300. Osterhoff, C., Ivell, R. & Kirchhoff, C. Cloning of a human epididymis-specific mRNA, HE6, encoding a novel member of the seven transmembrane-domain receptor superfamily. *DNA Cell Biol* **16**, 379-389 (1997).

301. Davies, B. *et al.* Targeted deletion of the epididymal receptor HE6 results in fluid dysregulation and male infertility. *Mol Cell Biol* **24**, 8642-8648 (2004).

302. Hannan, F.M., Kallay, E., Chang, W., Brandi, M.L. & Thakker, R.V. The calcium-sensing receptor in physiology and in calcitropic and noncalcitropic diseases. *Nat Rev Endocrinol* **15**, 33-51 (2018).

303. Gorvin, C.M. *et al.* AP2sigma Mutations Impair Calcium-Sensing Receptor Trafficking and Signaling, and Show an Endosomal Pathway to Spatially Direct G-Protein Selectivity. *Cell reports* **22**, 1054-1066 (2018).

304. Nesbit, M.A. *et al.* Mutations in AP2S1 cause familial hypocalciuric hypercalcemia type 3. *Nat Genet* **45**, 93-97 (2013).

305. Gorvin, C.M. Insights into calcium-sensing receptor trafficking and biased signalling by studies of calcium homeostasis. *J Mol Endocrinol* **61**, R1-R12 (2018).

306. Ray, K. Calcium-Sensing Receptor: Trafficking, Endocytosis, Recycling, and Importance of Interacting Proteins. *Prog Mol Biol Transl Sci* **132**, 127-150 (2015).

307. Varshney, S. *et al.* Simultaneous expression analysis of vitamin D receptor, calcium-sensing receptor, cyclin D1, and PTH in symptomatic primary hyperparathyroidism in Asian Indians. *Eur J Endocrinol* **169**, 109-116 (2013).

308. Kantham, L. *et al.* The calcium-sensing receptor (CaSR) defends against hypercalcemia independently of its regulation of parathyroid hormone secretion. *Am J Physiol Endocrinol Metab* **297**, E915-923 (2009).

309. Sudhaker Rao, D., Han, Z.H., Phillips, E.R., Palnitkar, S. & Parfitt, A.M. Reduced vitamin D receptor expression in parathyroid adenomas: implications for pathogenesis. *Clin Endocrinol (Oxf)* **53**, 373-381 (2000).

310. Brown, E.M. *et al.* Calcium-regulated parathyroid hormone release in primary hyperparathyroidism: studies in vitro with dispersed parathyroid cells. *Am J Med* **66**, 923-931 (1979).

311. Trogden, K.P. *et al.* Regulation of Glucose-Dependent Golgi-Derived Microtubules by cAMP/EPAC2 Promotes Secretory Vesicle Biogenesis in Pancreatic beta Cells. *Curr Biol* **29**, 2339-2350 e2335 (2019).

312. Hatakeyama, H., Takahashi, N., Kishimoto, T., Nemoto, T. & Kasai, H. Two cAMP-dependent pathways differentially regulate exocytosis of large dense-core and small vesicles in mouse beta-cells. *J Physiol* **582**, 1087-1098 (2007).

313. Sedej, S., Rose, T. & Rupnik, M. cAMP increases Ca2+-dependent exocytosis through both PKA and Epac2 in mouse melanotrophs from pituitary tissue slices. *J Physiol* **567**, 799-813 (2005).

314. Gambardella, J., Lombardi, A., Morelli, M.B., Ferrara, J. & Santulli, G. Inositol 1,4,5-Trisphosphate Receptors in Human Disease: A Comprehensive Update. *J Clin Med* **9** (2020).

315. Shah, S.Z.A., Zhao, D., Khan, S.H. & Yang, L. Regulatory Mechanisms of Endoplasmic Reticulum Resident IP3 Receptors. *J Mol Neurosci* **56**, 938-948 (2015).

316. Quinton, T.M. & Dean, W.L. Cyclic AMP-dependent phosphorylation of the inositol-1,4,5-trisphosphate receptor inhibits Ca2+ release from platelet membranes. *Biochem Biophys Res Commun* **184**, 893-899 (1992).

317. Murthy, K.S. cAMP inhibits IP(3)-dependent Ca(2+) release by preferential activation of cGMP-primed PKG. *American journal of physiology. Gastrointestinal and liver physiology* **281**, G1238-1245 (2001).

318. Hauser, A.S., Attwood, M.M., Rask-Andersen, M., Schioth, H.B. & Gloriam, D.E. Trends in GPCR drug discovery: new agents, targets and indications. *Nat Rev Drug Discov* **16**, 829-842 (2017).

319. Inoue, A. *et al.* Illuminating G-Protein-Coupling Selectivity of GPCRs. *Cell* **177**, 1933-1947 e1925 (2019).

320. Irannejad, R., Tsvetanova, N.G., Lobingier, B.T. & von Zastrow, M. Effects of endocytosis on receptor-mediated signaling. *Curr Opin Cell Biol* **35**, 137-143 (2015).

321. Ellaithy, A., Gonzalez-Maeso, J., Logothetis, D.A. & Levitz, J. Structural and Biophysical Mechanisms of Class C G Protein-Coupled Receptor Function. *Trends Biochem Sci* **45**, 1049-1064 (2020).

322. Salmaso, V. & Jacobson, K.A. Purinergic Signaling: Impact of GPCR Structures on Rational Drug Design. *ChemMedChem* **15**, 1958-1973 (2020).

323. Morgan, R.K. *et al.* The expanding functional roles and signaling mechanisms of adhesion G protein-coupled receptors. *Annals of the New York Academy of Sciences* **1456**, 5-25 (2019).

324. Demberg, L.M. *et al.* Activation of Adhesion G Protein-coupled Receptors: AGONIST SPECIFICITY OF STACHEL SEQUENCE-DERIVED PEPTIDES. *The Journal of biological chemistry* **292**, 4383-4394 (2017).

325. Monk, K.R. *et al.* Adhesion G Protein-Coupled Receptors: From In Vitro Pharmacology to In Vivo Mechanisms. *Mol Pharmacol* **88**, 617-623 (2015).

326. Stephenson, J.R. *et al.* Brain-specific angiogenesis inhibitor-1 signaling, regulation, and enrichment in the postsynaptic density. *The Journal of biological chemistry* **288**, 22248-22256 (2013).

327. Arac, D., Strater, N. & Seiradake, E. Understanding the Structural Basis of Adhesion GPCR Functions. *Handbook of experimental pharmacology* **234**, 67-82 (2016).

328. Manglik, A. *et al.* Crystal structure of the micro-opioid receptor bound to a morphinan antagonist. *Nature* **485**, 321-326 (2012).

329. Renault, N., Gohier, A., Chavatte, P. & Farce, A. Novel structural insights for drug design of selective 5-HT(2C) inverse agonists from a ligand-biased receptor model. *Eur J Med Chem* **45**, 5086-5099 (2010).

330. Wifling, D., Bernhardt, G., Dove, S. & Buschauer, A. The extracellular loop 2 (ECL2) of the human histamine H4 receptor substantially contributes to ligand binding and constitutive activity. *PLoS One* **10**, e0117185 (2015).

331. Woolley, M.J. & Conner, A.C. Understanding the common themes and diverse roles of the second extracellular loop (ECL2) of the GPCR super-family. *Molecular and cellular endocrinology* **449**, 3-11 (2017).

332. Patwardhan, A., Cheng, N. & Trejo, J. Post-Translational Modifications of G Protein-Coupled Receptors Control Cellular Signaling Dynamics in Space and Time. *Pharmacological reviews* **73**, 120-151 (2021).

333. Hoare, S.R.J., Tewson, P.H., Quinn, A.M., Hughes, T.E. & Bridge, L.J. Analyzing kinetic signaling data for G-protein-coupled receptors. *Scientific reports* **10**, 12263 (2020).

334. Grundmann, M. & Kostenis, E. Label-free biosensor assays in GPCR screening. *Methods Mol Biol* **1272**, 199-213 (2015).

335. Rocheville, M., Martin, J., Jerman, J. & Kostenis, E. Mining the potential of label-free biosensors for seven-transmembrane receptor drug discovery. *Prog Mol Biol Transl Sci* **115**, 123-142 (2013).

336. Schroder, R. *et al.* Applying label-free dynamic mass redistribution technology to frame signaling of G protein-coupled receptors noninvasively in living cells. *Nat Protoc* **6**, 1748-1760 (2011).

337. Hennen, S. *et al.* Decoding signaling and function of the orphan G protein-coupled receptor GPR17 with a small-molecule agonist. *Science signaling* **6**, ra93 (2013).

338. Luo, R. *et al.* Mechanism for adhesion G protein-coupled receptor GPR56-mediated RhoA activation induced by collagen III stimulation. *PloS one* **9**, e100043 (2014).

339. Ehrenmann, J. *et al.* High-resolution crystal structure of parathyroid hormone 1 receptor in complex with a peptide agonist. *Nat Struct Mol Biol* **25**, 1086-1092 (2018).

340. Gkountelias, K. *et al.* Alanine scanning mutagenesis of the second extracellular loop of type 1 corticotropin-releasing factor receptor revealed residues critical for peptide binding. *Molecular pharmacology* **75**, 793-800 (2009).

341. Balenga, N.A. *et al.* Heteromerization of GPR55 and cannabinoid CB2 receptors modulates signalling. *Br J Pharmacol* **171**, 5387-5406 (2014).

342. Balenga, N.A. *et al.* GPR55 regulates cannabinoid 2 receptor-mediated responses in human neutrophils. *Cell Res* **21**, 1452-1469 (2011).

343. Sun, Y. *et al.* Optimization of a peptide ligand for the adhesion GPCR ADGRG2 provides a potent tool to explore receptor biology. *The Journal of biological chemistry* (2020).

344. Patat, O. *et al.* Truncating Mutations in the Adhesion G Protein-Coupled Receptor G2 Gene ADGRG2 Cause an X-Linked Congenital Bilateral Absence of Vas Deferens. *American journal of human genetics* **99**, 437-442 (2016).

345. Yang, B. *et al.* Pathogenic role of ADGRG2 in CBAVD patients replicated in Chinese population. *Andrology* **5**, 954-957 (2017).

346. Rosa, M., Noel, T., Harris, M. & Ladds, G. Emerging roles of adhesion G protein-coupled receptors. *Biochem Soc Trans* **49**, 1695-1709 (2021).

347. Sun, Y. *et al.* Optimization of a peptide ligand for the adhesion GPCR ADGRG2 provides a potent tool to explore receptor biology. *J Biol Chem* **296**, 100174 (2021).

348. Jin, Z. *et al.* Disease-associated mutations affect GPR56 protein trafficking and cell surface expression. *Hum Mol Genet* **16**, 1972-1985 (2007).

349. Zhang, D. *et al.* Function and therapeutic potential of G protein-coupled receptors in epididymis. *Br J Pharmacol* **177**, 5489-5508 (2020).